"Arctic climate variability during the past millennium : combining model simulations and proxy data"

Crespin, Elisabeth

Abstract

The Arctic is one of the regions that experienced the fastest and highest warming of the planet during the recent decades, and changes in its environment had worldwide implications. Studying climate changes during the past is essential for a comprehensive understanding of the climate system, particularly to provide insights into the processes involved in the recent Arctic warming, in order to assess future global climate changes. Information about past climate evolution can be extracted from “proxy” data, while climate models can be used to interpret the observed changes. In this doctoral thesis, we have taken advantage of the complementarity of model results and proxy data, through data assimilation, to provide reliable simulations of the Arctic climate over the past millennium that are in agreement with all the possible sources of information: proxies, physics of the model and external forcings. Those simulations have then been used to analyse the role played by different forci...

Document type : *Thèse (Dissertation)*

UNIVERSITÉ CATHOLIQUE DE LOUVAIN
FACULTÉ DES SCIENCES, ECOLE DE PHYSIQUE
EARTH AND LIFE INSTITUTE
GEORGES LEMAÎTRE CENTRE FOR EARTH AND CLIMATE RESEARCH

ARCTIC CLIMATE VARIABILITY DURING THE PAST MILLENNIUM: COMBINING MODEL SIMULATIONS AND PROXY DATA

DOCTORAL DISSERTATION PRESENTED BY

ELISABETH CRESPIN

IN FULFILLMENT OF THE REQUIREMENTS
FOR THE DEGREE OF DOCTOR IN SCIENCES

THESIS COMMITTEE:

Prof. Thierry Fichefet (Supervisor)	Université catholique de Louvain
Prof. Hugues Goosse (Supervisor)	Université catholique de Louvain
Prof. Michel Crucifix	Université catholique de Louvain
Dr. Didier Swingedouw	Université de Bordeaux
Dr. Martin Widmann	University of Birmingham
Prof. Marie-Laurence De Keersmaecker (Chair)	Université catholique de Louvain

LOUVAIN-LA-NEUVE
JUNE 2014

Une thèse, quelle aventure ! D'aucuns diront que c'est une longue et redoutable épreuve... mais le chemin devient clair et agréable lorsqu'on est bien entouré ! Je voudrais remercier toutes les personnes qui ont fait en sorte que cette expérience soit une réussite.

Je commence, bien sûr, par mes deux promoteurs, les Professeurs Thierry Fichefet et Hugues Goosse, qui m'ont encadrée et soutenue tout au long de ma thèse. Merci, Thierry, de la confiance que tu m'as témoigné en me proposant de faire un doctorat à la fin de mon mémoire, et de ton exemple de rigueur et pertinence. Hugues, merci pour ton enthousiasme et ton optimisme hors pair, et pour ces nombreuses discussions desquelles j'ai énormément appris. A tous deux, merci pour votre disponibilité sans faille, votre bienveillance, votre patience et vos encouragements opportuns. Ça a été un plaisir et une chance de pouvoir travailler avec vous.

Je remercie également tous les autres membres du jury d'avoir accepté ce rôle. Merci Didier, Martin et Michel pour l'intérêt que vous avez porté à mon sujet de thèse, pour la lecture attentive du manuscrit, les commentaires pertinents et les discussions constructives qui ont permis d'améliorer mon travail.

Merci à l'École de physique de l'UCL de m'avoir accordé un mandat d'assistante. Cette opportunité fut une expérience très enrichissante.

En sept ans à l'Institut, on en voit défiler du monde ! Je voudrais remercier tous mes collègues, anciens et nouveaux (si nombreux qu'il serait difficile de tous les citer), pour tous les bons moments passés ensemble, et pour l'aide scientifique, technique et administrative que j'ai reçue. Plus particulièrement, merci à tous ces collègues qui sont devenus, avec le temps, de bons amis. D'abord merci à Violette. Mazette ! Je n'aurais pu trouver meilleure collègue de bureau. Entre discussions de chats, potager, syndic et autres parapluies de l'EGU, je pense que nous avons créé une synergie parfaite. Merci à Yoann, dont l'enthousiasme et la capacité innée à ronchonner ont égayé le groupe pendant deux trop courtes années, et dont l'expertise a fait faire un bond énorme à cette thèse. Merci Oli, mon pote des TPs et mon compagnon d'infortune de fin de thèse, pour ton soutien de tout instant. Merci aussi pour les weekends de camping à Sérigny qui resteront, j'espère, une longue tradition. Merci au reste de la bande: François, Pierre-Yves, Aurélien, Svetlana, Pierre, Alice, Antoine, pour ces nombreux bons moments passés autour d'un petit verre de jus de tomate en terrasse, d'un match de badminton, d'un barbecue ou d'un souper de Noël. Merci Marie-France, pour ton amitié et tous nos midis sportifs. Merci Francisco, d'avoir rendu, grâce à ta bonne humeur permanente, tous mes passages aux laboratoires de didactique si plaisants. Finalement, j'ai une

pensée émue pour Ralph, qui nous a quitté beaucoup trop tôt. Merci Ralph pour tous tes conseils de vieux sage ; tu as été celui qui a trouvé les mots les plus justes lors de mes périodes de démotivation et de stress.

Merci à toute ma famille, surtout à mes parents qui ont, depuis toujours, joué leur rôle à merveille. Merci aux frères et soeur, pour leurs "y el clima sigue calentándose..." d'encouragement. Merci aussi à ma belle-famille pour toutes leurs attentions.

Merci enfin à tous ces amis qui m'ont également soutenue pendant ces longues années: aux clans orchestra, au clan des physiciens, a los amigos de Bolivia. Merci à tous pour votre amitié, votre précieux soutien et votre patience les nombreuses fois ou je vous ai cassé les oreilles au sujet de ma thèse !

Une thèse est une longue et éprouvante aventure, c'est bien connu... Mais, tout compte fait, ce parcours n'est-il pas encore plus difficile pour la personne qui accompagne le doctorant au jour le jour, en supportant tous ses états d'humeur ? Merci Tom, d'avoir toujours été là, de m'avoir soutenue du début à la fin, contre vents et marées. Tu as autant de mérite que moi dans ce travail !

CONTENTS

CHAPTER 1

INTRODUCTION

1.1 Generalities on Arctic climate changes

The Arctic is the northernmost region of the Earth, surrounding the North Pole. Different limits defining this region have been proposed. Most commonly, the Arctic is defined as the area located north of the Arctic Circle, an imaginary circle at 66.56°N which corresponds to the approximate limit latitude of the midnight Sun or the polar night, that is, the latitude at which the Sun is above or below the horizon for 24 continuous hours during the solstices. Alternatively, the region can be limited by the mean July 10°C isotherm, corresponding roughly to the northernmost tree line. The boundary of this region is also sometimes taken at 60°N, and this is the definition we adopt in the context of this thesis. With its cold weather and vast ice-covered ocean, the Arctic is one of the most inhospitable regions of the globe, but also one of the most interesting and important place to study. Indeed, the Arctic environment is extremely vulnerable to climate change, and because it interacts with the climate of the entire Northern Hemisphere, through the atmosphere and oceans, changes in Arctic environmental conditions have worldwide implications (http://nsidc.org/cryosphere/arctic-meteorology/arctic.html, ACIA, 2005).

The reasons justifying the interest in the Arctic region can be summarized as follows. The Arctic is one of the regions that experienced the fastest and highest warming in recent decades (ACIA, 2005). During the past century, the average surface temperature in the Arctic has increased by about $0.09°C$ per decade, which is about twice the global mean value (ACIA, 2005). Climate projections presented in the recent report of the Intergovernmental Panel of Climate Change (IPCC, 2013) suggest that this strong warming will continue and range from approximately $2°C$ to $10°C$ by the year 2100 in winter, and from about $1°C$ to $5°C$ in summer, depending on the model and forcing scenario. This warming is associated with a substantial melting of sea ice (Fig. 1.1). The IPCC states that the annual mean Arctic sea ice extent has very likely decreased with a rate between 3.5 and 4.1% per decade over the period 1979-2012, corresponding to a decrease of 0.45 to 0.51 million km^2 per decade (Vaughan et al., 2007). Those changes in sea ice, as well as in snow cover, affect the atmospheric and oceanic circulations and the Earth's energy balance, which can in turn impact the regional or global climate. Therefore, because of this essential role played by the Arctic climate at global scale, it is primordial to understand the processes involved in Arctic warming and their global implications in order to be able to assess global climate changes and their impacts (ACIA, 2005).

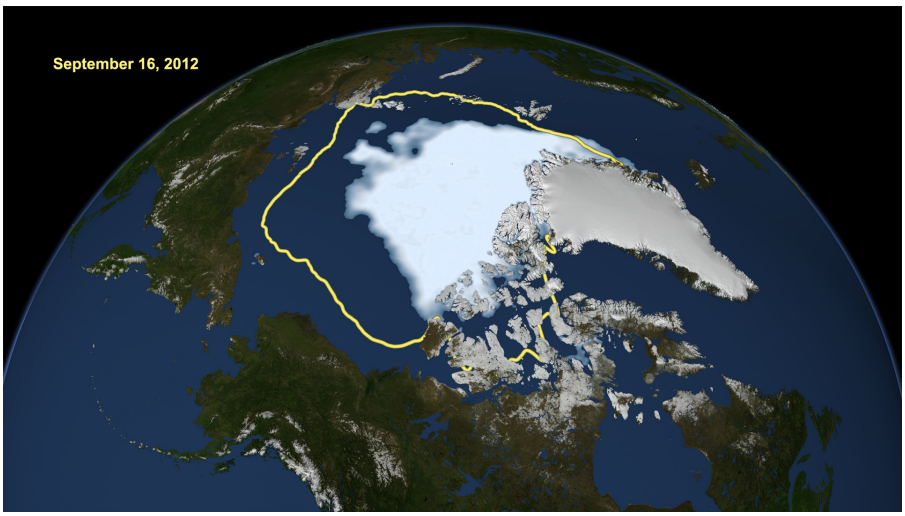

Figure 1.1: Arctic sea ice on September 16, 2012, identified as the minimum extent reached in 2012, compared to the averaged sea ice minimum from 1979 to 2010 (yellow line) (http://www.nasa.gov/topics/earth/features/2012-seaicemin.html).

For instance, the snow and sea ice are two prominent features of the Arctic and play a key role in the climate changes, in particular because of their high reflectivity, low thermal conductivity and because of the high latent heat required to melt the snow/ice. They are associated with positive feedbacks that, along with other processes, result in what is called the Arctic amplification, which corresponds to the fact that temperature changes in the Arctic tend to be larger than those of the Northern Hemisphere or the globe as a whole (Serreze and Barry, 2011). When talking about Arctic amplification, the principal process brought to the table is the snow and ice albedo feedback, although it is also strongly influenced by changes in atmospheric and oceanic poleward heat transport, by the water vapour feedback (due to the greenhouse effect of additional water vapour), the lapse rate feedback (associated with the vertical structure of the warming) and the cloud feedbacks (changes in the effect of clouds on Earth's radiative balance) (Pithan and Mauritsen, 2014). Here, only the processes linked to sea ice and snow will be described. The snow and ice albedo feedback is associated to a reduction of sea ice or snow extent that has the effect of increasing an initial warming. If the temperature becomes higher, the high albedo of sea ice and snow is replaced by the lower albedo of water and land surfaces, that subsequently absorb more solar radiation, leading to an additional heating of the surface and further loss of sea ice and snow. This feedback does work in reverse too. Another influence of snow and sea ice retreat concerns the modifications in the exchange of heat fluxes between ocean and atmosphere. Indeed, a smaller or thinner sea ice cover leads to a lesser insulation effect and then to an increased heat flux from the relatively warm ocean to the cold atmosphere in winter. Those feedbacks have a strong seasonal expression, since the winter in the Arctic is characterized by a low amount or absence of sunlight and a sea ice extent (about 15 millions km^2) more than double the extent in summer (about 6 millions km^2). Another negative feedback that has the potential to affect Arctic climate and cause global effects results from the reduction in the intensity of the global-scale oceanic overturning circulation. This is discussed in more details in Section 1.5.

Putting the recent Arctic climate change in a longer-term context is certainly useful to improve our understanding of the important mechanisms taking place in this region and their relative contributions to the observed variability. In this thesis, we focus our attention on the time period spanning the last millennium. This period turns out to be most relevant to assess the potential uniqueness of recent events (Jones and Mann, 2004). Indeed, the principal natural factors responsible for climate variability during the past millennium, as for instance the Earth's orbital geometry, were not very different compared to the actual period. The climate variability during the last millennium is then

supposed to be similar to the variability during the present century without taking into account the human influence. The comparison between the recent period and the previous centuries can thus be used to estimate the importance of the anthropogenic forcings on present and future climate changes. Furthermore, the study of the climate of the last millennium provides insights on the main mechanisms and feedbacks controlling the climate that could help the general understanding of Arctic climate.

The Arctic climate is a complex system, and the physical processes that have to be combined to explain the climate changes taking place in this region are numerous. Part of the variability observed in the Arctic climate can be related to external forcings which perturb the radiative balance of the Earth. However, significant part of the variability cannot be linked to any modification in external forcing, but rather to the internal dynamics of climate, that is, the variability associated with the chaotic nature of the system. For the last millennium, external forcings play a dominant role at hemispheric scale, but their contributions to the climate variability compared to internal variability become weaker for smaller spatial and temporal scales (Hawkins and Sutton, 2009). At regional scale and at mid- and high latitudes, the dominant cause of climate changes is generally the internal variability (Goosse et al., 2005).

The different external forcings are usually divided into two categories, according to their origin: natural or anthropogenic. Depending on the timescale considered, the dominant forcing factors may vary. The variations in greenhouse gas concentrations, in total solar irradiance, in the Earth's orbital parameters, in land use and land cover, and in volcanic activity are the main natural preindustrial external forcings responsible for climate variability during the last millennium. Other forcings such as dust or other natural aerosols may have also played a role, but they are not yet sufficiently documented (Moberg, 2013). In absence of human interference, variations in greenhouse gas concentrations results from natural feedbacks between the carbon cycle and climate changes. Those variations are reconstructed from ice core analysis. Since the beginning of the industrial period, the human influence on the atmospheric composition has increased dramatically. The higher emissions of greenhouse gases have resulted in an increase in radiative forcing of up to 2.5 Wm^{-2} compared to the preindustrial period (Forster et al., 2007). Additionally, during the industrial period, other anthropogenic forcings, that were nonexistent or not important before, have influenced the climate: the variations in tropospheric ozone and atmospheric aerosols such as anthropogenic sulfate aerosol load.

The forcing due to changes in the Earth's orbital geometry is the only one that can be computed numerically based on astronomical considerations (Berger et al., 1993). It modifies the amount of solar energy received in a particular season and location. This astronomical forcing plays a much weaker role during the past millennium than over much longer time-scales, when it can be a dominant forcing. The magnitude of the influence of this forcing on the climate of the last millennium strongly depends on the considered time of the year and location, but for some latitudes and seasons, it can be locally as large as the radiative forcing changes due to changes in anthropogenic greenhouse gas concentrations. The release of aerosols into the atmosphere during major volcanic eruptions affects the climate at both regional or large-scale. By reflecting the solar radiation back to space, these aerosols lead to a negative radiative forcing. Large individual volcanic eruptions can represent a forcing twice as large as the current greenhouse gas forcing, but their effect on climate last only for a few years (Moberg, 2013). The volcanic activity history is typically reconstructed from sulphate aerosol layers in ice cores (e.g. Crowley et al., 2008). One of the most uncertain and controversial forcing is the one related to solar irradiance variability. The solar irradiance forcing shows an 11-year cycle and has a relatively small amplitude compared to the volcanic or greenhouse gas forcing for instance. The proxy indices that seem to correlate with the total solar irradiance variations measured over the very short satellite period (3 last decades) are sunspot numbers, which are available back to the beginning of 17th century, and isotopic information recorded in tree rings or ice cores. Due to the high uncertainty concerning the long-term variations in solar irradiance during the last millennium, a set of alternative forcings of different magnitudes have been proposed, ranging from a 0.04 to 0.4% increase in total solar irradiance between a specific period, the Maunder minimum (1645-1715), and the recent solar minima (Schmidt et al., 2012). The land use change forcing has been estimated from historical evidence such as deforestation or maps and reconstructions of agricultural areas (Ramankutty and Foley, 1999; Pongratz et al., 2008). The increasing albedo associated with the land changes results in an increasing negative radiative forcing over the last 3 centuries. The magnitude of this change is ten times smaller than the one of the greenhouse gas forcing, and of opposite sign (Moberg, 2013).

Internal dynamics, through the interactions between the various elements of the climate system, can be an important cause of climate variability in the absence of any significant change in external forcing. Much of the observed changes in the Arctic are thought to be related to patterns of atmospheric circulation. A major mode of atmospheric variability in the Northern Hemisphere is the Arctic/North Atlantic Oscillation (AO/NAO) (ACIA, 2005). It

is characterized by relatively high frequency variations. The NAO is linked to the co-variability in sea level pressure between the Icelandic Low and the Azores High. The pressure difference between these regions is responsible for westerly winds characterizing the atmospheric circulation in the North Atlantic at mid-latitudes. A positive NAO index corresponds to a higher than normal pressure in the Azores High and a lower than normal pressure in the Icelandic Low, leading to stronger than average westerlies. If the pressure is lower than normal in the Azores High and higher than normal in the Icelandic Low, the index is negative and the westerlies are weaker than the mean. The AO, defined as the leading mode of variability of the Northern Hemisphere sea level pressure, is a larger scale oscillation of the pressure between subtropical areas and high latitudes. It is highly correlated with the NAO, which is usually considered as a regional manifestation of the AO.

Identifying and analysing in detail the different contributions to climate variability in the Arctic over the last millennium is our main objective. Even though numerous studies are devoted to the reconstruction of the climate conditions that prevailed during the last millennium, the understanding of the climate changes over this period is still fragmentary. One of the principal limitations for reconstructing temperature variations during the last millennium is certainly the lack of direct meteorological measurements that were not available prior to the mid-19th century. Before the instrumental period, the absence of direct climate observations urges us to rely on other types of information present in natural archives, that can provide an estimation of both the climate conditions and of the forcing factors that drive the climate (see Section 1.2 for more information on those proxy data). These data are, however, characterized by a poor temporal and geographical distribution, especially in the Arctic, and their number is still relatively low. Also, their reliability as indicators of climate varies from one to the other, and the reconstructed climate signal or forcing history are thus associated with a relatively large degree of uncertainty. In complement to those data, numerical models of the climate system, driven by the estimated external forcings, can be used to interpret the observed changes and to analyse the response of the system to changes in the forcings (see Section 1.3 for more information). However, models are also characterized by deficiencies, and no matter how complex they are, they can never be expected to reproduce exactly the real climate. In this thesis, we combined those two ways of analysing past climate changes, proxy data and climate models, to take advantage of the different information provided by both of them. The studies performed in this context contributed to the development of a method of data assimilation, which is addressed in Section 1.5.

1.2 Proxy data and proxy-based climate reconstructions

The proxy data are natural indirect indicators that contain biological, chemical or physical properties that are related to climate phenomena. In addition to the natural archives, written archives from historical documents can also be a source of information. The temporal resolution recorded in the proxies varies according to the type of indicator. Some of them, such as sediment cores or pollen, have poor chronologies and are thus only useful to describe changes at decadal to centennial or even longer time scales. Higher-resolution proxy records are needed when the interest is focused on the past millennium. Annually or seasonally resolved proxies can be obtained from historical documents, corals, ice cores, lake sediment cores, and from the most important and geographically widespread proxies used to reconstruct climate over the past millennium: growth and density measurements from tree rings. For a complete review of proxy records, the reader can refer, for instance, to Jones and Mann (2004) and Jones et al. (2009).

The amount of proxy data spanning the past one or two millennia has increased very rapidly during the last decades and is now quite substantial (Ljungqvist, 2009). Those proxy records can be assembled together, using statistical models, to produce a climate reconstruction over the past centuries. Because of the indirect nature of the proxy informations and the fact that they include non-climatic noise, a relatively high level of uncertainty is related to the data. In order to be reliable, those reconstructions, based on indirect climate indicators, need to be calibrated and independently validated against instrumental data during a common period of overlap (Jones and Mann, 2004). Many of the studies dealing with climate reconstructions based on proxy data are devoted to the reconstruction of regional, hemispheric or global mean temperature (e.g. Mann et al., 2008; Crowley, 2000; Overpeck et al., 1997; Kaufman et al., 2009; Ljungqvist, 2010; Moberg et al., 2005), while some others are focused on spatial patterns of past surface temperature (e.g. Briffa et al., 1994; Rutherford et al., 2005; Luterbacher et al., 2004; Mann et al., 2009; Xoplaki et al., 2005). Finally, other studies have also focused on the reconstruction of different climate variables and indices (see the review of Jones and Mann, 2004), but in the context of this thesis, we will only concentrate on temperature reconstructions.

We basically describe here two approaches for combining proxies: the "composite plus scale" (CPS) method, used to reconstruct large-scale mean climate, and the "climate field reconstruction" (CFR) methods, to reconstruct spatial patterns of past climate changes. The first technique aims at selecting proxy

series (either of the same or different type) assumed to be sensitive to a certain climatic signal, temperature for instance, and at assessing which part of the year the proxy responds to. After scaling the proxy data to the local instrumental data, they are composited (averaged) and the resulting series is regressed or scaled against the equivalent instrumental series to form a regional or hemispheric reconstruction of surface temperature (e.g. Mann et al., 2008). In the CFR approaches, the proxy network is calibrated against the spatial information contained within the instrumental temperature field over the period of overlap between the proxy and instrumental data (Mann et al., 2009). This kind of method makes use of the covariance within the proxy data, within the instrumental data and between proxy and instrumental data. Although very different methods are applied in CPS or CFR approaches, those reconstructions are generally based on a regression relationship, often linear, between the proxy and a particular climate variable (the temperature in this context) over a calibration period, and it is assumed that this relationship is stationary (i.e., the proxy-temperature relationship does not change over time). The fundamental assumption of stationarity concerns both relationships between local proxies and local climate, and between local and large-scale climates, i.e., teleconnections (Mann et al., 1998, 1999; Lohmann et al., 2005; Groll and Widmann, 2006; Trenberth et al., 2007). However, this assumption of stationarity for local climate and for the fidelity of teleconnections needs to be verified (www.assessment.ucar.edu/paleo/past_stationarity.html#teleconnection, Ammann and Wahl, 2007).

Reconstructing climate variations in the Arctic region from proxy records is still a challenge, mainly because of the spatially incomplete and noisy information they provide. In order to obtain a large-scale spatial coverage, a multi-proxy approach has to be preferentially considered, since different types of proxies are distributed differently around the globe. Only a few high-resolution temperature reconstructions based on proxy records are available for the Arctic. Before Kaufman et al. (2009) did propose their quantitative reconstruction of decadally resolved summer Arctic temperature for the last 2000 years, the longest existing multi-proxy temperature reconstruction for the Arctic was the one of Overpeck et al. (1997). This last reconstruction spans the last four centuries. More recently Shi et al. (2012) presented a new Arctic summer temperature reconstruction with annual resolution based on multi-proxy records for the period covering the last 1400 years, using a novel ensemble method. Finally, the Past Global Changes (PAGES) 2k Network has assembled together a considerable number of high-resolution proxies and proposed a reconstruction for the past 2000 years (PAGES 2k Consortium, 2013). All those reconstructions have demonstrated that recent warmth is anoma-

lous compared to previous centuries (Fig. 1.2). But, although the temperature changes are similar from one reconstruction to another, there are also clear differences, bringing into question the accuracies and uncertainties of each reconstruction.

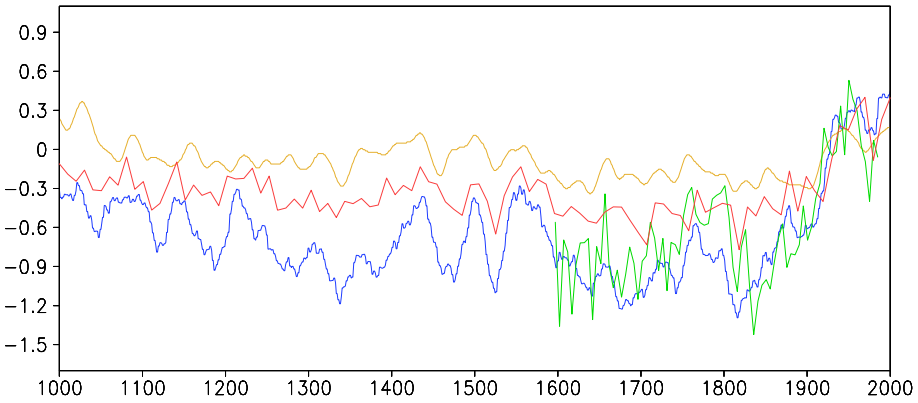

Figure 1.2: Proxy-based reconstructions over the past millennium of Arctic summer temperatures of Kaufman et al. (2009) in red, Shi et al. (2012) in yellow, and of Arctic annual mean temperature of PAGES 2k Consortium (2013) in blue (a 21-year running mean has been applied to this time series) and Overpeck et al. (1997) in green. The reference period is 1900-1970.

1.3 Modelling of Arctic climate changes

While proxy-based reconstructions provide information only for a limited number of climate variables, climate model simulations include a more complete representation of past climate states. When driven by appropriate external forcing changes, climate models can provide very useful insights concerning physical and dynamical processes that may have governed the climate system evolution during the last centuries. These models contain interactive representations of the physical behaviour of the atmosphere, ocean and sea ice, and sometimes of the carbon cycle, the vegetation dynamics and the ice sheets. Different types of models are available, that differ in their temporal and spatial resolution and on the degree of simplification of the description of the processes governing climate. We can distinguish models with a highly simplified representation of the dynamics of the system (Energy Balance Models or EBMs) from those which try to account for all the important properties of the system at a high-resolution (General Circulation Models or GCMs). Between those two extremes, EMICs (Earth System Models of Intermediate Complex-

ity) propose more sophisticated atmospheric and oceanic components than EBMs, but still include simplifications and parameterisations for some processes to enhance the computational efficiency. All these types of models have their advantages and brought different insights according to the scientific objectives. For instance, the simplest models do not take into account the high frequency variability of the atmosphere, and are then lacking any representation of internal variability. The simulated changes are thus, to a large extent, only a response to the external forcings. These models have the advantage to be very efficient in terms of computational time and can thus be used to perform easily a large number of simulations to improve our understanding of this response. Nevertheless, it is difficult to perform model-data comparisons with these simulations, particularly at regional scale where the role of internal variability can be very important. More complex models are thus needed to represent the variability on interannual to centennial timescales. In this thesis, an EMIC is used, to take advantage of both the possibilities to perform numerous simulations because of its low demand of computational time, and to provide simulations that include the contributions from internal and forced variations. These conditions fit well with the requirements needed to perform this thesis' tasks and follow its objectives, as will be explained in the next sections.

The Paleoclimate Modeling Intercomparison Project Phase 3 (PMIP3) was created to coordinate climate modelling activities, using GCMs and EMICs, over different past time periods, such as the last millennium. One of its task was to select a complete compilation of forcing reconstructions for this period (Schmidt et al., 2011), that were used to run most of the simulations presented in this thesis (some of these forcings are represented in Fig. 1.3). A group of approximately 15 models of different complexities have been driven by those forcings in the context of this project of intercomparison (https://pmip3.lsce.ipsl.fr). As an illustration, the available results of the mean Arctic surface temperature for five of these simulations are illustrated in Fig. 1.4. All results show relatively low temperatures between the 16th and 19th centuries, and a large warming during the 20th century. The differences in the high frequency variability between the different simulations are attributable, for instance, to the different resolutions of the models, the different representations of the system dynamics, or the choice of initial conditions. Furthermore, each simulation represents a possible evolution of the internal variability of the climate system, but almost certainly not the one followed in the real world (Goosse et al., 2008). Under these conditions, it is generally impossible to state if a particular difference between models is due to deficiencies in models and forcings, or simply to a different realisation of internal variability. This is why,

when it is possible, performing an ensemble of simulations with a particular model is very useful. Such an ensemble is obtained with exactly the same forcing but slightly varying the initial conditions to end up with a range of independent samples of the internal variability. The consistency between model and proxy data can then be verified if the data are well within the range of the ensemble of simulations. If an ensemble is available, the mean over all the members can be used to isolate and analyse the forced response of the system, as the internal variability is filtered by the averaging procedure.

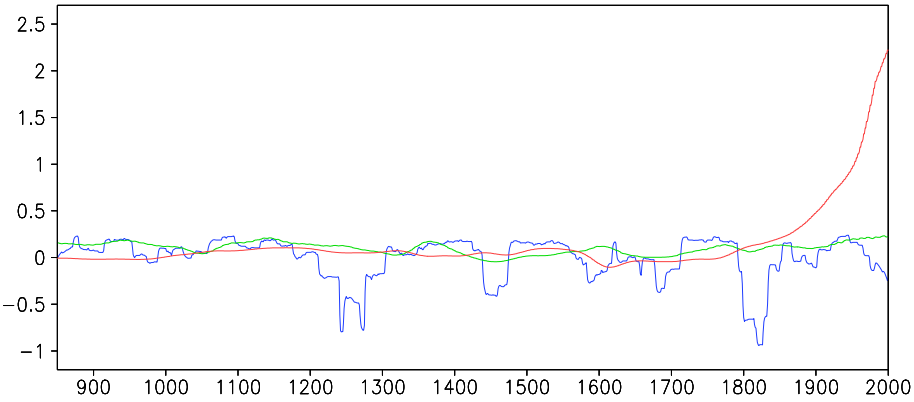

Figure 1.3: Estimates of past changes in annual mean radiative forcing (Wm^{-2}), as used in Crespin et al. (2012): solar forcing in green, volcanic forcing in blue, and greenhouse gas forcing in red. See Section 3.2 for references. A 25-year running mean has been applied to the time series.

1.4 Combining proxy data and model simulations

Separating the contributions of external forcings to the one of internal variability in present and past climate changes has been an arduous task of a number of recent studies (e.g. Jungclaus et al., 2010; Spangehl et al., 2010; Stendel et al., 2006; Hegerl et al., 2007; Crowley, 2000; Bauer et al., 2003; Goosse et al., 2005). Especially at regional scale, the role played by the internal variability is very important and can even mask the role of external forcing. For example, it is very hard to disentangle the response of atmospheric circulation to an external forcing from the internal variability of the system. As mentioned previously, climate model simulations can be used to isolate the response to external forcing, without forgetting that forcing reconstructions are also characterized by a certain degree of uncertainty. Having an ensemble of simulations is useful to sample the internal variability, but by using only the model results, it is

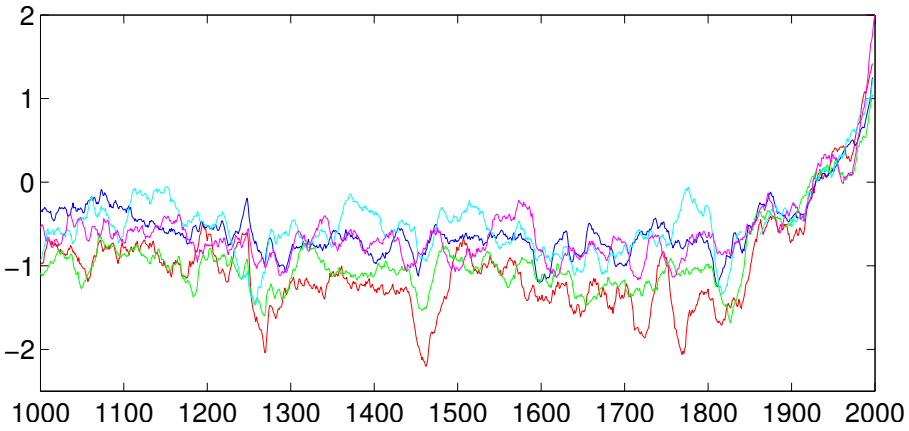

Figure 1.4: Anomaly in Arctic annual mean surface temperature (°C) simulated by 5 different GCMs: CCSM4 (USA) in red, GISS-E2-R (USA) in blue, IPSL-CM5A-LR (France) in green, MPI-ESM-P (Germany) in cyan, and Bcc-csm1-1 (China) in magenta. A 21-year running mean has been applied to the time series. The reference period is 1900-1970. (Data collected and processed by F. Klein).

not possible to determine which realisation is the closest to the real climate (Goosse et al., 2006b). In that sense, empirical information contained in proxy data can give an insight about the "real" evolution of climate conditions, but as they also include a component of non-climatic noise, it can be difficult to estimate the climatic signal and its causes. From this, it can be clearly deduced that very interesting insights can be obtained by combining the information available from observations and from model simulations. This is done by the means of a data assimilation method. The principle of this process is to optimise the agreement between model results and the proxy or instrumental data.

The general idea of data assimilation is to find, given a set of model variables contained in a vector x, an optimal analysis x^a for this set of variables, having a set of observed variables y^0 and a background knowledge x^b of the vector x. This last one is generally obtained using model simulations starting from a preceding analysis and run over the previous time interval (Kalnay, 2003). Mathematically, the computation of the analysis can be represented by

$$x^a = x^b + W(y^0 - H(x^b)) \tag{1.1}$$

where W is a weight matrix determined by accounting for uncertainties in model results and observations, and H is the observation operator, that performs a transformation of model results before they are compared to data. This transformation is needed because the variables y^0 and x^b are not usually obtained at the same locations, or because observations could provide a different variable than the one of the model.

This approach, consisting in integrating a model forward in time and updating periodically its solution using available observations before continuing the integration, is called sequential assimilation, also known as filter. Many data assimilation methods exist, based on different implementations to compute the analysis: nudging, Kalman filter, particle filter (Kalnay, 2003; van Leeuwen, 2009). Other techniques directly minimise a cost function, and are called variational data assimilation methods. The use of data assimilation techniques is relatively new in paleoclimate, while it is standard in meteorology for weather forecasting, to determine the initial conditions at a certain time from which the subsequent evolution of the system is deduced. Differences in the amount of data (hundreds of thousands of observations for weather forecast versus a few tens to hundreds of proxy data over the past millennium) and in the spatial and temporal resolutions (data available for weather forecast every few hours versus seasonal or annual resolution of proxy data) make it difficult to implement the standard methods applied in weather forecast over several centuries. For instance, assimilation methods are generally optimised for situations where a large set of reliable physical measurements is available, which is the case for weather forecasting or reanalysis projects, but not for paleoclimatology, where proxy data are sparse and have larger uncertainties. Also, these sophisticated methods used for weather forecasting are computationally expensive, and applying them over long time periods such as the last millennium is nearly impossible using a model with high CPU time requirement such as GCMs.

Because of these difficulties, only a few studies applying data assimilation over the last millennium have been performed (Widmann et al., 2010). The first technique proposed (von Storch et al., 2000) consisted in a nudging technique in which the atmospheric circulation is modified to remain close to a large-scale pattern reconstructed from the proxies. Later, van der Schrier and Barkmeijer (2005) proposed a more sophisticated method in which an artificial forcing is added to the model to ensure that the atmospheric circulation stays close to a reconstructed one. The approach proposed in this thesis, first presented in Goosse et al. (2006b), does not make direct use of information about the atmospheric circulation, which is only available over selected regions or

periods. This method aims at combining the results of an ensemble of climate simulations with the proxy data available at a specific time and location. It is based on a particle filter, which is one of the main ensemble methods along with the ensemble Kalman filter. A disadvantage of the latter compared to the particle filter is that the analysis is linearised and that it assumes Gaussian distributions. The particle filter does not imply a modification of the solutions provided by the model, contrary to the ensemble Kalman filter. The idea of particle filtering is to approximate the statistical behaviour of the nonlinear model by a finite ensemble of simulations, called particles, which are initialised from slightly different states. In order to sample as many realisations of internal variability as possible, a high number of ensemble members is required. The climate model used to run the ensemble of simulations must then not be too demanding in terms of computational cost. Then, at some specific time (after one year of simulation in our studies), a weight is attributed to each particle, based on its agreement with the proxy data available at that time. In our studies, the target variable is the surface air temperature. In a simple version of the particle filter, the model-data agreement is computed according to the Euclidian distance between model results and proxy data. We select, among the different realisations of model's internal variability, the one that is the closest to the climate state inferred from this data. This particle is then used as the basis for the initial condition of the new ensemble of simulations performed until the next assimilation step, and the procedure is repeated. In a more advanced version of the particle filter, the particle filtering with sequential resampling (van Leeuwen, 2009), the weight attributed to each particle is computed assuming a Gaussian likelihood. The particles are then resampled according to their weight: large-weight particles are duplicated in proportion to their weight while small-weight particles are simply eliminated. The best estimate of the state is then given by the sum of the results of each particle multiplied by the corresponding weight. A small perturbation is then added to the duplicated particles before they are again propagated forward in time by the model. More detailed explanations of these techniques are given in Chapters 2 and 4, and the reader is referred to Dubinkina et al. (2011) for a complete presentation.

An important issue about the data assimilation method is the size of the ensemble of particles. Geophysical systems such as the atmosphere or the ocean have a large number of degrees of freedom, that have to be represented by an ensemble of model simulations. Unfortunately, for high dimensional systems, the particles tend to drift apart during their evolution and, after a few data assimilation steps, none or a too limited number of ensemble members may be close to the assimilated data. Consequently, all except one particles have

weights close to zero and the filter becomes degenerated. The statistical information in the ensemble that has collapsed to a single particle could then be too low to be meaningful.

The size of the ensemble has then to be chosen carefully, so that the ensemble reproduces the observational data correctly, at a reasonable computational cost and avoiding filter degeneracy. In paleoclimatology, the fact that observations have larger uncertainties than in meteorology, and that observations are sparse and available at seasonal resolution at best, implies that a small number of the degrees of freedom of the system can be reconstructed, and there is thus a larger chance to find particles that have a good agreement with the data in a small sample (Dubinkina et al., 2011). It has been demonstrated in other studies (Dubinkina et al., 2011; Goosse et al., 2006b) that it is possible to reproduce large-scale annual mean temperature patterns over a wide region with a number of particles of the order of 100. The way the ensemble of particles is generated is also an important issue. The perturbation applied to create the ensemble must ensure a good spread of atmospheric and oceanic variables within the ensemble members. This is done by perturbing the atmospheric streamfunction in the simple data assimilation method, and the surface temperature in the more advanced technique. These techniques favour the generation of rapid perturbations in the atmospheric dynamics, but not in the ocean. Even if the second choice of perturbation ensures a better dispersion of oceanic variables than the first one, ongoing studies still focus on the way to perturb surface and subsurface oceanic variables to enlarge the range of oceanic states in the ensemble.

1.5 Contributions and outline of the thesis

The principal goal of this thesis is to study the physical processes ruling the changes of Arctic climate over the last millennium and, in particular, to separate the contribution of internal versus forced variability. In this context, a first priority is to provide estimates of past Arctic climate variations as reliable as possible. We thus aim to take advantage of the complementarity of model results and proxy data, through data assimilation. Compared to studies using only empirical information from proxy data, or relying only on a particular numerical model, our data assimilation method yields a climate reconstruction that follows the actual realisation of past climate variability as represented in proxy data, and that is consistent with basic climate physics and dynamical processes represented in the model. Some methodological issues rose throughout the evolution of this thesis and had to be tackled, moving us temporarily away from our initial goal of providing a comprehensive un-

derstanding of past Arctic climate changes.

The data assimilation method based on a particle filter has been used in this thesis in its simplified and advanced versions, and has led to one first author publication in the journal Climate of the Past (Crespin et al., 2009), four publications of which I am coauthor (Goosse et al., 2009, 2010b, 2012b; Dubinkina et al., 2011) and several other studies (Goosse et al., 2012c,a; Mairesse et al., 2013; Mathiot et al., 2013; Zunz et al., 2013). All these studies have proven that the particle filter works efficiently and provides promising results to improve our understanding of past climates. The climate model used in this context is LOVECLIM (Goosse et al., 2010a), an EMIC well suited for the requirement of the data assimilation method. Indeed, because of its coarse resolution compared to GCMs, and the simplifications applied, particularly in the atmospheric component, it is affordable to perform large ensembles of long past climate simulations. This model has demonstrated to be suitable to study past climate changes, particularly at mid- and high latitudes, and has, for instance, be involved in an intercomparison project of a group of EMICs that contributed to the 5th Assessment Report of the IPCC, Working Group 1. My contribution to this project resulted in three coauthored publications (Eby et al., 2013; Zickfeld et al., 2013; Weaver et al., 2012).

LOVECLIM reproduces correctly the major characteristics of present-day and past climates. For instance, the large-scale structure of the near-surface circulation is well reproduced. In the Northern Hemisphere, the first principal component of the geopotential height at 800 hPa in LOVECLIM is an annular mode similar to the AO (Goosse et al., 2005). The simulated geopotential height decreases as expected with latitudes, and presents local minima in the North Altantic and the North Pacific. Compared to observations, the simulated winds are weaker in both hemispheres, except for the Aleutian low, because the model underestimates the gradients of geopotential height. The direction of the winds east of Greenland are also wrong, because the simulated geopotential height minimum is located too far eastwards, over Baffin Bay instead of Iceland (Goosse et al., 2010a). It is important to keep in mind when interpreting our results that LOVECLIM's representation of atmospheric dynamics is simpler than in complex GCMs, and the interpretation of dynamical processes have then to be taken with caution. For instance, our model does not include an interactive representation of stratospheric dynamics, and this may explain the small magnitude of the simulated changes in the NAO/AO in response to changes in external forcings. Indeed, changes in solar irradiance, for example, can lead to modifications in the stratosphere that influence in turn the atmospheric circulation. In LOVECLIM, changes in atmospheric cir-

culation due to changes in solar irradiance are related to different processes: for instance, a warming at high latitudes due to forcing changes leads to a decrease of geopotential height at 800 hPa, and thus to stronger winds at mid-latitudes (positive NAO/AO index). Additionally, the model formulation leads to strong biases that cannot be reduced without affecting the main advantages of LOVECLIM. The most significant biases occur at low latitudes. Indeed, the temperature is overestimated and the atmospheric circulation is too weak in the subtropics. Furthermore, the model does not reproduce some dominant modes of variability in these regions, like ENSO. The land surface model in LOVECLIM is also rather simple compared to GCMs and the land use changes must be applied in LOVECLIM only through a reduction in the area covered by trees and an increase in grassland. The vegetation changes affect the land-surface albedo and surface evaporation.

The present thesis consists of four studies, each of them presented in a different chapter, two of them in their original peer-reviewed journal publication versions. In Chapter 2, we present the results obtained using the simple particle filter over the last millennium with the model LOVECLIM constrained by the proxy-based reconstructions of local temperature of Mann et al. (2008). Our analysis focuses on a substantial warm event that occurred in the Arctic during the period 1470-1520, with the objective to propose an hypothesis for the mechanisms that were dominant at that time. In this case, internal variability of the system seems to be the responsible for the changes in atmospheric circulation that leads to the warming. This chapter has been published in Climate of the Past (Crespin et al., 2009).

Following this study of the Arctic climate variability, we focus on the analysis of the responses to external forcings taken individually, on an annual and seasonal point of view. Chapter 3 takes advantage of about fifty simulations that were run with LOVECLIM in the context of PMIP3 by A. Mairesse, without data assimilation. The new forcing reconstructions proposed by PIMP3 were used individually to drive an ensemble of simulations. We then examine the contribution of each individual forcing to the large seasonal contrast in temperature changes observed during the last millennium. The main factor responsible for the seasonal differences in those experiments is the astronomical forcing, and more surprisingly, we conclude that the response to land use changes has a significant impact on the Arctic temperature, even though those changes are localised at lower latitudes. In parallel, the results obtained in this chapter provide an important conclusion concerning the interpretation of proxy-based reconstructions used in other studies. Our results highlight the importance of a correct estimation of the season represented in proxy data, in

order to avoid a significant bias in their calibration against a much different annual or seasonal mean temperature. This study has been published in the journal The Holocene (Crespin et al., 2012).

Chapter 2 has put in evidence the skills and weaknesses of the data assimilation technique and demonstrates that several improvements were possible. The following Chapters 4 and 5 revisit the method and contribute to the development of a more advanced version of the particle filter. The most important improvements of this new method are a better use of the information available within the ensemble and the inclusion of the uncertainties of proxy-based reconstructions in the data assimilation process. More specifically, Chapter 4 deals with the reconstruction of the North Atlantic meridional overturning circulation (MOC). A study of the MOC is justified by the very important role it plays in the Northern Hemisphere climate, particularly in the North Atlantic and Arctic regions. The formation of North Atlantic deep waters takes place in the high latitudes of the North Atlantic Ocean leading to a southward deep current of cold water. Any change in the climate conditions of those regions can influence the behaviour of the MOC, by modifying the density of water at the surface of the deep convection zones. In turn, a change in the intensity of the MOC can substantially influence the climate of the Northern Hemisphere, following modifications of the northward ocean heat transport. For these reasons, the knowledge of recent variations of the MOC intensity, which are still very uncertain because of the lack of direct observations, has to be improved. In this context, sophisticated methods using complex models and a large quantity of surface and subsurface oceanic data have been used, but have the disadvantage to provide reconstructions that can only be obtained over the last few decades (e.g. Wunsch and Heimbach, 2006; Stammer et al., 2002; Balmaseda et al., 2007). The goal of this study presented in Chapter 4 is to test a new methodology that enables the reconstruction of the MOC evolution over time periods such as the last century or the last millennium, using the data assimilation method and only the little amount of data available over these periods, that is, data of surface temperature and pressure. The results obtained using twin experiments turn out to be more satisfying when the data of temperature are used to constrain the model rather than the pressure data. We then propose a reconstruction of the MOC evolution for the past 155 years, based on instrumental data of surface temperature. Unfortunately, the diversity of reconstructions of the MOC presented in other studies prevents us to give more precisions about the validity of our method.

In Chapter 5, we conduct experiments applying the advanced particle filter, hoping to obtain a robust reconstruction of Arctic climate over the last millen-

nium. To increase the spatial distribution of proxy data in the region, a new set of proxies provided by PAGES2k has been utilized in addition to those already used in Chapter 2. Those new proxies were furnished without being processed. So, a first step of this study consisted in their selection and calibration against temperature observations. During this process, we became aware of the impact of the calibration method used to reconstruct past temperatures on the results of our simulations with data assimilation. The magnitude of the reconstructed variability has to be high enough to be correctly assimilated, in order to include the right amplitude of the climatic signal during the assimilation procedure. Besides, because of the uncertainty in proxy data, linked to the non-climatic noise recorded by the proxies (a residual variance uncorrelated with the true state of the climate), the total variance is overestimated by the proxy-based reconstruction, but this can be taken into account by the assimilation process. The best simulation obtained shows good correlations with proxy data at the exact location where those data are available, but is not able to follow the signal where no proxy exists. This is probably due to the small number of proxies available and to inconsistencies between proxy series. We conclude on the necessity to apply a spatial filter to the proxy-based reconstructions before the assimilation process to obtain coherent spatial patterns of anomalies that could be reproduced by the model.

In Chapter 6, we finally conclude the thesis with a summary of the most important findings and perspectives.

CHAPTER 2

THE 15TH CENTURY ARCTIC WARMING

This Chapter is based on the following paper: Crespin, E., Goosse, H., Fichefet, T., Mann, M. E., 2009. The 15th century Arctic warming in coupled model simulations with data assimilation. Climate of the Past 5, 389–401.

Abstract

An ensemble of simulations of the climate of the past millennium conducted with a three-dimensional climate model of intermediate complexity are constrained to follow temperature histories obtained from a recent compilation of well-calibrated surface temperature proxies using a simple data assimilation technique. Those simulations provide a reconstruction of the climate of the Arctic that is compatible with the model physics, the forcing applied and the proxy records. Available observational data, proxy-based reconstructions and our model results suggest that the Arctic climate is characterized by substantial variations in surface temperature over the past millennium. Though the most recent decades are likely to be the warmest of the past millennium, we find evidence for substantial past warming episodes in the Arctic. In partic-

ular, our model reconstructions show a prominent warm event during the period 1470-1520. This warm period is likely related to the internal variability of the climate system, that is the variability present in the absence of any change in external forcing. We examine the roles of competing mechanisms that could potentially produce this anomaly. This study leads us to conclude that changes in atmospheric circulation, through enhanced southwesterly winds towards northern Europe, Siberia and Canada, are likely the main cause of the late 15th/early 16th century Arctic warming.

2.1 Introduction

Studies of the Arctic climate indicate a considerable warming in this region in recent decades. For the past 100 years, the Arctic has warmed twice as much as the global average (Trenberth et al., 2007). This warming has been associated with a substantial diminution of sea ice thickness (Serreze et al., 2000) and extent (Meier et al., 2005).

While recent Arctic warmth appears anomalous, observational and proxy data indicate substantial long-term temperature variability in the region. A multidecadal interval of relative warmth, for example, can be found during the early 20th century, between the 1920s and 1940s, when conditions were only slightly less warm than today (Johannessen et al., 2004). While instrumental temperature data are relatively sparse during the first half of the last century, the early 20th century Arctic warm period appears to have been characterized by a large-scale spatial pattern different from the current warm period. The early 20th century warming was largely confined to the Arctic alone (i.e. the region north of 60°N), while the recent warming has been more widespread, with a pronounced warming in the Eurasian mid-latitudes (Kuzmina et al., 2008; Trenberth et al., 2007; Johannessen et al., 2004; Overland et al., 2004).

The dynamical processes underlying those two Arctic warm periods are also likely different. For the most recent decades, it is almost certain that the anthropogenic greenhouse gas forcing has dominated over the contribution from internal variability (defined here as the variability related to the internal dynamics of the climate system, i.e. that would be present in the absence of any change in natural or anthropogenic forcing) (Johannessen et al., 2004), though the extent of the role played by natural multidecadal variability has not yet been entirely resolved (Polyakov and Johnson, 2000). By contrast, during the early 20th century when anthropogenic forcing was considerably weaker than today, the observed Arctic warming was likely due, at least in substantial part, to the natural variability of the climate system. The natural external forcing

resulting from solar irradiance variations and volcanic eruptions could have played some role in this early warming, but the precise role is difficult to assess due to the uncertainties in the forcings. It has been proposed that the early 20th century warming was caused by increased southwesterly winds and oceanic heat transport into the Barents Sea region (Bengtsson et al., 2004; Overland et al., 2004; Rogers, 1985). There is evidence that these changes were, in turn, associated with purely internal, multidecadal oscillatory variability of the climate system (Bengtsson et al., 2004; Johannessen et al., 2004; Overland et al., 2004; Delworth and Mann, 2000; Delworth and Knutson, 2000; Przybylak, 2000; Mann and Park, 1994).

The absence of widespread direct instrumental data before the mid-19th century at high latitudes (though there are sparse records reaching back to the late 18th century (e.g. Moberg et al., 2003; Vinther et al., 2006)) requires the use of climate "proxies", such as tree rings, ice cores, lake sediments and historical documents, from which we can infer some key characteristics of climate changes in past centuries. Such compilations for high northern latitudes (e.g. Jiang et al., 2005; Jennings and Weiner, 1996; Massé et al., 2008; D'Arrigo and Jacoby, 1993; Jacoby and D'Arrigo, 1989; Overpeck et al., 1997; Ogilvie and Jónsson, 2001) suggest that similar Arctic warm events may have occurred in past centuries. In this study, we focus on the evidence and dynamical explanations for any such extended periods of Arctic warmth during the past millennium. Proxy reconstructions of global or hemispheric mean surface temperature (e.g. Mann et al., 1999; Briffa et al., 2001; Jones et al., 2001; Esper et al., 2002; Mann and Jones, 2003; Jones and Mann, 2004; Mann et al., 2005b; Jansen et al., 2007; Mann et al., 2008) reveal the existence of a period of modest large-scale warmth covering the 10th to 12th centuries, though it does not rival current warmth. This so-called "Medieval Warm Period" is followed by a period of relative large-scale coolness over the 15th-19th centuries known as the "Little Ice Age". At the hemispheric or global scale, these temperature changes are largely consistent with the response of the climate system to external changes over the past millennium in natural (and after the 19th century, anthropogenic) radiative forcing (e.g. Crowley, 2000). At regional or local scales, however, the influence of the forced response of the climate may be overwhelmed by the contribution of internal climate dynamical processes (Goosse et al., 2005).

In this study, we seek, as in previous studies (e.g. Goosse et al., 2008), to merge the observational information contained in available proxy records with the physical and dynamical constraints present in forced climate model simulations to interpret past climate changes. Our focus is on using such analyses

to interpret the impacts of large-scale dynamics, as well as radiative forcing changes, on the inferred pattern of past regional temperature changes.

We employed LOVECLIM1.1 (Goosse et al., 2007) for our model simulations. A set of five different experiments covering the past millennium were run with data assimilation. More specifically, the evolution of the model was constrained by selecting, among all available realisations, the realisation of the internal variability that most closely matches the information from the proxies. Those estimates of past climate changes based on model simulations using data assimilation will be referred to as "reconstructions", even though the methodology used in this framework differs from the more traditional, statistically-based approach to reconstructing climate over the past millennium. The model simulations allow us to advance hypotheses about the mechanisms associated with any particular interval of Arctic regional warming. We performed a parallel ensemble of simulations without data assimilation. The ensemble mean in the latter case can be used to define the response of the system to the external forcing alone, since the influence of the natural internal variability, which differs from one realisation to another, is heavily damped by the averaging process. Comparisons between these two parallel sets of experiments allow us to isolate the relative contributions of both external forcing and internal variability.

We first describe the model and experimental design, the forcings applied and the data assimilation technique. The assimilated proxy records are taken from a recent compilation (Mann et al., 2008) of a large network of high-resolution (that is, decadally or annually-resolved) climate proxy data. Our focus is on a particularly warm event taking place during the period 1470-1520 that is evident in the proxy data. Using the model data assimilation experiments, we analyse the role of various physical and dynamical processes that appear responsible for the pattern of the observed Arctic warmth, and demonstrate that this pattern likely arises from dynamical variability.

2.2 Model description and experimental design

The different simulations examined in this study were performed with LOVECLIM1.1 (Driesschaert et al., 2007; Goosse et al., 2007), a three-dimensional climate model of intermediate complexity which includes representations of the atmosphere, the ocean and sea ice, the terrestrial biosphere, the oceanic carbon cycle and the polar ice sheets. As the last two components were not activated in this study, they will not be described here. The atmospheric component of LOVECLIM is ECBILT2 (Opsteegh et al., 1998), a quasi-geostrophic

model of horizontal resolution T21 and three vertical levels, with simple parameterisations for the diabatic heating due to radiative fluxes, the release of latent heat, and the exchanges of sensible heat with the surface. The oceanic component is CLIO3 (Goosse and Fichefet, 1999). This model is made up of a primitive-equation, free-surface ocean general circulation model coupled to a thermodynamic-dynamic sea-ice model. Its horizontal resolution is 3° in longitude and latitude, and there are 20 unevenly spaced vertical levels in the ocean. The terrestrial vegetation module VECODE (Brovkin et al., 2002) computes annually the evolution of trees, grass and deserts. It has the same resolution as ECBILT. More information about the model can be obtained at: http://www.astr.ucl.ac.be/index.php?page=LOVECLIM%40Description.

All the simulations were driven by the same forcings. The model includes three natural forcings, namely the changes in the Earth's orbital parameters, the volcanic activity and the variations in solar irradiance, as well as three anthropogenic forcings, i.e., the changes in greenhouse gas concentrations, including tropospheric ozone, the variations in sulphate aerosol loading, and the forcing due to changes in land-use. The temporal evolution of some of these forcings is shown in Fig. 2.1. The variations of the Earth's orbital parameters follow Berger (1978). The effect of volcanism is derived from Crowley (2000) and is included through changes in solar irradiance. The evolution of solar irradiance follows the reconstruction of Muscheler et al. (2007). The total solar irradiance changes have been scaled to provide an increase of 1 Wm^{-2} between the Maunder minimum and the late 20th century. The evolution of greenhouse gas concentrations is based on a compilation of ice cores measurements (J. Flueckiger, pers. comm., 2004). The influence of anthropogenic sulphate aerosols is taken into account through a modification of surface albedo (Charlson et al., 1991). The changes in land-use are based on Ramankutty and Foley (1999) and are applied in the model through a reduction in the area covered by trees and an increase in grassland as VECODE does not include a specific vegetation type corresponding to cropland.

The goal of this study is to obtain a simulation of the Arctic climate for the last millennium that is not only consistent with our model and the forcings applied, but also with the data available for that period. For that purpose, we constrain the model results using the recent compilation of well-calibrated surface temperature proxy records of Mann et al. (2008) and a new version (see Goosse et al., 2009) of the data assimilation technique described in Goosse et al. (2006b). We proceed in the following manner: we start the simulation at the year 1000, from a condition obtained from a long simulation covering the whole Holocene (Goosse et al., 2007). By introducing small perturbations in

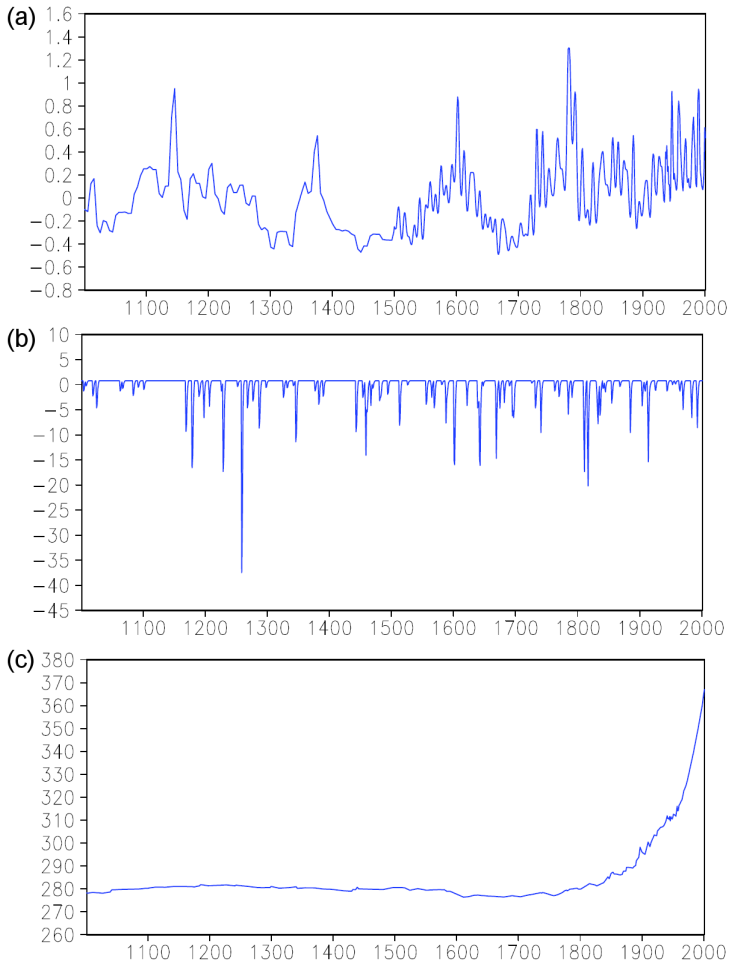

Figure 2.1: (a) Global mean radiative forcing (Wm^{-2}) used to drive LOVECLIM simulations for the last 1000 years associated to variations in the total solar irradiance based on Muscheler et al. (2007). (b) Radiative forcing (Wm^{-2}) associated to volcanic activity according to Crowley (2000) for the region including latitudes from 35°N to 90°N, incorporated in LOVECLIM through a modification in the solar irradiance. (c) Time series of CO_2 concentrations ($ppmv$).

the atmospheric streamfunction, we generate an ensemble of 96 simulations for a short period of time (1, 5, 10 or 20 years). We choose the number of ensemble members for technical reasons: we want around a hundred simulations in order to have enough realisations of the internal variability of the

system, and it is easier to run 96 simulations in parallel (3 groups of 32 simulations, each of them on 32 CPUs of a cluster). Then, we select among those 96 representations of the model internal variability the one that is the closest to the proxy records available for the period of time investigated. This is achieved by using the following cost function:

$$CF_k(t) = \sqrt{\sum_{i=1}^{n} w_i (F_{obs_i}(t) - F^k_{mod_i}(t))^2} \tag{2.1}$$

$CF_k(t)$ is the value of the cost function for each member k of the ensemble for a particular period t. n is the number of proxies used in the model/data comparison. $F_{obs}(t)$ is the value of the variable F (the surface temperature in this case) in the proxy records at the location where they are available, and $F^k_{mod}(t)$ is the value of the same variable simulated by the model in the simulation k at the same location as the proxy record. w_i is a weight factor. The experiment k which minimizes the cost function $CF_k(t)$ is selected for that particular period of time, and the end of this simulation is used as the basis for the initial condition of the new ensemble of simulations performed over the next period. The procedure follows in the same way for the whole millennium. As this method requires a large number of simulations, LOVECLIM coarse resolution and low computer-time requirements are appropriate.

A set of 56 annual or decadally-resolved proxy series (or regional composites thereof) screened for a local temperature signal (Mann et al., 2008) is used to constrain the model. The proxy data set is derived largely from tree-rings, ice cores, some lake sediments and historical documents. The screening procedure retains only those proxy data exhibiting a statistically significant correlation with local (5 degree latitude x longitude) gridbox instrumental surface temperature data (Brohan et al., 2006) during the calibration interval (1850-1995). When proxy records reflect temperature variations at sub-annual resolution, they are averaged to obtain annual mean values. All proxy records available over a gridbox region are averaged to produce a regional gridbox composite. The proxy gridbox series are then decadally-smoothed using a low pass filter, and averaged and scaled to the same mean and decadal standard deviation as the associated instrumental gridbox temperature series over the calibration period. For the purpose of the ensuing analysis, we have kept only those records available back to the year 1400, and which extend through 1995. The proxy data are primarily terrestrial, and cover tropical, extratropical, and polar regions, though the greatest coverage is provided northward of 30°N. The locations of the proxy gridbox series available in the Arctic region over the time interval of our analysis are shown in Fig. 2.3. The available data sam-

ple Scandinavia, Siberia and western North America, while there is a dearth of coverage in certain regions such as eastern North America.

We present in this paper the results obtained from 5 different numerical experiments using data assimilation. They start from the same initial conditions, but use different approaches to placing constraints on the model and different periods of time in the computation of the cost function. In the first experiment, the weight factors w_i are the same for all the proxy records and the cost function is evaluated for 1-year averages. In the other four simulations, in order to give a larger weight to proxies which are more reliable, the value of the weight factors w_i is proportional to the correlation between the proxy records and the observations of temperature obtained during the instrumental period. In these 4 experiments, the averaging period in the computation of the cost function is set to 1, 5, 10 and 20 years, in order to test if this has an impact on our results. For instance, for 20-year mean, processes responsible for interannual variability may be filtered, while they can play an important role in the selection of the best experiment when 1-year mean are analysed. These different experiments allow us to test the robustness of our results, by assuring that we obtain similar and internally consistent results regardless of the precise method by which we constrain the model evolution to be consistent with the proxy data. The ensemble mean over the 5 experiments provides a better estimate of the true climatic variability by averaging out the 'noise', while the within-ensemble variance provides an appropriate estimate of the component of uncertainty associated with the sensitivity to the precise constraint method used.

In addition, an ensemble of 10 simulations was performed without data assimilation. This ensemble was run with the same model and the same forcings used in the simulations with data assimilation, but with slightly different initial conditions used for each ensemble member. The ensemble mean allows us to diagnose the response of the system only to the external forcings, and by comparing it with the experiments with data assimilation, we can attempt to separate the relative roles of internal variability and external forcing in the observed climate history.

2.3 Validation of the assimilation method using modern observations

In order to test the ability of the model to follow true, observed changes when using the method described in Section 2.2, a validation exercise was

performed in which we assimilated HadCRUT3 annual surface temperature observations (Brohan et al., 2006) between years 1850 and 2000. In the first experiment, we constrained the model with observed temperatures over the region located northward of 30°N. We divided this region into six boxes: Atlantic, Pacific, Europe, Asia, America and Arctic. The average surface temperature over each box was computed for both the observational data and the model results, using only those locations where observations are available, and the cost function was then evaluated using these six averages. This approach insures that each region has the same weight, even if one region has less data than another (this approach is similar to that used for examining surface temperatures in the Southern Hemisphere by Goosse et al. (2009)). In a second experiment, we constrained the model using only the instrumental surface temperature observations at gridboxes where proxy data are available. This exercise was used to establish whether the model can successfully reproduce a coherent evolution of the surface temperature field when constrained only with relatively sparse data, as it is the case when using proxy networks such as that used in our current study.

Figure 2.2 shows the results from these model simulations. Each experiment was conducted twice, using an averaging period of 1 and 5 years, respectively, for the computation of the cost function. The agreement between the simulated surface temperatures and observations in the Arctic (region northward of 64°N) is reasonably good for the 20th century. The experiments performed with the complete HadCRUT3 data set (dark and light blue curves) are very close to the observations (red curve). Likewise, the experiments using the sparser "proxy site" observations (dark and light green curves), are also in good agreement with the observations. While the sparseness of the available proxy data is a primary limiting factor with the technique used in this study, we nevertheless find that the model yields satisfactory results for the Arctic, even when constrained by relatively sparse observations at high latitudes (23 series north of 55°N in this case).

2.4 Comparison of model results with proxy data

Before analysing the climate evolution obtained in our simulations over the past millennium, we sought to establish the robustness of the technique of data assimilation and the quality of model results by comparing them with the proxy records used to constrain the model. The comparison between the annual mean surface temperature anomaly pattern directly indicated by the proxies and the model simulation (we have retained only those model locations where proxy information is available) is shown in Fig. 2.3. We chose

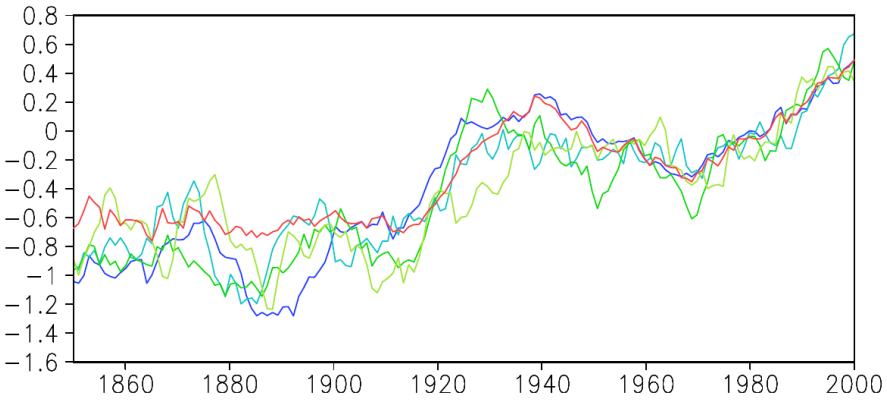

Figure 2.2: Anomaly in annual mean surface temperature (°C) in the Arctic over the last 150 years. The red line is the HadCRUT3 data set (Brohan et al., 2006). The dark and light blue lines are the results from model simulations using the complete HadCRUT3 data set to constrain the model, for the cost function evaluated for 1 and 5 years averages respectively. The dark and light green lines are the results from model simulations constrained by data from HadCRUT3 only at the locations where proxies are available, for the cost function evaluated for 1 and 5 years averages respectively. An 11-year running mean has been applied to the time series. The reference period is 1960-2000.

to examine a representative set of warm and cold periods, averaged over 50 years, which take place during years 1470-1520 and 1600-1650, respectively. In general, the spatial pattern of surface temperature simulated in the model is reasonably close to the proxy data, although some substantial local differences can be observed, for example over the North American region. Possible explanations for these local discrepancies are that (i) the proxies contain sizeable non-climatic sources of noise or bias which are not correlated over local scales, and that (ii) the model may be deficient in representing the variability at such scales (i.e. one model gridbox). Both factors could lead to substantial local differences between model results and the proxy observations. On the other hand, as shown in Fig. 2.4, the model results exhibit a better agreement with proxy records at regional scales. The temporal evolution of surface temperature averaged over three representative regions where proxies are available (boxes in Fig. 2.3a define these different regions), indicates good agreement between the surface temperature computed in each one of the 5 model simulations and the proxy-based reconstruction. For the average over each region, we measure the misfit between model results (mean of the 5 experiments) and proxy series by calculating the root mean-square error (RMSE) for the period 1400-1995. In the first (RMSE = 0.08) and second (RMSE = 0.1)

regions, all simulations are in good agreement with the proxy records. The third region (RMSE = 0.21) presents good results as well, although some discrepancies with proxy data and a larger variance between model simulations is observed. For instance, the amplitude of the early 17th century cooling in that region is larger in the proxies than in the different model simulations, and this minimum is shifted.

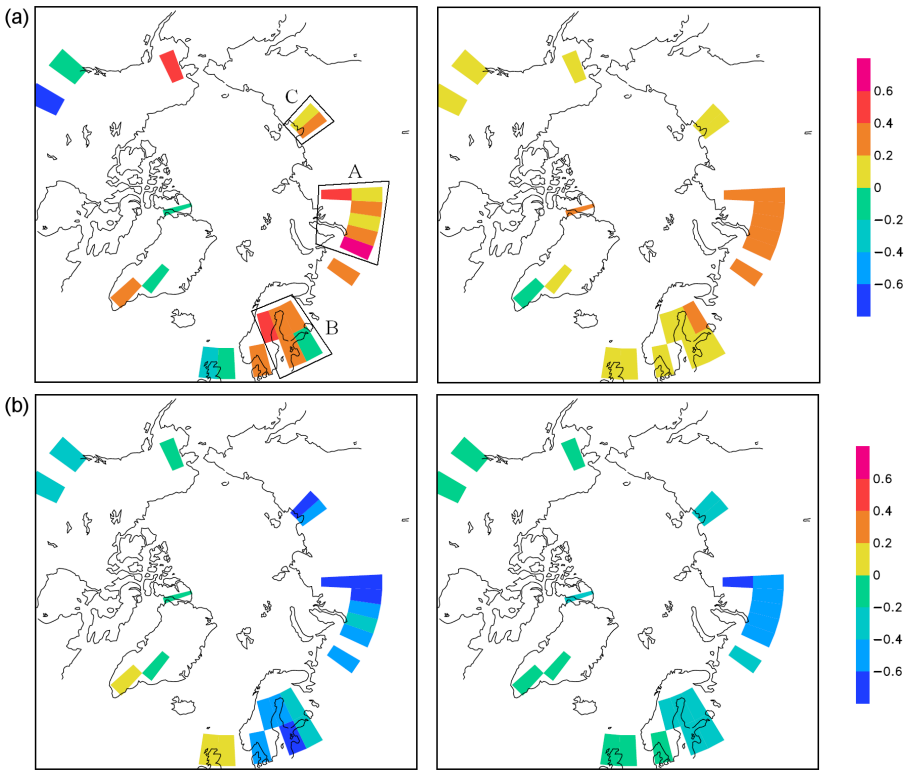

Figure 2.3: Anomaly in annual mean surface temperature (°C) during a warm and a cold period in the proxy data (left column) and the model results averaged over the 5 simulations (right column). The model results are shown only at the locations where the proxies are available. (a) 1470-1520 and (b) 1600-1650. The reference period is 1600-1950. The boxes in (a) correspond to the regions over which averages are performed to obtain the time series shown in Fig. 2.4.

In Fig. 2.4d, we compare the annual mean surface temperature averaged over the whole Arctic obtained in the different simulations with the high-

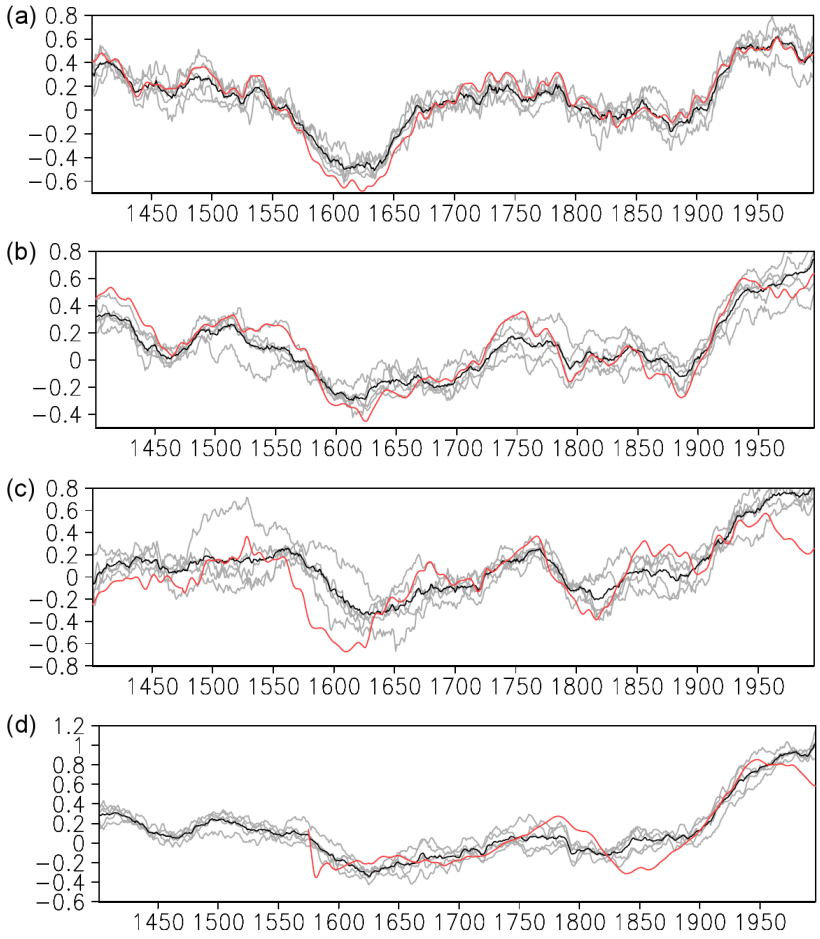

Figure 2.4: (a) Time series of the anomaly in annual mean surface temperature (°C) over the last 600 years for the region in the box A in Fig. 2.3. The black line is the mean over the 5 model simulations, the red line is the average over the 6 proxy data contained in box A in Fig. 2.3, and the grey lines are the results of the 5 different model simulations. (b) Same as a) for the mean over box B in Fig. 2.3 (5 proxies). (c) Same as a) for the mean over box C in Fig. 2.3 (2 proxies). (d) Anomaly of annual mean surface temperature in the Arctic for the last 600 years. The Arctic area corresponds to the mean over all longitudes between 64°N and 80°N. The red curve is the reconstruction of Overpeck et al. (1997). A 51-year running mean has been applied to all time series. The reference period is 1600-1950.

latitude summer-weighted annual temperature reconstruction of Overpeck et al. (1997). It is worth mentioning that this reconstruction is not totally independent from ours, since some of their proxies are also included in this study. The "Little Ice Age" and subsequent warming recorded by this compilation are reproduced in the model simulations. The agreement between model and proxy data is quite good overall, though the mid-19th century is colder in the Overpeck et al. (1997) reconstruction than in our model. The model also tends to simulate slightly too high temperatures at the end of the 20th century.

2.5 The 1470-1520 warm period

The annual mean surface temperature in the Arctic in the 5 simulations including data assimilation (Fig. 2.5a, blue curve) shows the relative warmth during the first five centuries that is evident in hemispheric climate reconstructions (e.g. Jansen et al., 2007; Mann et al., 2008). The mean surface temperature northward of 64°N during the 12th century is about $0.2^{\circ}C$ warmer than over the reference period 1600-1950. The cooling that follows, starting at the beginning of the 13th century, is interrupted by some warming periods. Two important peaks of temperature are observed during the periods 1400-1450 and 1470-1520. They correspond to the warmest periods of the last millennium before the industrial period for the mean over the 5 experiments, i.e. that, in our simulations, they are warmer than the so-called "Medieval Warm Period" in the Arctic. The "Little Ice Age" then follows, with relatively cool temperatures during the 16th, 17th and 19th centuries. From the beginning of the 20th century to the present, there was an abrupt increasing trend in surface temperature, associated with anthropogenic forcing.

As an expected result of the data assimilation method, from the 14th century onwards, the mean over the Arctic of the proxy data used to constrain the model (Fig. 2.5b, red curve) exhibits almost the same temperature evolution than the mean of the model results taken only at the locations where the proxies are available (Fig. 2.5b, black curve). In particular, we observe in the proxy series the two maxima of temperature during the years 1400-1450 and 1470-1520. Their presence in our simulation with data assimilation is thus clearly related to the signal recorded by the proxies. For the first 4 centuries, the model is less constrained by the proxies, the number of proxies available during this period being probably too small in the Arctic region. The largest discrepancy is observed at the end of the 12th century where proxies recorded a clear cooling.

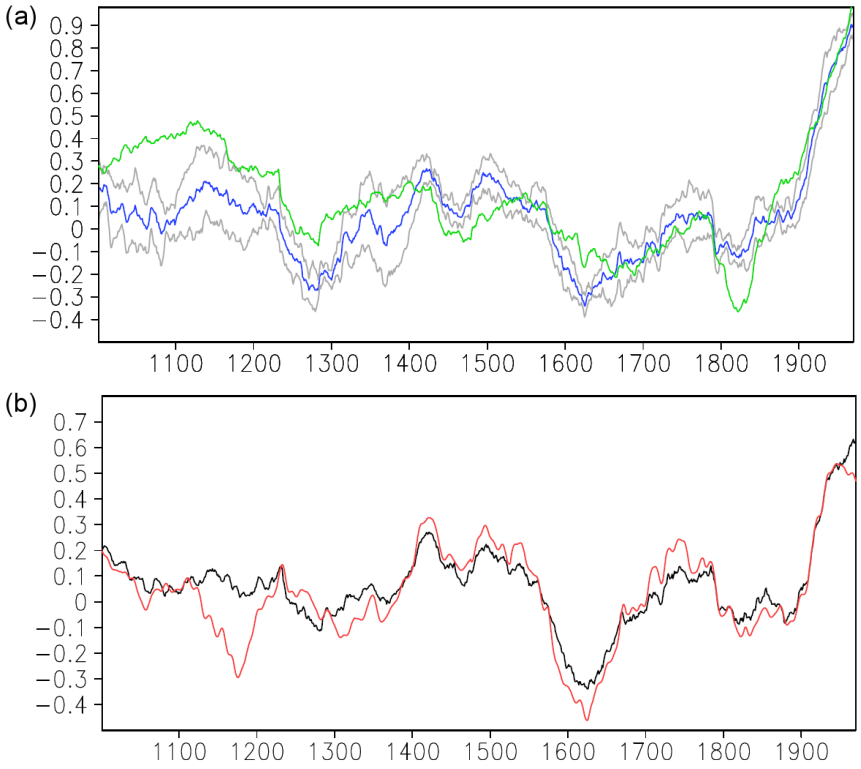

Figure 2.5: Anomaly in annual mean surface temperature (°C) in the Arctic over the past millennium. (a) The blue line is the average over the 5 model simulations performed with data assimilation, and the grey lines are the mean plus and minus one standard deviation of the ensemble. The green curve is the mean of an ensemble of 10 simulations made without data assimilation. (b) The red line corresponds to the average of the proxy series used to constrain the model over the Arctic. The black line represents the mean of the 5 model simulations with data assimilation averaged over the grid points where proxies are available. A 51-year running mean has been applied to the time series. The reference period is 1600-1950.

The scatter between the 5 experiments with data assimilation (Fig. 2.5a, grey curves) is measured by the standard deviation of the 5 members. During the first 4 centuries of the last millennium, a fewer number of proxies is available. The variance between the different model simulations is thus larger than for the next centuries. The low standard deviation observed for the 15th century period (standard deviation = 0.06°C) indicates a good agreement between

model results.

To interpret the simulated temperature changes, we compare our experiments with data assimilation with those without data assimilation (forced response). The peak medieval Arctic warmth is greater in the simulations without data assimilation (Fig. 2.5a, green curve). Averaged over the years 1100 to 1150, the temperature is almost $0.5^{\circ}C$ higher than the mean over the reference period in the forced response. The millennial-scale cooling trend (approximately half a degree over the millennium) is thus more pronounced in the forced response than in the simulations with data assimilation. Several causes might be responsible for this discrepancy. The forcing used in the model (and thus the forced response) is uncertain and prone to potential systematic error (e.g. Jones and Mann, 2004). Internal variability of the system at any low-frequency may induce a cooling in the Arctic, counterbalancing the effect of the forcing. On the other hand, there are uncertainties in the proxy temperature reconstructions themselves, which become increasingly substantial in the earlier centuries of the past millennium (Mann et al., 2008) and the number of proxies available for the data assimilation is low during the first 4 centuries. Although this difference between the simulations with data assimilation and without is intriguing, we will thus focus in this study on a period for which we have more data and thus likely more robust results: the period 1470-1520, corresponding to warmest period of the millennium before the 20th century.

The first maximum of temperature observed during the period 1400-1450 appears consistent with the forcing: it has low volcanic activity and is preceded by a maximum of the solar forcing ($0.5\ Wm^{-2}$) (see Fig. 2.1). By contrast, the second maximum of temperature taking place during the period 1470-1520 is less clear in the forced response of the model. It is possible that the response of the model to the external forcings is actually not correct and that the data assimilation technique takes charge to head the system in the good direction. For instance, the response of the atmospheric circulation to external forcings, such as solar and volcanic forcings, is weak in LOVECLIM (Goosse and Renssen, 2004), while it has been suggested that the Arctic Oscillation/North Atlantic Oscillation (e.g. Shindell et al., 2001) and El Niño-Southern Oscillation (Mann et al., 2005a) response to external radiative forcings has a strong impact on past regional climatic changes. However, the period 1470-1520 corresponds to a minimum ($-0.3\ Wm^{-2}$) in the solar forcing which would rather lead to a cooling over large parts of the Arctic, even if the dynamical response is taken into account (Shindell et al., 2001), and it does not include any explosive volcanic events (Fig. 2.1). It is thus difficult to envision a substantial role for external forcings. It appears considerably more likely that this event arises

simply as a realisation of the internal variability of the system.

In order to find the causes of the changes in temperature during the period 1470-1520 simulated by our model including data assimilation, we analyse the anomalies in atmospheric and oceanic heat transports, an information not available from proxy records. The mean of the 5 model simulations performed with data assimilation is used in the following patterns.

The simulated spatial distribution of annual surface temperature anomaly for the warm period averaged over the years 1470 to 1520 (Fig. 2.6), shows an overall warming over the Arctic region. The few proxy records available in this region (23 proxy series north of 55°N) for that period are in good agreement with the model results (Fig 2.3a). This pattern is robust in our model as each individual simulation gives similar ones (not shown). The largest warming is observed in the Canadian Archipelago and Eurasian Arctic, with the maximum in the Barents Sea, whose temperature is almost $0.6°C$ higher than in the reference period.

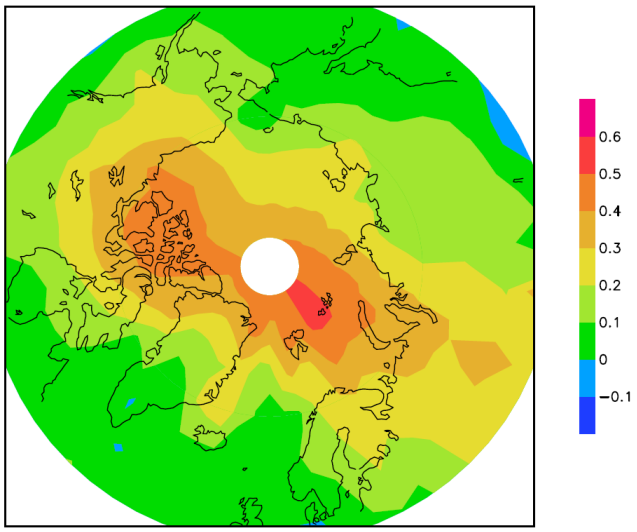

Figure 2.6: Anomaly in annual mean surface temperature (°C) over the 1470-1520 warm period for the model results averaged over the 5 simulations with data assimilation. The reference period is 1600-1950.

The pattern of the annual mean anomaly of the geopotential at 800 hPa, averaged over the period 1470-1520 (Fig. 2.7), is consistent with the particu-

larly warm conditions of that period. The negative anomaly west of Iceland produces an increased inflow of warm air coming from the south, leading to the warming over northern Europe, the Barents Sea and the western Siberian region. Similarly, the negative anomaly centered over the Bering Strait induces a warming over Canada. By contrast, in regions characterized by winds anomaly coming from the north, such as the Baffin Bay and the eastern Siberia, the temperature anomaly is weak and even negative in some regions. The geopotential anomaly corresponds thus to the right combination of anomalies in both the Atlantic and Pacific sectors that leads to a warming of nearly all regions in the Arctic and a clear signal on the regional mean shown in Fig. 2.6.

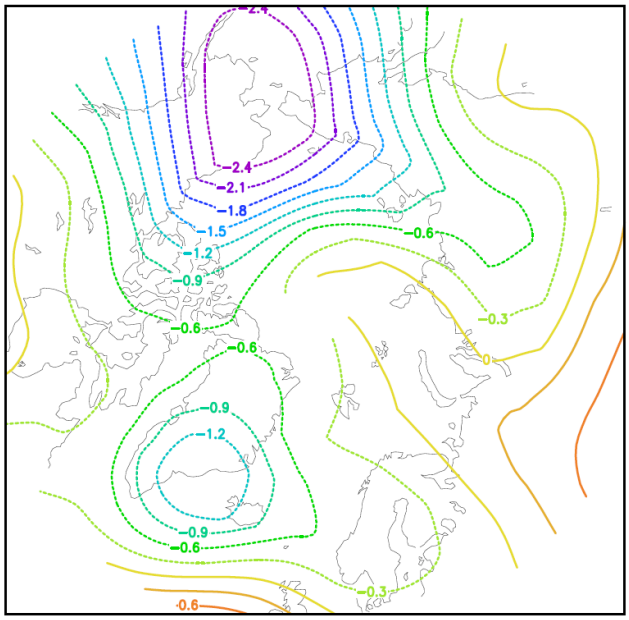

Figure 2.7: Anomaly in annual mean 800 *hPa* geopotential height (*m*) over the 1470-1520 warm period for the model results averaged over the 5 simulations with data assimilation. The reference period is 1600-1950.

The pattern of surface temperature anomaly in the simulation performed without data assimilation for the period of interest 1470-1520 (not shown) is not at all similar to the one observed in the simulation with data assimilation. A weak cooling (up to $-0.1°C$ relative to the reference period) is even observed over large areas in North America and Siberia. The pattern of anomaly of the 800 *hPa* geopotential height is neither similar. This clearly shows that, if

not helping the model through constraining internal variability in the simulations, the external forcings are not able to induce a large-scale warming as described in the proxies (Fig 2.3a) and thus the role of these external forcings in our model is weak.

The behaviour of the sea ice is consistent with the evolution of the surface temperature. For the whole Arctic, we notice a decrease of approximatively 2% in sea ice area and 6% in sea ice volume between the periods 1250-1300 and 1470-1520. The decrease in annual mean sea ice concentration is the largest in the Eurasian Arctic and the North of Canada, while a small increase is seen in Chukchi Sea (Fig. 2.8) compared to the reference period. A minimum in sea ice concentration anomaly is seen in the Barents Sea, with a decrease of almost 3% averaged over the whole period (this is mainly a winter signal, since there is no sea ice in that region during the summer).

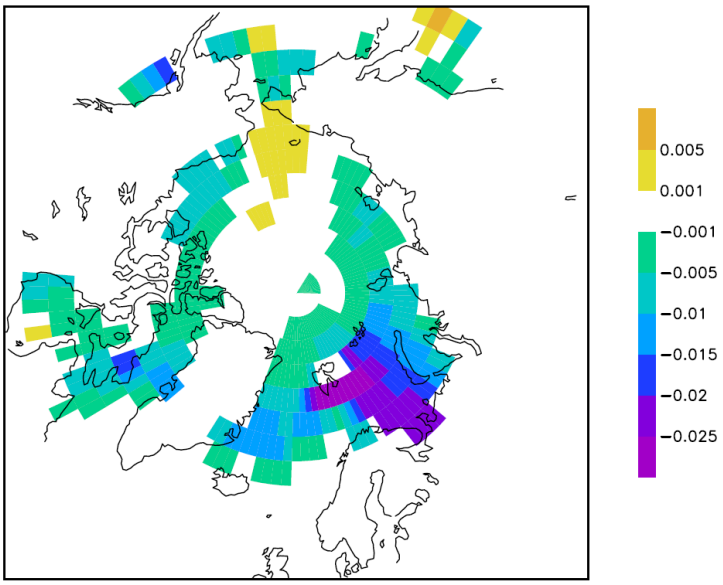

Figure 2.8: Anomaly in annual mean sea ice concentration over the 1470-1520 warm period for the model results averaged over the 5 simulations with data assimilation. The reference period is 1600-1950.

Many studies have shown that a link may exist between anomaly in sea ice concentration and changes in atmospheric circulation (e.g. Slonosky et al., 1997; Alexander et al., 2004). In particular, because of the simulated reduc-

tion of sea ice cover in winter in the Barents Sea, the cold atmosphere is less isolated from the ocean, and is thus warmed by the oceanic heat fluxes. This warming can then impact on the atmospheric circulation. For instance, a reduction in Barents Sea ice coverage can trigger an important local decrease in atmospheric pressure, and thus, an enhanced cyclonic atmospheric circulation (e.g. Guemas and Salas-Mélia, 2008). This anomaly in atmospheric circulation enhances the northward inflow of warm air into the Barents Sea region, favoring further melt of sea ice. Such a positive feedback mechanism has also been suggested previously by Goosse et al. (2003) in a study using an earlier version of LOVECLIM. Bengtsson et al. (2004) proposed as well that the anomaly in atmospheric circulation during the early 20th century warming in the Arctic was most likely induced by a reduced sea ice cover, mainly in the Barents Sea and that this circulation anomaly in turns strongly influences the ice concentration. Such a positive feedback could thus also play a role in both the persistence of the anomaly in atmospheric circulation and in sea ice concentration in the region of the Barents Sea during the period 1470-1520 obtained here.

Changes in oceanic circulation could also have an impact on regional temperature changes during the last millennium. However, the model does not simulate any clear oceanic signal during the period 1470-1520. For instance, Fig. 2.9 shows that the meridional transport of heat in the North Atlantic Ocean towards the Arctic does not experience any large variations over the last millennium in our simulations. Consequently, our results do not support attribution of the warming observed in the Arctic Seas during the period 1470-1520 to changes in oceanic circulation. A slight increase in the poleward heat transport is observed in our simulations over the course of the past millennium, bearing some similarity with the trend shown in Fig. 2.5a. Nevertheless, changes are not significantly different from zero. This weak oceanic response in the model may be due to the experimental design: we are not constraining directly the oceanic changes since the proxies selected for the data assimilation are located only on continents and continental shelves. Though some oceanic proxies at high latitudes are available, including, for instance, records derived from benthic and planktonic foraminifera, stable isotopes and diatom assemblages (Sicre et al., 2008; Eiríksson et al., 2006; Lund et al., 2006; Klitgaard Kristensen et al., 2004; Jiang et al., 2002; Mikalsen et al., 2001; Black et al., 1999), the number of continuous high-resolution marine sedimentary proxy records in the Arctic Ocean over the past millennium is rather small. Furthermore, the uncertainty associated with the calibration and dating of the marine records is generally larger than with other types of proxy records (Jones and Mann, 2004). As a consequence, incorporating such proxy data into our data assim-

ilation procedure is not currently feasible. Most studies suggest that some regional temperature variability coincides with changes of oceanic circulation in the North Atlantic region, in particular, some indicate a role of the ocean in the Atlantic decadal variability. However, none of these studies highlight particular conditions during our period of interest that would suggest a clear underestimation of the role of the ocean in our simulations.

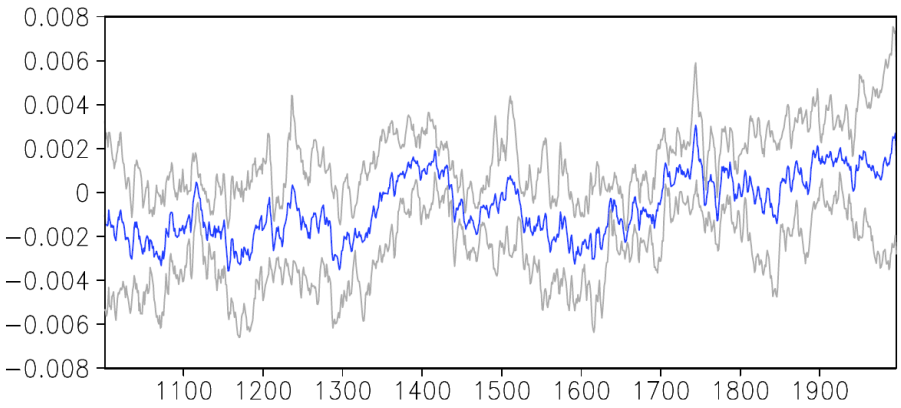

Figure 2.9: Anomaly in meridional heat transport in the North Atlantic Ocean at 70°N (*PW*) for the average over the 5 model simulations performed with data assimilation, the grey lines are the mean plus and minus one standard deviation of the ensemble. A 51-year running mean has been applied to the time series. The reference period is 1600-1950.

To conclude this section, we have compared qualitatively our model results with proxy data that have not been used in the data assimilation process. Some recent proxy-based reconstructions agree pretty well with our warm conditions during the 15th and early 16th century. For instance, a record of temperature based on sedimentary diatoms from a lake in Northern Fennoscandia (Weckström et al., 2006) shows a warm period during 1470-1500, which suits very well to our results. Bird et al. (2009) identified two relatively warm periods from 1350 to 1450 and 1500 to 1620 in a varve-based record from a lake in Alaska. The climate record inferred from varved lake sediments on Northeast Baffin Island studied by Thomas and Briner (2009) also suggests that the warmest pre-20th century interval during the last millennium occurred between 1375 and 1575. Finally, in an ice core record from Lomonosovfonna, Svalbard (Kekonen et al., 2005), the 15th and mid-16th century corresponds to the warmest part of the δ^{18}O profile. Sodium and chloride concentrations are high during this period, which is explained in the study of Kekonen et al.

(2005) by a smaller sea ice extent, which allowed an increased sea-salt aerosols transport form the ocean. This reduced sea ice area is in accordance with the results obtained in our study. Furthermore, the higher sodium and chloride concentrations might possibly also suggest an increase in southerly winds intensity during that period, as proposed in our study.

2.6 Conclusions

In our simulations using LOVECLIM with data assimilation, we find the warmest pre-industrial conditions in the Arctic to have occurred during the period 1470-1520. During this period, the simulated temperatures are even higher than during the so-called "Medieval Warm Period". As the forced response of the model does not produce such an event, this warm period is interpreted as having resulted from internal adjustments of the climate system.

The advantage of the data assimilation technique used in this study is that we obtain a reconstruction of the climate of the past that is consistent with the proxy records, the forcing applied and the physical and dynamical processes included in the model. We can then provide additional information on a plausible large-scale pattern associated with the warming recorded locally in the proxies and on the dynamical processes that were responsible for this warming. There are still some limitations with this new method, and further refinements will be attempted in future studies. When combining proxies and model results, we benefit from the advantages of both proxies and models, but this also leads to some limitations. The assimilation of proxy data insures that the reconstructed climate follows, if imperfectly, the actual realisation of internal climate variability experienced in the past climate evolution, while the use of physically-based model insures that the estimated climate history is consistent with basic climate physics and dynamical processes. This latter property of our approach allows us, furthermore, to interpret the estimated past climate history in terms of climate dynamical hypotheses. We cannot, however, deduce a precise explanation for the pattern of anomalies evident at any particular time, or the precise reason for the long-term persistence of particular patterns.

While not constituting a conventional detection/attribution analysis, our approach can nonetheless establish whether observed changes are consistent with the modelled response to forcing. For those changes which appear unrelated to any forcing, the most reasonable remaining hypothesis is that they arise from the internal variability of the system, though we cannot, of course, completely rule out a bias in the forcing time series used or in the model re-

sponse to the forcing. It is important to keep in mind that LOVECLIM is a model of intermediate complexity and, by definition, its representation of atmospheric dynamics is simpler than in climate general circulation models. Such a simplified model is required in the context of studies such as ours, due to the high computational demand of the data assimilation technique. While LOVECLIM has been successfully employed in a number of past studies focused on the climate variability of the past millennium (e.g. Goosse et al., 2005), some caution is nonetheless advised in interpreting the dynamical response of the atmosphere to past forcing. For instance, the data assimilation scheme can induce a particular phase of the NAO during some periods that would be interpreted based only on LOVECLIM results as mainly due to internal variability, while in the real world (and in more sophisticated models), this can be largely attributed to a response of the system to the forcing and a much weaker contribution of the internal variability. Nevertheless, the volcanic and solar forcing did not appear to be particularly important during the period analysed here.

Another limitation of our study is the low amount of data available. Because of the absence of proxy records in the central Arctic, our simulated pattern of anomaly can thus not be validated by observations there. Our results are then presented as hypotheses of changes, which could then be tested when new reconstructions become available, and used to provide information about mechanisms which could possibly explain the observed changes. It should be reminded that our results are certainly more robust in areas where a lot of proxies are available, such as over Scandinavia and Siberia.

Our model results clearly show that the simulated 1470-1520 Arctic warming is almost entirely explainable in terms of changes in atmospheric circulation, with a clear influence of the negative geopotential anomalies west of Iceland and in the North Pacific. The decrease in sea ice concentration in the Barents Sea region associated with the warming probably contributes to the persistence of those anomalies, at least in the European sector.

The patterns of surface temperature and sea level pressure over the years 1470-1520 is somewhat similar to the early 20th century Arctic warm event. The available data indicates that the winter times in the 1920s were characterized by increased warm air inflow into Europe, while the Baffin Bay experienced a cooling (Overland et al., 2004; Bengtsson et al., 2004). The pattern of sea level pressure (SLP) anomalies during this period is comparable with the pattern of the 1470-1520 warming period obtained in our model reconstructions (the geopotential height being the closest variable to the SLP in the model).

The early 20th century warm event might thus not have been unique in the recent past. Furthermore, the negative anomaly centered over Bering Strait is responsible of the warming over the Canadian Archipelago. The relatively large event during the period 1470-1520 appears thus as a consequence of coincident changes in the European and Pacific sectors that also play a role in variations of Arctic climate during the 20th and early 21st centuries (e.g. Overland and Wang, 2005).

No robust change in the patterns of oceanic circulation could be found in our model results to explain the changes observed in the Arctic Seas during the 1470-1520 warm event. The absence of strong response of the ocean in our simulations covering the past millennium may be due to the data assimilation and in particular to the lack of well calibrated oceanic proxies for the past millennium. Evidence has indeed been provided in past studies (e.g. Delworth and Mann, 2000; Knight et al., 2005) for the existence of a mode of multidecadal variability in the North Atlantic, related to fluctuations in the intensity of the thermohaline circulation. Such persistent patterns of variability could explain some of the low-frequency temperature variability observed at high latitudes (Zhang et al., 2007). The intensification of the Atlantic water inflow to the Arctic, which appears to explain some of the recent warming of the Arctic Ocean (Zhang et al., 1998; Gerdes et al., 2003), could provide an analog for past episodes of Arctic warming. As a consequence, additional work will be required both in terms of the implementation of the data assimilation technique and the inclusion of additional marine proxies, to investigate the role of oceanic circulation in past changes in the Arctic.

CHAPTER 3

ANNUAL AND SEASONAL RESPONSES TO EXTERNAL FORCINGS

This Chapter is based on the following paper: Crespin, E., Goosse, H., Fichefet, T., Mairesse, A., Sallaz-Damaz, Y., 2012. Arctic climate over the past millennium: Annual and seasonal responses to external forcings. The Holocene 23, 321–329.

Abstract

The annual and seasonal temperatures in the Arctic over the past 1150 years are analysed in simulations performed with the three-dimensional Earth system model of intermediate complexity LOVECLIM forced by changes in solar irradiance, volcanic activity, land use, greenhouse gas concentrations and orbital parameters. The response of the system to individual forcings for each season is examined in order to evaluate the contribution of each forcing to the seasonal contrast. For summer, our results agree relatively well with the reconstruction of Kaufman et al. (2009). Our modelling results suggest that the temperature changes during this period were characterized by large seasonal

differences. In particular, while annual mean temperatures display a decreasing trend during the preindustrial period, spring temperatures appear to rise. The variations in the Earth's orbital parameters are the main cause for those seasonal differences. Larger climate variations are simulated in autumn compared to the other seasons in response to each forcing, particularly in response to changes in greenhouse gas concentration during the industrial period and in response to land use forcing, which surprisingly has a significant impact on Arctic temperature. These contrasting changes for the different seasons also underline the need for an adequate estimate of the season represented by a proxy.

3.1 Introduction

Many studies have been devoted to the reconstruction and understanding of the annual mean, large-scale temperature changes over the past millennium, using both proxy-based reconstructions and models (e.g. Crowley, 2000; Briffa et al., 2001; Jones and Mann, 2004; Rutherford et al., 2005; Osborn and Briffa, 2006; Osborn et al., 2006; González-Rouco et al., 2006; Mann et al., 2008, 2009; Jones et al., 2009; Goosse et al., 2010b). Less attention has been paid to seasonal trends at the regional scale, except maybe for Europe (see, for instance, Luterbacher et al., 2004; Xoplaki et al., 2005; Goosse et al., 2006a; Guiot et al., 2010; Hegerl et al., 2011). However, it is important to improve our knowledge of the evolution of seasonal temperatures, because they may behave very differently from the annual ones (Jones et al., 2003; Bauer and Claussen, 2006). This has been clearly shown over the last 150 years, as the instrumental records exhibit a larger warming over the Northern Hemisphere in winter than in summer (Jones et al., 2003). These differences between changes in annual and seasonal temperatures can be explained by the response of the climate system to a specific forcing which may vary from one season to another and from one region to another (Zveryaev and Gulev, 2009; Bauer and Claussen, 2006; Shindell et al., 2003). For instance, over the preindustrial period, Shindell et al. (2003) showed that solar and volcanic forcings lead to spatially and seasonally different climate responses in the Northern Hemisphere. When analysing the average over the Northern Hemisphere in the CLIMBER model, Bauer and Claussen (2006) identified the changes in orbital parameters as responsible for an increase in seasonal differences in the temperature over the past millennium, and the deforestation and variations in atmospheric carbon dioxide concentration as the main forcings responsible for a decrease in this difference over the past century.

None of the above mentioned studies has specifically investigated the Arctic climate. However, a deeper analysis of this region is justified by placing the rapid and large temperature variations observed in the Arctic during the last century in a wider context (e.g. McBean et al., 2005; Serreze and Francis, 2006). Additionally, a polar amplification of temperature changes is simulated in climate models driven by an increased radiative forcing, because of positive climate feedbacks involving, among other processes, albedo changes due to the decrease in sea ice and snow coverages (e.g. Holland and Bitz, 2003; Serreze and Francis, 2006). An evaluation of model behaviour at the scale of the millennium thus appears to be of interest.

Multi-proxy climate reconstructions are currently available for the Arctic region (Overpeck et al., 1997; Kaufman et al., 2009). The most recent one (Kaufman et al., 2009) consists of decadally resolved summer proxy temperature records covering the past 2000 years. According to this reconstruction, a long-term decreasing trend in summer Arctic temperatures occurs over this period, except for the last century, and is attributed to the steady reduction in summer insolation. However, because of the lack of widespread data and since most proxies do not reflect annual conditions but just the ones of the warmest months of the year, much less information is available on changes in the annual cycle through time. Climate model simulations are thus necessary, in complement to the proxy-based reconstructions, to help to confirm the proposed hypotheses and to improve the understanding of climate variations in this region, both for annual and seasonal means.

In this framework, the goal of this study is to document the differences in the Arctic temperature changes over the past millennium between the various seasons and to understand the causes of those differences. To do so, we analyse the annual and seasonal responses of the Arctic climate to natural and anthropogenic forcings such as solar, volcanic, astronomical, greenhouse gas and land use, in the Earth system model of intermediate complexity LOVECLIM (Goosse et al., 2010a). With a coarser spatial resolution and a simpler representation of the physical processes than in climate general circulation models, LOVECLIM has the advantage of being much faster than the latter and, consequently, of being affordable for performing the large ensembles of long simulations required here. These advantages inevitably come with some limitations, such as, for instance, a smoothed topography and a lack of a representation of stratospheric dynamics. However, the model is suitable for studying long-term climate changes at mid- and high latitudes (Goosse et al., 2010a).

The present paper is organized as follows. First, a brief description of the model and forcings used is presented in Section 3.2. The evolution of the simulated temperatures over the last millennium in response to the different forcings is analysed in Section 3.3, a subsection being devoted to the contribution of each forcing. A final discussion of the results follows in Section 3.4, including a brief discussion of the implications of our results for the calibration and interpretation of proxy data.

3.2 Model description and experimental design

The simulations analysed here were conducted with the Earth system model of intermediate complexity LOVECLIM1.2 (Goosse et al., 2010a). This three-dimensional model includes representations of the atmosphere, the ocean and sea ice, the land surface and its vegetation, the carbon cycle and the polar ice sheets. However, the last two components are not activated in this study. The atmospheric component, ECBilt2 (Opsteegh et al., 1998), is a quasi-geostrophic model with a resolution of 5.6° in longitude and latitude and three vertical levels. The oceanic component, CLIO3 (Goosse and Fichefet, 1999), is a primitive-equation, free-surface ocean general circulation model, with a resolution of 3° in longitude and latitude, and 20 unevenly spaced vertical levels. It is coupled to a thermodynamic-dynamic sea ice model, where sea ice is assumed to behave as a two-dimensional viscous-plastic continuum for the computation of sea ice dynamics. Its representation of sensible heat storage and vertical heat conduction within the snow and ice are based on a three-layer model, and the energy budget at the bottom and top boundaries of the snow-ice cover and in leads determines the vertical and lateral growth and decay of sea ice (Fichefet and Morales Maqueda, 1997). The component representing the terrestrial vegetation is named VECODE (Brovkin et al., 2002) and simulates the annual evolution of trees, grassland and deserts, at the same resolution as ECBilt. The computed vegetation changes affect both the surface albedo, surface evaporation and water storage. LOVECLIM has been used successfully in many studies focused on recent, past or future climate changes at hemispheric and regional scales (e.g. Renssen et al., 2005; Driesschaert et al., 2007; Crespin et al., 2009; Goosse et al., 2005, 2006a). More information about LOVECLIM is available at: www.climate.be/LOVECLIM.

All the simulations start at year 850 AD and end in 2000 AD, following the experimental design of the third phase of the Paleoclimate Modelling Intercomparison Project (PMIP3) until the year 1850 AD, and the fifth phase of the Coupled Model Intercomparison Project (CMIP5) afterwards. The initial conditions come from a 1000-year long, quasi-equilibrium run, using the

greenhouse gas and astronomical forcings corresponding to 850 AD. The simulations are driven by the forcings adopted by PMIP3 (v1.0), i.e., variations in solar irradiance, volcanic activity, orbital parameters, land use and greenhouse gas concentrations (Schmidt et al., 2011). The solar irradiance follows the reconstruction from Delaygue and Bard (2011) between 850 and 1609 AD, and from Wang et al. (2005) between 1610 and 2000 AD. The Earth's orbital parameters vary according to the calculations of Berger (1978). The forcing due to volcanic activity is derived from Crowley et al. (2008) and is implemented through anomalies in solar irradiance at the top of the atmosphere. The anthropogenic land use changes are based on the reconstruction of global agricultural areas and land cover of Pongratz et al. (2008) from 850 to 1700 AD and on the reconstruction of Ramankutty and Foley (1999) from 1700 AD onwards. This forcing is applied in LOVECLIM through a reduction in the area covered by trees and an increase in grassland since VECODE does not include a specific vegetation type corresponding to cropland. The evolutions of the concentration of the main greenhouse gases (CO_2, CH_4, and N_2O) are provided by Joos and Spahni (2008). For a detailed description of all these forcing reconstructions, see Schmidt et al. (2011). After 1850 AD, the changes in sulfate aerosol load are taken into account through modifications in the surface albedo (Charlson et al., 1991), and the variations in tropospheric ozone concentration are included after 1950 AD. In addition to the simulations including all those forcings, the contribution of each of them (with the exception of sulfate aerosol and ozone, because of our focus on the whole millennium) is evaluated in a set of experiments driven by one forcing at a time.

Each experiment set consists of an ensemble of ten simulations with identical forcing, in which the different members differ only in their initial conditions, with a small noise being added to the atmospheric streamfunction (as in Goosse et al., 2010b). The ensemble mean of these simulations provides an estimate of the response of the system to each forcing, as the influence of the natural variability simulated by the model, which differs in each member of the ensemble, is reduced by the averaging process. In our study, winter is taken as the months of January, February and March (JFM), spring as April, May and June (AMJ), summer as July, August and September (JAS), and autumn as October, November and December (OND). This choice is justified by the fact that, in the Arctic, spring starts later than at mid-latitudes, the maximum sea ice extent being observed for instance in February-March (Chapman and Walsh, 1993; Stroeve et al., 2007; Comiso and Nishio, 2008). Furthermore, this definition groups months with similar tendencies and thus gives more contrasted results between the seasons, as discussed in the next section. In the following analysis, the Arctic is defined as the region located north of 64°N.

3.3 Temperature response to different forcings

3.3.1 Response to greenhouse gas forcing

The climate response to changes in greenhouse gas concentrations is rather weak in the Arctic during the first centuries of the millennium (Fig. 3.1a). In contrast, a rapid rise in surface temperature is simulated after 1850 AD. The temperature difference due to the greenhouse gas forcing between the last and first decades of the 20th century for the Arctic region amounts to $1.7°C$ in our simulations. The corresponding value for the Northern Hemisphere is much lower ($0.7°C$), in accordance with the Arctic amplification of the warming.

The temperature increase varies considerably between the seasons. The maximum change occurs in autumn ($2.5°C$ between the end and the beginning of the 20th century), and the smallest increase in summer ($0.9°C$). During autumn, the direct effects of the temperature-albedo feedback are relatively weak at high latitudes, because of the weak incoming solar radiation. It is likely the insulation effect of sea ice which is instead responsible for the larger temperature response to the forcing in this season compared to the others. The process leading to this has been observed and explained in other studies (e.g. Manabe et al., 1992; Vavrus et al., 2012). During summer, the amount of heat stored in the Arctic Ocean increases with the rise of greenhouse gas concentrations. This absorption of heat by the ocean is enhanced by the decrease in surface albedo resulting from the reduction in sea ice extent. However, the temperature variability and the response to the forcing are relatively low in summer, as temperatures remain mainly at the freezing point due to the melting of sea ice. In contrast, a decrease in the ice cover in summer has a large impact on the temperature in autumn and winter. During these seasons, the production of sea ice is slowed down because of the increased summer heat storage in the mixed layer of the ocean. The thinner and less extensive ice cover allows greater heat transfer from the ocean towards the cooler atmosphere and thus a large air temperature increase. This process appears valid in the response of LOVECLIM to each of the forcings, as shown in the following sections. This is confirmed by the changes in sea ice extent (average over area with at least 15% sea ice concentration), depicted in Fig. 3.6 for the response to all forcings combined, which indicate a decrease in sea ice extent that is almost twice as large in summer as the other seasons between 1850 and 2000 AD.

3.3.2 Response to volcanic forcing

As only a few major eruptions took place between 850-1200 AD, the Arctic mean temperature is relatively stable during that period in our simulations

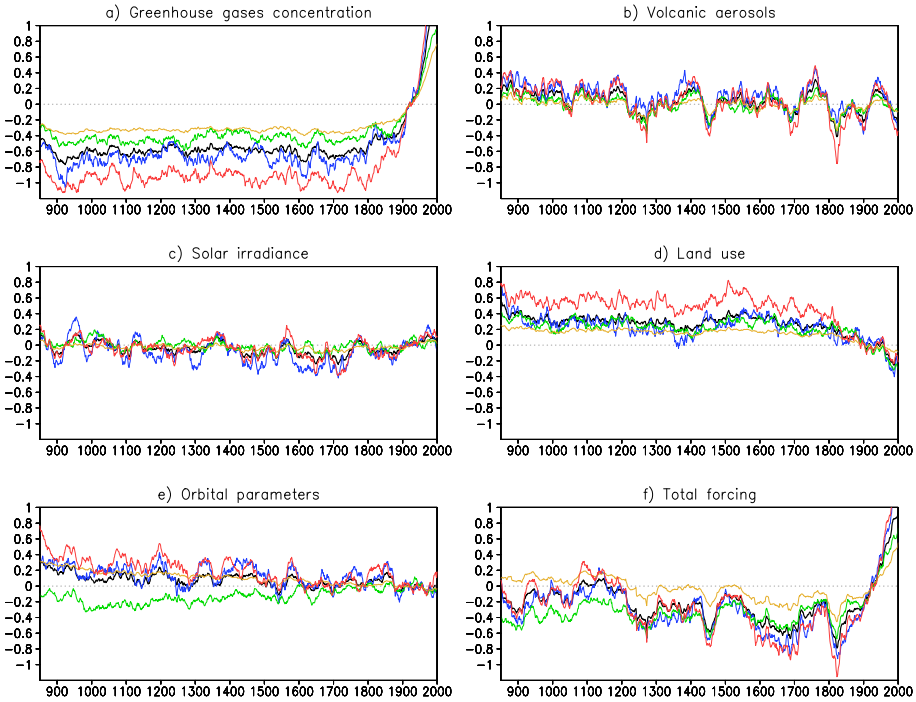

Figure 3.1: Anomaly in annual and seasonal mean surface temperature (°C) in the Arctic (north of 64°) over the last 1150 years as simulated by LOVECLIM in response to different forcings. Each time series represents the mean of an ensemble of 10 simulations. The annual mean is displayed in black, the winter (JFM) in blue, the spring (AMJ) in green, the summer (JAS) in yellow, and the autumn (OND) in red. The reference period is 1850-1980 AD. A 31-year running mean has been applied to the time series.

driven by the volcanic forcing only (Fig. 3.1b). For the last 800 years, a long-term cooling trend is observed, because of the higher frequency of eruptions, in addition to the abrupt temperature drops coinciding with the strong volcanic eruptions. Over the 1150 years of simulation, this cooling rate is equal to $-0.016 \pm 0.006°C$ per century (95% confidence interval for the trend).

A cooling is observed after a major eruption in all seasons. No significant seasonal contrast is observed over the last millennium in our simulations, except a larger temperature response in autumn than for other seasons. For instance, in some periods with intense volcanic activity, such as between 1745-1775 AD and 1810-1840 AD, during autumn the temperature drops by up to $1.2°C$ (averaged over a 31-year period), while in summer the difference reaches only

$0.45°C$. The end of the last century also presents large seasonal differences with a drop in autumn and winter temperatures of almost $0.6°C$, but with five times smaller changes in summer and spring. These seasonal differences cannot be explained by the seasonal variability of the forcing itself, since on average it is the strongest during winter and spring and the weakest in autumn. Here again, it is suggested that it is the insulation effect of sea ice which leads to this larger response, as explained in the previous section.

3.3.3 Response to solar forcing

Changes in irradiance due to variations in solar activity have little influence on the temperature evolution in the Arctic during the last millennium in our simulations. The temperature response (Fig. 3.1c) is relatively weak, with a small long-term cooling trend until 1850 AD ($-0.013 \pm 0.006°C$ per century) and a small warming during the last 150 years ($0.14 \pm 0.08°C$ per century). Decadal-to-centennial fluctuations correspond roughly to positive and negative anomalies in solar activity, suggesting a simple, quasi-linear response to the forcing (after applying a 31-year running mean, the correlation between the solar forcing and the ensemble mean temperature response to this forcing in the Arctic is 0.57). These numbers should, however, be taken with caution. The signal is small, with a standard deviation of the temperature in the ensemble mean of simulations run with solar forcing reaching $0.08°C$, compared to $0.06°C$ in a control experiment without forcing. Ten ensemble members is too few in this case to precisely assess the contribution of solar forcing compared to a run without forcing, but we can confidently state that it is weak.

Whilst the Arctic receives little to no incoming solar radiation during winter, summer is characterized by high amount of incoming solar radiation due to the long period when the Sun is above the horizon. Nevertheless, as observed in Fig. 3.1c, the seasonal responses to solar forcing do not display large differences. This weak seasonal contrast is due to the low absorption of solar radiation by the surface, even during summer (because of the high albedo of sea ice and snow) and to a memory effect related to sea ice, explained in Section 3.3.1: a summer warming induces a decrease in ice thickness, leading to larger oceanic heat fluxes towards the atmosphere in autumn and winter, and thus to a surface temperature increase during these seasons, although no direct effect of solar radiation is expected at high latitudes.

We must caution that the solar forcing selected in this study, and this is also the case for the other alternative solar reconstructions proposed by PMIP3 (v1.0, Schmidt et al., 2011), has a substantially smaller amplitude compared

to some reconstructions used previously to drive models over the last millennium. This choice is justified from our present-day understanding of solar physics (e.g. Foukal et al., 2006). However, uncertainties remain large. Using an alternative reconstruction displaying larger variations, such as the one of Shapiro et al. (2011) included in those proposed in the version 1.1 of PMIP3 forcings (Schmidt et al., 2012), would lead to a more significant contribution of solar forcing to temperature changes during the past millennium. A new set of simulations would be required to estimate the influence of this forcing. However, we can infer from the quasi-linear behaviour of the temperature response to the solar forcing that this response will not change much qualitatively, but its magnitude would be much larger, as the Shapiro et al. (2011) reconstruction presents a TSI amplitude variance one order of magnitude larger than the reconstruction used in this study.

3.3.4 Response to land use changes

Surprisingly, the temperature evolution in the Arctic is strongly influenced by the deforestation taking place at lower latitudes. The land use forcing produces a significant cooling that reaches an annual mean of almost $0.6^{\circ}C$ over the last four centuries (Fig. 3.1d). This forcing leads to different magnitudes of temperature change for the various seasons. The largest cooling is observed in autumn, where it reaches almost $1^{\circ}C$ since 1600 AD. The cooling is substantially weaker during summer, reaching only $0.3^{\circ}C$.

This strong cooling is investigated in more detail by depicting the geographical distribution of the temperature response to deforestation (Fig. 3.2). The land use changes at mid-latitudes lead to a cooling in the entire Arctic region in winter, spring and autumn, when comparing the periods 1950-2000 AD and 1550-1600 AD. In summer, the signal is less clear, with still an overall cooling, but also a warming in some regions (Siberia and Canada). No significant change in either atmospheric or oceanic circulations is noticed in our simulations (not shown). Therefore, these temperature anomalies must be explained by radiative and thermodynamical effects rather than dynamical ones.

Deforestation has an impact both on the surface albedo and evaporation in LOVECLIM. The first effect induces a cooling, as the albedo of forests is lower than the one of grass or crops. This difference in albedo becomes larger when snow covers the deforested areas. Moreover, the initial cooling associated with deforestation is responsible for a delayed melting of the snow, thus leading to an additional increase in surface albedo and a subsequent cooling (Fig.

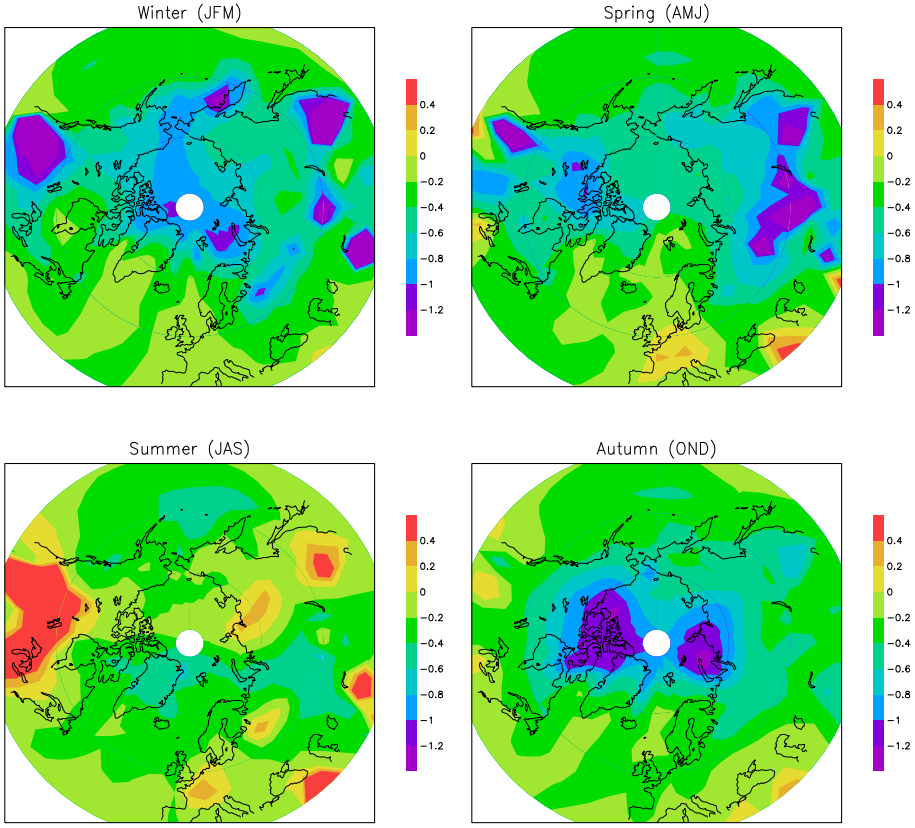

Figure 3.2: Surface temperature difference (°C) in the Arctic between 1950-2000 AD and 1550-1600 AD for the four seasons simulated by LOVECLIM, driven only by the land use forcing.

3.3b,c). The impact of changes in albedo is thus mostly visible during spring. As discussed above, the autumn and winter coolings are a consequence of the changes occurring during the other seasons (insulating effect of the sea ice), since little to no solar radiation reaches the surface during large parts of these seasons.

In summer, the reduced evapotranspiration, and hence the reduced surface latent heat flux (Fig. 3.3d), due to the decreasing number of trees in some regions, warms up the surface locally. However, the temperature trend in the Arctic during this season remains negative over the last 400 years, because of the cooling during the other seasons. In the Arctic, the sea ice concentration

increases by up to 10% in some regions in summer. The Arctic Ocean is thus more insulated from the cooler atmosphere, and the surface cooling is reinforced, mainly in autumn and winter, when the cooling in the centre of the Arctic is very large. This also increases the albedo and the amount of heat needed to melt the more extensive ice cover in summer. The net effect in this season is a cooling that overwhelms the influence of the slight warming at mid-latitudes due to the lower latent heat fluxes.

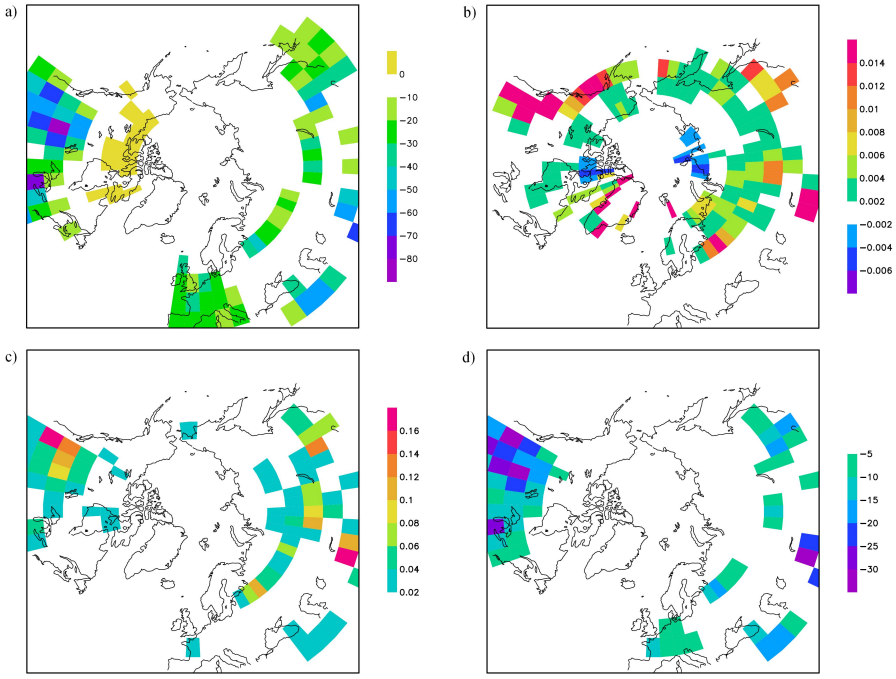

Figure 3.3: Difference in (a) annual mean tree fraction (%), (b) snow depth over land (m) in spring, (c) surface albedo in spring and (d) surface latent heat flux (Wm^{-2}) in summer between 1950-2000 AD and 1550-1600 AD as simulated by LOVECLIM driven only by the land use forcing.

3.3.5 Response to astronomical forcing

The variations in the Earth's orbital parameters over the last millennium are associated with a 20-day shift in the perihelion, but also changes in eccentricity and obliquity (Berger et al., 1993; Schmidt et al., 2011). This forcing induces negligible changes at the hemispheric scale on an annual average, but its ef-

fect can be more important for specific months at particular latitudes (Bauer and Claussen, 2006). In our simulations, contrasted temperature trends for the different seasons are observed. Indeed, the temperature response to the astronomical forcing is characterized by a positive trend during the spring, contrary to the other seasons which display negative trends (Fig. 3.1e). While the annual mean temperature in the Arctic decreases by about $0.15°C$ during the last millennium, the spring temperature experiences a rise of about $0.25°C$.

Figure 3.4 displays the insolation difference at 75°N between 1900-2000 AD and 850-950 AD for the different months of the year along with the temperature difference in the Arctic for the same periods. During the first months of the year, an increase in insolation is observed, with the largest change occurring in April ($1.5\ Wm^{-2}$). The anomaly becomes negative after May, reaches its lowest value in July ($-4\ Wm^{-2}$) and remains negative throughout the entire summer season. The region north of 75°N receives no solar radiation during November, December and January. The temperature response follows the forcing, but with a time-lag of one to two months, reflecting the thermal inertia of the system. The spring months then exhibit a warming, which reaches a maximum in May. The rest of the year displays a cooling, with the highest negative temperature anomaly occurring at the beginning of the autumn. The temperature difference between the months of May and September reaches up to $0.8°C$.

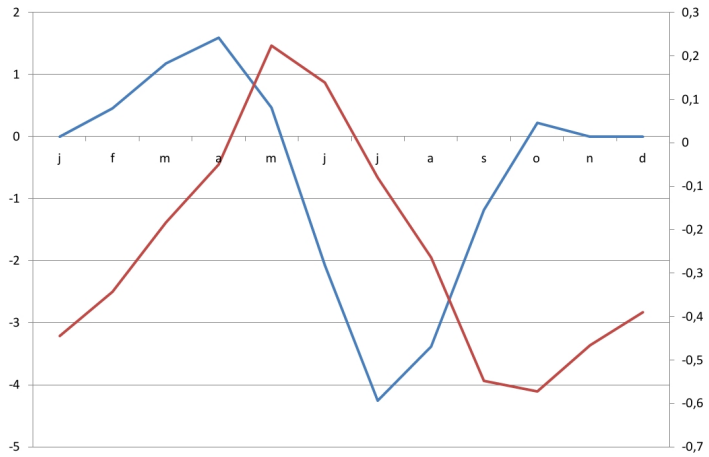

Figure 3.4: Insolation difference (Wm^{-2}) at 75°N (blue line) and temperature difference ($°C$) in the Arctic as simulated by LOVECLIM driven only by the orbital forcing (red line) between 1900-2000 AD and 850-950 AD.

Bauer and Claussen (2006) also showed that the astronomical forcing plays a role in their climate simulations over the last millennium. However, they document a temperature difference of $0.1°C$ only between winter (DJF) and summer (JJA) for the land areas located between 30 and 70°N. For this region, LOVECLIM displays a similar result. This is smaller than the result for the Arctic region in our simulations and clearly indicates that the astronomical forcing plays a more important role over the last millennium in the Arctic than at lower latitudes. This is mostly due to the fact that modifications in obliquity have a stronger influence at high, compared to low, latitudes (Berger et al., 1993) and to the positive feedbacks amplifying the changes.

3.3.6 Response to all forcings

In response to all forcings combined, the annual mean Arctic surface temperature (Fig. 3.1f) decreases slowly during the last millennium after a warm period around the 11th and 12th centuries, which is often referred to as the Medieval Warm Period. The impact of large volcanic eruptions is clear during the mid-13th, mid-15th, late 17th and early 19th centuries. During the industrial period, the warming due to the increase in greenhouse gas concentrations is attenuated by the cooling effect resulting from land cover changes (and sulfate aerosol loads changes that are not studied here). The climatic response to all forcings corresponds more or less to the sum of the contributions of each individual forcing. Indeed, the RMSE between the response to all the forcings combined and the sum of the responses to each single forcing, after applying a 31-year running mean, is equal to $0.15°C$. If we use this linearity, we can estimate the relative contribution of the different forcings to the cooling trend on an annual mean over the period 900-1850 AD. It amounts to $35 \pm 18\%$ for the volcanic forcing, $28 \pm 12\%$ for the astronomical forcing, $27 \pm 12\%$ for the solar forcing and $20 \pm 12\%$ for the land use forcing, while the trend of the greenhouse gas forcing is positive.

The low-frequency temperature evolution in the Arctic over the last millennium has similarities with that simulated by many models at the hemispheric scale and in the different latitude bands of the Northern Hemisphere (e.g. Crowley, 2000; Bauer and Claussen, 2006; Osborn and Briffa, 2006; Osborn et al., 2006; González-Rouco et al., 2006; Goosse et al., 2010b). However, its amplitude is significantly higher in the Arctic region because of the existing feedbacks related to snow and sea ice, pointing out an Arctic amplification of climate changes. The seasonal contrast is also much more pronounced in the Arctic than at the hemispheric scale in our simulations. The astronomical forcing seems to strongly contribute to the seasonal differences of the temperature

evolution during the last millennium, as the opposing seasonal temperature trends (positive in spring and negative for the other seasons) observed in the response to the astronomical forcing are also simulated by the model when driven by all the forcings.

Kaufman et al. (2009) attributed the millennial-scale cooling in the Arctic to the reduction in summer (defined here as the mean of June, July and August) insolation due to the variations in orbital parameters. If we again estimate the contribution of the different forcings to the cooling trend in our simulations but now for summer (over the period 900-1850 AD), we obtain a contribution of $22 \pm 11\%$ for the volcanic forcing, $57 \pm 5\%$ for the astronomical forcing, $12 \pm 5\%$ for the solar forcing, $15 \pm 5\%$ for the land use forcing and a positive trend for the greenhouse gas forcing. This confirms the role of orbital forcing proposed by Kaufman et al. (2009), but emphasizes that volcanic, land use and solar forcings also play a role in the cooling trend modelled by LOVECLIM. The time series of the model outputs and proxy-based data are depicted in Fig. 3.5. One sees a relatively good agreement between them (even though the mean of June, July and August does not exhibit the largest cooling in our simulation, since the temperature trend in June is still positive). The low frequency variability of our simulation is lower than in the Kaufman et al. (2009) reconstruction. This might be related to the climate sensitivity of the model or to the forcing applied. Averaging over the ensemble might also play a role, as this reduces the multidecadal internal variability. On the other hand, the amplitude of the changes is strongly seasonally-dependent and a small bias in the attribution of the signal of the proxy to a specific month in the Kaufman et al. (2009) reconstruction might also have a large impact on the model-data comparison. The reconstruction is, however, within the uncertainty range of the simulations, represented by two standard deviations of the ensemble, with the exception of two particular periods. Between years 900 AD and 1000 AD, the reconstruction shows a warming that is not simulated by the model. The model also fails in reproducing the mid-20th century warming (Goosse et al., 2010a). It thus appears that our experimental design satisfactorily captures the long-term trends but is not able to simulate these observed multidecadal fluctuations. The cause of this discrepancy will be investigated in a forthcoming study devoted to the origins of the warm periods in the Arctic.

In contrast, the comparison of our summer model results with the Kinnard et al. (2011) reconstruction of August Arctic sea ice extent is less satisfactory (Fig. 3.6, model results are represented for summer but do not differ much from the August mean). The magnitude of the changes is much larger in the reconstruction throughout the whole period. The decrease in sea ice extent

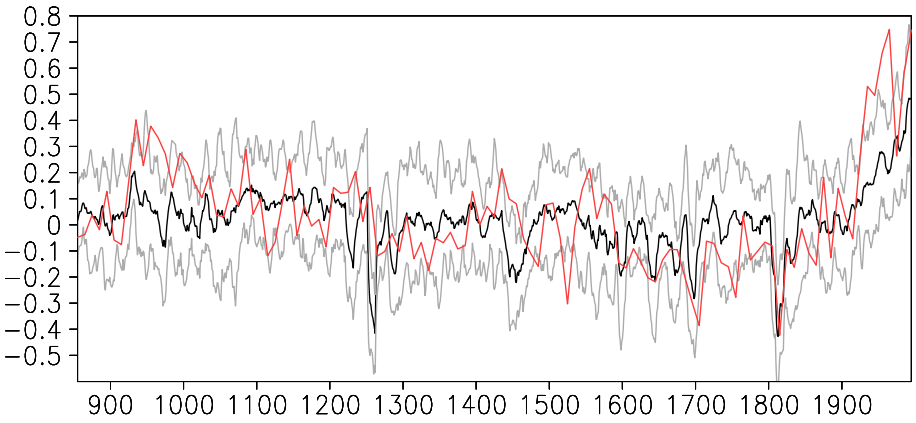

Figure 3.5: Anomaly in temperature (°C) averaged over the months of June, July and August in the Arctic over the last 1150 years. The black line is the mean of an ensemble of ten simulations using LOVECLIM driven by all the forcings. The grey lines are the mean plus and minus two standard deviations of the ensemble. The red line corresponds to the reconstruction of Kaufman et al. (2009). The reference period is 855-1855 AD. An 11-year running mean has been applied to the model time series.

during the industrial period started earlier in the model than in the reconstruction and the decreasing trend is much larger in the latter. Compared to observations, the decline in summer sea ice extent in the Arctic is underestimated in LOVECLIM. The trends computed between 1979 and 2007 AD are equal to $-0.056 \times 10^6\ km^2/yr$ in the observations and $-0.046 \pm 0.013 \times 10^6\ km^2/yr$ in the model (Goosse et al., 2010a). Note that the trend in the Kinnard et al. (2011) reconstruction during this very recent period is likely influenced by the use of the 40-year filter. Additionally, the reconstruction is characterized by a period with reduced sea ice extent during the late 16th and early 17th centuries (period with particularly low temperatures) which is not simulated by the model. However, before 1200 AD, the reconstruction and the model agree on periods with relatively low sea ice extent and, between 1200 and 1450 AD, an extensive sea ice extent is present in both of them.

3.4 Discussion and conclusions

This study aimed at improving our understanding of the evolution of the Arctic temperature during the last millennium using the Earth system model of intermediate complexity LOVECLIM. The modelled temperature response to external forcings agrees reasonably well with the reconstructed tempera-

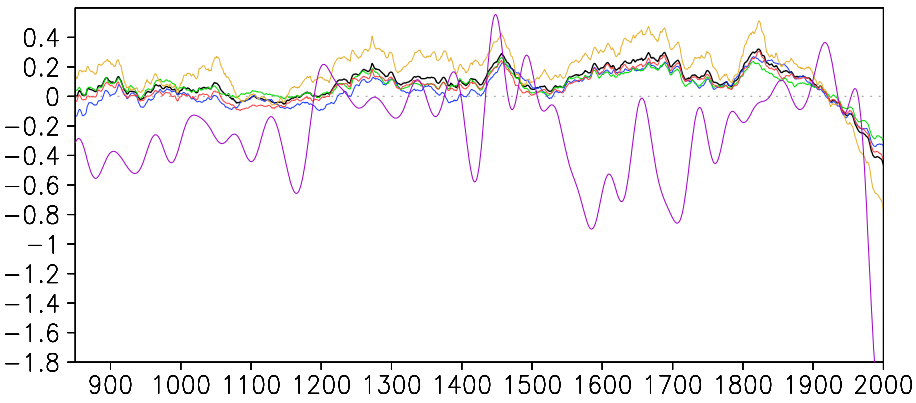

Figure 3.6: Anomaly in annual mean sea ice extent (area with at least 15% sea ice concentration) in the Northern Hemisphere (10^6 km^2) over the last 1150 years as simulated by LOVECLIM in response to all forcings. Each time series represents the mean of an ensemble of 10 simulations. The annual mean is displayed in black, the winter (JFM) in blue, the spring (AMJ) in green, the summer (JAS) in yellow, and the autumn (OND) in red. A 31-year running mean has been applied to the time series. The 40-year smoothed reconstructed August Arctic sea ice extent from Kinnard et al. (2011) is displayed in purple. The reference period is 1850-1980 AD.

ture of Kaufman et al. (2009). Volcanic, astronomical, greenhouse gas and, to a smaller extent, solar forcings all contribute to the simulated temperature changes over the 1150 years of simulation. More surprisingly, land use changes in mid-latitudes also have a significant impact on Arctic temperatures. An Arctic amplification of the temperature changes is simulated in the responses to each of the forcings.

Our results show considerable differences between the four seasons. This seasonal contrast is mainly caused by the variations in orbital parameters of the Earth, which induce an increase of 1.5 Wm^{-2} in spring insolation and a decrease of 4 Wm^{-2} in summer insolation at 75°N during the past millennium. This astronomical forcing is larger than at lower latitudes and amplified more strongly in the Arctic by positive feedbacks involving snow and sea ice. This leads to larger differences between the seasons in that region compared to lower latitudes, with a positive long-term temperature anomaly trend during spring and a negative one during the three other seasons. During the 20th century, the larger autumn and winter warming trends are due to a stronger response to the variations in greenhouse gas concentrations during these seasons than in summer. The land use forcing has an opposite effect over this period: it leads to a larger cooling in spring, autumn and winter than in sum-

mer in the Arctic. In the study of Bauer and Claussen (2006), comparable results have been found for land areas from 30 to 70°N, except for the cooling obtained in response to land use forcing which is larger in summer than in winter in their study, in contrast to our results.

The contributions of the solar and volcanic forcings to the seasonal differences are relatively small for the past millennium in our simulations. Nevertheless, in addition to the direct radiative impact of volcanic eruptions or changes in solar irradiance, the dynamical response of the system can yield contrasting changes between the seasons in some regions, in particular over the mid-latitude continents. Indeed, the warming of the stratosphere (by absorption of both solar and terrestrial radiations) after a large volcanic eruption in the tropics is larger at low than high latitudes, leading to a strong meridional temperature gradient, especially during winter. The resulting changes in tropospheric circulation can induce a winter warming over the continents, which overwhelms the direct radiative cooling effect of volcanic eruptions (Robock, 2000). Furthermore, the tropospheric circulation can also be affected by variations in solar irradiance, which influences the distribution of ozone in the stratosphere, affecting in turn its temperature and winds (e.g. Shindell et al., 2001). Because of the absence of a representation of the dynamics of the stratosphere in LOVECLIM, these effects can not be studied here (Goosse and Renssen, 2004). Since the radiative scheme used in the model is very simple, it was also not possible to include solar spectral irradiance variations (Schmidt et al., 2012), which also have a clear impact on stratospheric dynamics. These constitute limitations to our study that must be kept in mind when interpreting our results. Finally, our results clearly depend on the choice of forcings. Alternative reconstructions (such as Shapiro et al. (2011) for the solar forcing and Kaplan et al. (2011) for the land use forcing) could lead to different results, although we do not expect that they would qualitatively affect our conclusions. The response to the alternative vegetation reconstruction is particularly difficult to assess, as the Kaplan et al. (2011) reconstruction is based on a very different assumption from the reconstruction used in this study. However, we expect a noticeable impact in the Arctic of land use changes at lower latitudes.

The significant seasonal contrast in trends underlined by our simulations may have consequences for the interpretation of the reconstructions of past temperature based on proxy-data. Indeed, our study indicates that some seasons are less representative of annual conditions than others. Because many proxies record changes during a specific part of the year or season (e.g. Jones and Mann, 2004), the calibration against annual temperatures may thus be biased (Briffa and Osborn, 2002; Jones et al., 2003, 2009). For the 20th cen-

tury, the trends have the same sign for all seasons and the correlation between proxy records and instrumental observations may be relatively similar for all of them. Unfortunately, looking at our model simulations, it is apparent that seasonal differences have not been stationary through the past millennium, with seasonal contrast being larger at the beginning than the end of the millennium. If the modelled temperature curves are scaled over the warming of the past 100 years, the difference between summer and spring temperature anomalies at the beginning of the millennium amounts to $0.6^{\circ}C$ in our experiments. This points out the need to carefully determine the season that most influences the proxies, as the May-June signal, for instance, is clearly different from that of July-August.

CHAPTER 4

TESTING A NEW DATA ASSIMILATION METHOD USING A PARTICLE FILTER TO RECONSTRUCT THE EVOLUTION OF THE NORTH ATLANTIC MERIDIONAL OVERTURNING CIRCULATION

4.1 Introduction

Because of the lack of direct observations, our knowledge of the variations of the North Atlantic meridional overturning circulation (MOC) intensity and the role they played in past climate changes is very uncertain. By combining available data with model results using a new data assimilation method, we aim in this chapter to test a methodology to reconstruct past changes in the intensity of the MOC over long time periods. Data such as instrumental observations of surface temperature (Brohan et al., 2006) and pressure (Allan and Ansell, 2006) are available over approximately the last 160 years. Sea surface salinity data is not sufficiently spatially and temporarily sampled before 1960 (Bingham et al., 2002) and we will therefore not employ them in this study. If we want to move further in the past, proxy-based reconstruc-

tions of surface temperature (e.g. Mann et al., 2009) and more precisely sea surface temperature (e.g. Keigwin, 1996; Calvo et al., 2002; Jiang et al., 2005; Sejrup et al., 2010; Sicre et al., 2011; Spielhagen et al., 2011) are available but the temporal and spatial coverage is lower and the uncertainties of the data larger. Considering the nature of the available data, the procedure introduced in the present chapter seeks to reproduce correctly the evolution of the intensity of the MOC assimilating only surface data of temperature and pressure. We follow the hypothesis that the link between the atmosphere and the MOC is sufficiently strong so that atmospheric variability controls the evolution of the MOC strength. For instance, previous studies using the model LOVECLIM proved that the wind forcing plays a substantial role in maintaining the MOC (Timmermann and Goosse, 2004). The main question that we try to answer in the present study is: is the knowledge of those surface data enough to reproduce adequately the evolution of the intensity of the MOC in our model or is it impossible to avoid using 3D data when seeking for reconstructing the MOC?

4.2 The North Atlantic meridional overturning circulation

4.2.1 Importance and past evolution of the MOC

The Atlantic meridional overturning circulation is one of the main agent responsible for the northward transport of heat in the North Atlantic Ocean. Indeed, at the surface, it carries northward warm tropical water via the Gulf Stream and the North Atlantic Drift, while a deep current of cold water flows southward (e.g. Bindoff et al., 2007; Lozier, 2012). This plays an important role in the Northern Hemisphere climate, since the release of the transported heat to the atmosphere contributes to the warming of Northern Europe, for example. It was proposed that variations in the MOC intensity may influence substantially the climate of the Northern Hemisphere, with global impacts, because of the associated modifications in the ocean heat transport (e.g. Vellinga and Wood, 2002). For these reasons, the analysis of such changes in the strength of the MOC during the recent and deeper past and in the future has been the focus of attention of numerous studies. However, robust conclusions regarding past changes in the strength of the MOC and underneath mechanisms are still lacking on all timescales (Bindoff et al., 2007). For instance, climate model intercomparison studies suggest that an increase in the concentration of greenhouse gases due to human activities could cause a weakening of the MOC strength (Gregory et al., 2005; Schmittner et al., 2005). Nevertheless, in spite of major efforts from several observational and modelling studies on observing this behaviour (see the sections below), it is still impossible

to affirm that the MOC associated to the present anthropogenic warming is currently slowing (Kerr, 2005).

It has been proposed that the climate of the North Atlantic region over the past millennium or during the Holocene has been influenced by fluctuations in the intensity of the MOC (Wanamaker et al., 2012; Denton and Broecker, 2008; Keigwin and Boyle, 2000). For instance, over the past millennium, events such as the Medieval Climate Anomaly (MCA) and the Little Ice Age (LIA) may have been influenced by the variations in the amount of heat transported by the MOC from lower to higher latitudes (Trouet et al., 2012; Miller et al., 2012), but the precise role played by those variations is still unknown. There are also evidences of several abrupt climate changes caused by sudden modifications of strength of the MOC during the last glacial period, the so-called Dansgaard-Oeschger events (Broecker and Denton, 1989), but the detailed description of those events should still be refined. As a consequence, large efforts are made in the observational data and modelling communities to characterize the MOC behaviour over the recent and distant past (see Sections 4.2.2 and 4.2.3), but the acquisition of new proxy data containing information about the MOC variability remains essential for the understanding of the link between MOC and climate changes (Wanamaker et al., 2012).

4.2.2 Observational estimates of the MOC variability

We describe here several recent studies whose goal was to provide continuous time series of the MOC. Five shipbased transatlantic sections at 26.5°N available for the period 1957-2004 were used to estimate the intensity of the MOC (Bryden et al., 2005). This study inferred a slowing of 30% (6 Sv) of the MOC between 1957 and 1992. However, even if this data highlights high short-term variability, the temporal sampling is too sparse to accurately estimate decadal variability or trends and the results are thus not highly robust (Cunningham et al., 2007). In 2004, a unique effort to provide a continuous monitoring of the MOC at the same latitude (26.5°N) started. It consists of measurements of zonal density gradients by moored profilers or sensors, completed by cable voltage measurements of mass transport across the Florida Straits, and satellite-based observations of wind stress (Cunningham et al., 2007; Baehr et al., 2007; Hirschi et al., 2003). Observations have also been taken at other locations, such as five hydrographic sections at 48°N (Lumpkin et al., 2008) between 1993 and 2000, and the transport at 41°N has been studied using satellite observations of sea surface height, combined with temperature, salinity and velocity data from profiling floats (Willis, 2010). More recently, an assessment of the variability of the MOC and associated heat flux across a

Greenland to Portugal line over 1993-2010 has been presented from six repeats of the OVIDE section, satellite altimetry and Argo float measurements (Mercier et al., 2013). Other processes related to MOC local changes have also been measured, such as the flux of the deep western boundary current (Schott et al., 2006), the convective activity in the Labrador Sea (Våge et al., 2009), or surface heat and freshwater fluxes (Josey et al., 2009).

On the basis of the available observations, Cunningham and Marsh (2010) mention in a recent review that observational estimates of the MOC during the 1990s and early 2000s generally show a decrease of its intensity, with magnitudes ranging from 1 to 3 Sv (e.g. Lherminier et al., 2007; Josey et al., 2009; Grist et al., 2009). However, no consensus is reached yet, since, for instance, another study (Lumpkin et al., 2008) shows no clear change in the MOC strength.

The data sets described above provide reliable information about the state of the MOC but are available for a very short time period, that is less than a decade. If we move back in time, we do not have any information aside from the data of Bryden et al. (2005) for the last 50 years, which are too scattered in time. To go back further in time, given the lack of longer instrumental records, geological proxy data able to provide information about the MOC are needed. For instance, Wanamaker et al. (2012) linked a shell-derived ^{14}C record from the North Icelandic shelf with the ocean circulation and concluded that the surface MOC was strong in medieval times and weak during the LIA, thus amplifying the warm conditions of the MCA and the cold conditions of the LIA in the North Atlantic region. Foraminifera from sediment cores in the Florida Straits were also used to show that the Gulf Stream experienced a reduced flow during the LIA (Lund et al., 2006).

4.2.3 Modelling studies of MOC changes

Models have also been used to study past changes of the MOC. A comparison of the different studies conducted is not straightforward, because of differences in the definitions and metrics used. A simple method using the available surface data is based on the close connection deduced from model results between the MOC and the large-scale sea surface temperature (SST) anomalies (Latif et al., 2006, 2004; Knight et al., 2005). In these studies, it is indeed suggested that the North Atlantic SST anomalies are a good predictor of the MOC anomalies, and by simply computing the difference in the observed SST between two regions located in the North and South Atlantic, we can infer the strength of the MOC. However, these findings are based on the results of a

particular climate model and more studies on the subject are thus necessary (Latif et al., 2004). Other modelling studies use oceanic and coupled climate model simulations to estimate the MOC variability (e.g. Swingedouw et al., 2013; Menary et al., 2013; Grist et al., 2009; Lozier et al., 2010; Drijfhout and Hazeleger, 2007; Böning et al., 2006; Marsh et al., 2005), but each individual study relies on the physics of a particular model, and could lead to different results. Finally, a different and more complex approach consists of ocean reanalysis experiments using advanced data assimilation techniques (Lee et al., 2011; Baehr, 2010; Balmaseda et al., 2007). Dynamically consistent oceanic state estimates can be obtained combining all available large-scale 3D ocean data sets and general circulation models. This has first been done for a 10-year period starting in 1992 (Wunsch and Heimbach, 2006; Stammer et al., 2002) and has then been extended back to 1952 (Köhl and Stammer, 2008).

No consensus can be found between all these different modelling studies, neither in the magnitude nor the sign of the MOC changes (Lozier et al., 2010; Cunningham and Marsh, 2010). The results can be divided in two opposing groups, either showing an increase or a decrease of the MOC intensity over the last few decades. Among the studies inferring an increase, Latif et al. (2006) suggest that the MOC strength increases since the 1980s, applying the proposed relationship between SST gradients and the MOC strength to SST observations. Knight et al. (2005) also infer an increase in the intensity of the MOC between the 1970s and 2000. A period of strong MOC is also suggested around 1950, compared to two weaker periods around 1920 and 1970. Menary et al. (2013) also suggest a 20% increase in the strength of the MOC between 1860 and 2005 and attribute a role in this strengthening to the anthropogenic aerosol forcing. Lozier et al. (2010) found a slight strengthening of the MOC in the subpolar gyre and a slight weakening in the subtropical one. Finally, according to the reanalysis from Lee et al. (2011) and Köhl and Stammer (2008), the MOC increased over the last 6 and 4 decades (before 2000) respectively.

On the other hand, several studies propose that a slowdown of the MOC took place in the recent decades, such as the one of Balmaseda et al. (2007) for the period 1959-2006. A comparison between 16 CMIP5 (Coupled Model Intercomparison Project) models is presented in Menary et al. (2013). The majority of model time series of MOC strength show a stable or declining AMOC since 1860; only two models exhibit a strengthening. The study of Drijfhout and Hazeleger (2007) also mention a weakening of the MOC in response to different increasing greenhouse gas concentration scenarios. Seemingly in opposition to Lozier et al. (2010), Marsh et al. (2005) simulation proposes a decline of the MOC in the northeast Atlantic of $\sim$20% over the 1990s, and an increase

in the subtropics, simulated at location where monitoring in underway. Grist et al. (2009), on the other hand, do not detect a trend within the high multi-decadal variability over the period 1958-2007. Baehr et al. (2007) study come to a similar conclusion.

4.3 Data assimilation method and experimental design

The evident conflicts between the results obtained by the different studies presented in the previous section justify the need for further investigations concerning the behaviour of the MOC. The absence of agreement between them unables us to draw solid conclusions about the past and current states of the MOC. The disadvantage of the more complete short-term studies available is that they make use of advanced techniques which require high computational time, complex climate models and subsurface oceanic data, and are then available only for the past few decades, 50 years uttermost. In this study, we present, in complement to all these different methods, an alternative approach to reconstruct the temporal evolution of the MOC for time periods extending from a century to a millennium, making use of a new data assimilation technique consisting in a particle filter.

4.3.1 The particle filter

The data assimilation method used in this study differs from the one presented in Chapter 2. Let's first recall the principle of this method, which was successfully applied in different past climate studies (e.g. Goosse et al., 2009; Crespin et al., 2009; Goosse et al., 2010b). In this method, the different members of an ensemble of model simulations and a proxy-based reconstruction of annual surface temperature, interpolated on the model grid, are compared using the Euclidean distance between the data and the model results (Eq. 2.1) to isolate, at each step of the analysis, the member of the ensemble that best reproduces the climate state represented by the proxies. If we call "particles" the different members of the ensemble of simulations, then this data assimilation method retains only one particle at each assimilation step, the closest one to the data. Taking into account that the average number of particles used in the published experiments mentioned above is almost a hundred, retaining only a single particle and discarding all the others results in the lost of a big part of the information from the ensemble. Furthermore, the uncertainty on proxy data was neglected in this method, leading to another important simplification.

In this chapter, we test a more sophisticated data assimilation scheme corresponding to an approach in which the information within the ensemble is used more efficiently. This is done by applying a particle filter with resampling, as described in van Leeuwen (2009). At each assimilation step, we select a significant fraction of the particles, each of them associated with a weight related to its agreement with observational data. It works in the following way. Starting from specified conditions, a different initial state is created for each particle by adding a small perturbation to the atmospheric streamfunction in the same way as in Chapter 2. The particles are propagated in time with the climate model for a period of one year. We assume that this finite number of random model states or particles represents well enough the statistical behaviour of the system. Then, we associate to each particle a weight that is computed according to its likelihood, which is computed from the difference between observations interpolated on the model grid and the simulated results at all available locations. The likelihood, which is based on a Gaussian probability density, is defined as the conditional probability of the observations given the model solution, i.e., it registers how "likely" is the observed data given the model state. The weight for each member of the ensemble i is computed as follows:

$$w_i = \frac{exp\left[-\frac{1}{2}(d - H(\psi_i))^T C^{-1}(d - H(\psi_i))\right]}{\sum_{j=1}^{N} exp\left[-\frac{1}{2}(d - H(\psi_i))^T C^{-1}(d - H(\psi_i))\right]} \tag{4.1}$$

Each ψ_i is a vector representing a variable of one of the N members of the ensemble, d is the observational data that contains information about that variable, H is an operator that selects the model values only at the grid points where the observations are available, and C is the error covariance matrix of the data. This last element corresponds to the discrepancy between the model results and the observations and adds up two different matrices, describing the instrument or the proxy errors (assumed to be uncorrelated) and an error of representativeness, corresponding to the misfit between the spatial scale of a coarse resolution model such as LOVECLIM and the spatial scale of the observational data. The latter is approximated using the internal variability of the model (the covariance between states variables in a long control model run), including a scale parameter chosen to be of the order of one but that could vary between applications. The fact that the uncertainties in the observations play a role in the computation of the likelihood constitutes an improvement compared to the previous version of the method where data were

considered as perfect.

After a weight is attached to each particle, we proceed to the resampling following Liu and Chen (1998). The particles with largest weights are duplicated multiple times, while small weight particles are eliminated. The best estimate of the state is given by the sum of the results of each particles multiplied by the corresponding weight. The number of copies of high-weight particles is proportional to their weight, and the total number of particles remains equal to N. The new weight of each particle is then set to one, and the atmospheric streamfunction of the copied particles is perturbed again to obtain different model initial states for the next step. The model is then propagated again in time until the subsequent year and the whole procedure is repeated until the final year. More details about the method are given in Dubinkina et al. (2011).

When using a particle filter, caution has to be taken to avoid filter degeneracy. This may occur when, after a few analysis steps, the large majority of particles drift far away from the observations. Consequently, only one or a very low number of particles get all the weights while all the other particles have an almost zero weight. The following steps of assimilation will then start from a very reduced number of model states and the system has high probability to be maintained in a state differing significantly from the observations. Note that the previous version of the method can be considered as a degenerated particle filter, as only one particle was kept at each assimilation step. A particle filter can degenerate because of the large spatial and temporal scales involved in the problem, and the large space state cannot be entirely represented by the particles. In order to avoid dealing with this filter degeneracy, the computation of the annual mean is performed and a spatial filter retaining only the large-scales is applied to the data before calculating the likelihood, as this helps reducing the number of degrees of freedom of the climate system. Indeed, filtered fields have lower spatial degrees of freedom and lower dimensionality of state space. The number of particles needed to represent all these degrees of freedom is required to be large, in order to cover a sufficiently wide range of internal variability compared to the observed one. Besides, the number should be small enough to avoid prohibitive computational costs. The use of an intermediate complexity model such as LOVECLIM is then adequate for its implementation, because of its key advantage regarding low computing demands (reduced mainly thanks to important simplifications applied to the atmospheric component). A too small number of members may also cause a problem of degeneracy of the method, that is why the choice of the number of particles needed to reproduce correctly the observations has to be determined properly.

4.3.2 Twin experiments

The present study focuses first on testing the ability of the new data assimilation method to detect changes in the MOC at decadal timescales in an idealized framework. As the main source of data over past periods consists of surface observations of temperature and, since the mid-19th century, surface observations of pressure, these data will be assimilated in the model with the purpose to try reproducing correctly the evolution of the MOC intensity. However, as we do not have any accurate reconstruction of MOC variability for the past centuries, the results that could be obtained after assimilating observations of surface temperature or pressure cannot be compared with or validated by real observations of the state of the MOC. A way to test the validity of the method, i.e., to determine if the data and the assimilation scheme could work for real data, is then to perform what is called "twin experiments", also referred to as perfect model approach. In these experiments, the assimilated data is extracted from a simulation performed by the same model than the one used to run the data assimilation experiments, replacing the real observations (after adding a small perturbation). This data, called pseudo-observations, is assimilated in a model run starting from independent initial conditions. The target, the MOC intensity, is then well defined and is used to test whether the state of the MOC can be estimated correctly by this method. The advantage of this procedure is that it allows us focusing just on the data assimilation method, as uncertainties in forcing or model physics have no influence on the results.

4.3.3 Experiments over the period 1850-2005

In a second phase, we perform simulations using real observations of surface temperature from the HadCRUT3 dataset (Brohan et al., 2006). The experiments start in 1850 and run for 155 years. The data assimilation method is used in the same way than before. All natural and anthropogenic forcings described in Chapter 3 are used. One experiment is conducted using all the available data north of 30°N and another using only the data in the North Atlantic region. Those two experiments are performed to test the robustness of the results. For comparison, an ensemble of 10 experiments without data assimilation is also performed over the same period and with the same forcings. The mean over those 10 members is presented in the Section 4.4.

4.3.4 Experimental design

The Earth system model of intermediate complexity LOVECLIM (Goosse et al., 2010a), described briefly in Chapters 2 and 3, was used to perform all the fol-

lowing simulations. A first run was performed, starting from equilibrium initial conditions, to generate the data used as the pseudo-observations for the subsequent data assimilation experiments. No external forcings were used in this simulation. The last 100 years of the simulation, which was run for 500 years, were taken as pseudo-observations, to ensure an equilibrium state. We make sure afterwards to start our data assimilation experiments from different initial conditions than those of the pseudo-observations, since starting from "perfect" initial conditions is not conceivable in real test cases. In order to mimic the error associated with real instrumental or proxy data, a Gaussian error term or noise was added to these pseudo-observations.

In a first step, in order to compare the new particle filter with the previous method used in Chapter 2 (referred to as the simplified version of the method from now on), we use the maximum of the MOC strength as the observed variable. This corresponds to the most favorable case in which the MOC is already well-known from observations. Of course, having direct observations of the MOC would exempt us from doing data assimilation. The purpose of this approach is actually to test the improvements of the new particle filter concerning the spread of oceanic variables in the ensemble. Then, two different variables were used as pseudo-observations to perform different test cases: the surface temperature and the 800 hPa geopotential height, which corresponds to the variable closest to surface pressure in the model.

A spatial filter is applied to the data before calculating the likelihood. This filter emphasizes the contribution of large-scale structures by removing spatial variations with scales lower than a few thousand kilometers. We also restrict the data assimilation to the region northwards of 30°N. This region is selected because the skill of LOVECLIM is much higher in the extra-tropics than in tropical regions (Goosse et al., 2010a). These two factors help reducing the degrees of freedom. The optimal choice concerning the number of particles has been studied in Goosse et al. (2006b) and Dubinkina et al. (2011). Some test run with different total number of particles were also carried out in the context of the present study. We used 96 particles, as those experiments have shown that such a number represent a good compromise between a good agreement between model results and observations and a reasonable computational cost.

In real cases, the error of the observational data is derived from the characteristics of instruments and of the observation network. In the case of the twin experiments, the value is taken according to the Gaussian noise added to the pseudo-observations. For the parameter scaling the representativeness error, some freedom is available. In the case of experiments with pseudo-

observations, the error of representativeness is small and hence the parameter too. Only the tests with the most satisfactory results are shown in the following section. For the simulation over the period 1850-2005, all the natural and anthropogenic forcings described in Chapter 3 are used. The initial conditions come from a long simulation run over the past millennium.

4.4 Results of the simulations performed with LOVECLIM

4.4.1 Test of the validity of the method

We first present the idealized experiments carried out in order to test the validity of the method, assuming that we do have reliable observations of the MOC strength. In LOVECLIM, we use the maximum of the intensity of the MOC in the North Atlantic between latitudes 45°N and 75°N as an index of the MOC strength. A first experiment was performed using the simplified version of the technique, assimilating directly pseudo-observations of the MOC maximum, in which we added a Gaussian error term of standard deviation 0.5 Sv (about $1/4$ of the variable standard deviation) to represent the uncertainty (an observation error). This test identifies a weakness of the simplified method when dealing with oceanic variables. In Chapter 2, we showed a very weak oceanic response to temperature changes in our model, probably due to the experimental design (Fig. 2.9). Goosse et al. (2010b) also pointed out that the dynamics of the ocean may not be perturbed enough during the generation of the different members of the ensemble. Those are created by introducing small perturbations in the quasi-geostrophic potential vorticity field of the atmosphere, thus favouring the generation of rapid perturbations in the atmospheric dynamics rather than in the ocean. This leads to a very small range of oceanic states in the model, as can be seen in Fig. 4.1a, where, at each time step, all the particles of the ensemble are represented in grey and the best one in black. Each particle propagates in similar directions, resulting in oceanic states that can quickly differ from the observations (in blue). Once the initial model states are far from the observations, the probability to find a particle close to the observations in the very small range of oceanic states obtained after one year of simulation becomes very low. We can then point out here that, unless we have a significant range in the initial conditions in the data assimilation procedure, the model cannot be constrained properly to follow the observations. Perturbing only the initial conditions of the best member of the ensemble at each time step is thus not sufficient to obtain a large enough range of climate states in the ocean.

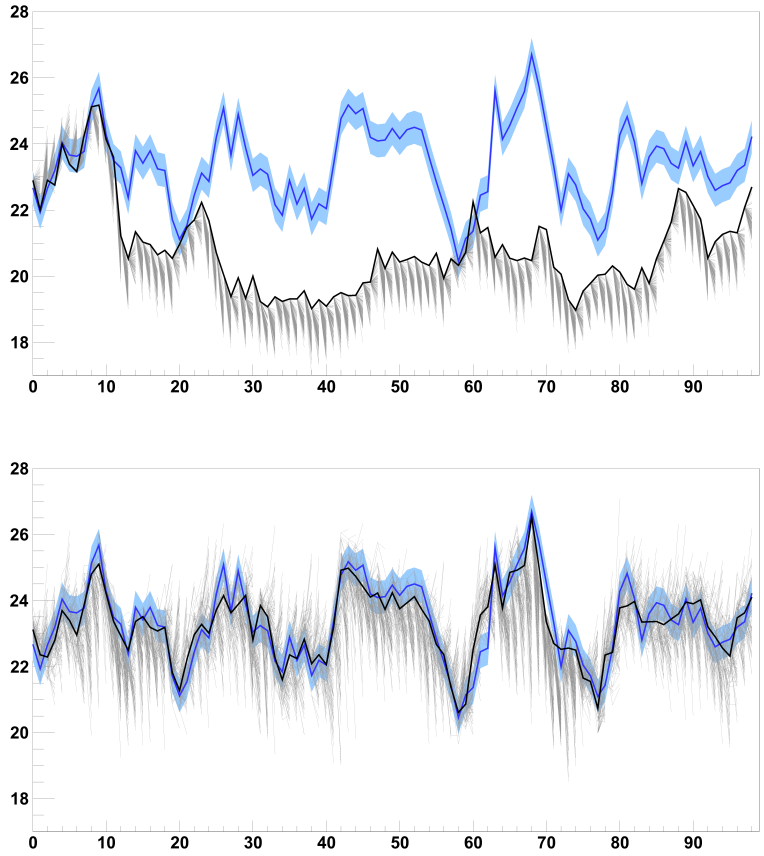

Figure 4.1: Time series of the annual mean of the MOC maximum in the North Atlantic (Sv). The blue line represents the pseudo-observations with a 0.5 Sv range, and the black line corresponds to the result of the model simulations performed with (a) the simplified version of the technique and (b) the particle filter, accompanied at each assimilation step by all 96 members of the ensemble in grey. The assimilated variable is the maximum of the MOC in the North Atlantic.

When using the new particle filter, on the other hand, a much larger dispersion of the initial conditions at the beginning of each time step can be obtained (Fig. 4.1b), since the different members are not generated from only one single model state but from a larger ensemble of initial conditions. The spread within the ensemble members is much more important and the observations

are then more likely to fall within the range of simulated model states. This leads to a huge improvement in the results, with a correlation between the pseudo-observations and the model results obtained applying the particle filter reaching 0.93.

4.4.2 Assimilating pseudo-observations of temperature and geopotential height

As direct MOC observations are not available in real conditions, we now want to test if the assimilation of pseudo-observations of surface temperature (taken over the entire region north of 30°N) using the new particle filter helps the model to reproduce correctly the changes in MOC strength. A Gaussian error term of standard deviation 0.5°C is added to the pseudo-observations of temperature to mimic the instrumentation error. In addition, in order to take into account the uncertainties related to the estimation of forcings used in climate model simulations, each particle is driven by a small random forcing, following a Gaussian distribution. The results obtained in this experiment prove that knowing only the surface temperature data can help constraining the evolution of the MOC. Figure 4.2 presents this evolution, in blue for the pseudo-observations and in black for the mean of the model ensemble, plus and minus one standard deviation of the ensemble (in grey). The correlation

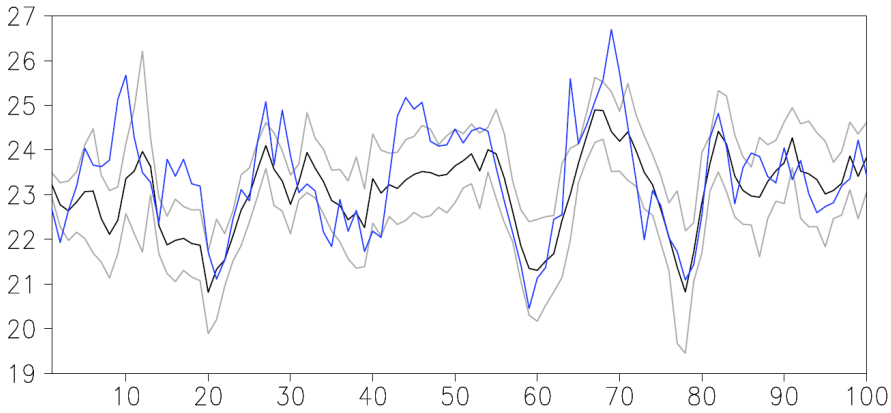

Figure 4.2: Time series of the annual mean of the MOC maximum in the North Atlantic (Sv). The blue line represents the pseudo-observations, and the black line corresponds to the result of the model simulation constrained by pseudo-observations of surface temperature using the particle filter. The grey lines are the mean of the ensemble plus and minus one standard deviation of the ensemble.

between the MOC pseudo-observations and the MOC obtained by the model with data assimilation is equal to 0.69. It can be observed that the pseudo-observations of the MOC lie within one standard deviation of the ensemble mostly in the second half of the simulation. At the beginning of the simulation, the model needs some time to adjust after being started from an initial state differing from the pseudo-observations, as it can be seen by the disagreement between the two curves during the first two decades of the experiment. Without taking into account these two decades, the computation of the correlation reaches 0.79.

The changes in meridional oceanic heat transport are depicted in Fig. 4.3. For this variable, the decadal variability is also similar between the pseudo-observations and the model results, except at the beginning of the simulation that presents a much lower variability. Regarding the surface temperature (not shown), the variable that has been assimilated, the correlation between the mean Northern Hemisphere temperature derived from the pseudo-observations and the model results is also equal to 0.7, and the variability of the modeled temperature is smaller than in the pseudo-observations, a classical feature in data assimilation methods using ensembles (Annan and Hargreaves, 2012).

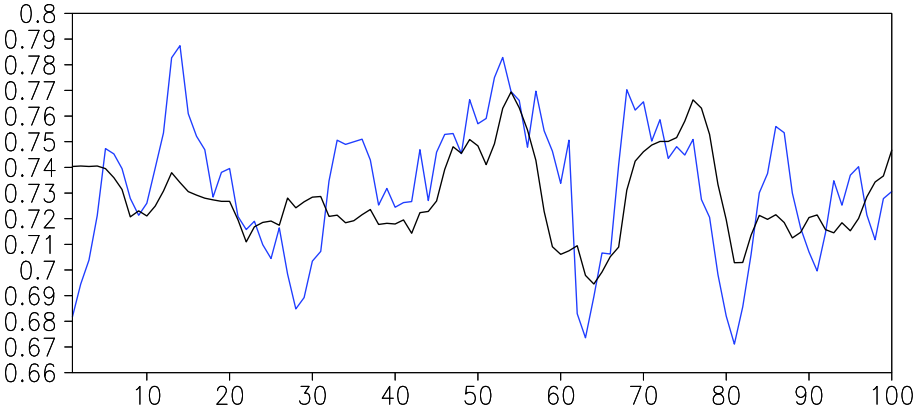

Figure 4.3: Time series of the annual mean meridional oceanic heat transport in the North Atlantic Ocean at 30°N (*PW*). The blue line represents the pseudo-observations, and the black line corresponds to the result of the model simulation constrained by pseudo-observations of surface temperature using the particle filter. A 5-year running mean has been applied to the time series.

In another experiment, we assimilate the 800 *hPa* geopotential height. This variable is the closest to the surface pressure in LOVECLIM. This experiment (Fig. 4.4) was conducted to evaluate the capacity of the model to reproduce the MOC with the information of wind patterns. The MOC is characterized by both a density-driven circulation (often called thermohaline circulation) and a wind-driven circulation, and the latter one plays a substantial role in maintaining the MOC (e.g. Timmermann and Goosse, 2004). Constraining the model with data of geopotential height could thus help reaching our goal. We obtain a correlation of 0.55, which is reasonable but less satisfying than the experiment with pseudo-observations of temperature.

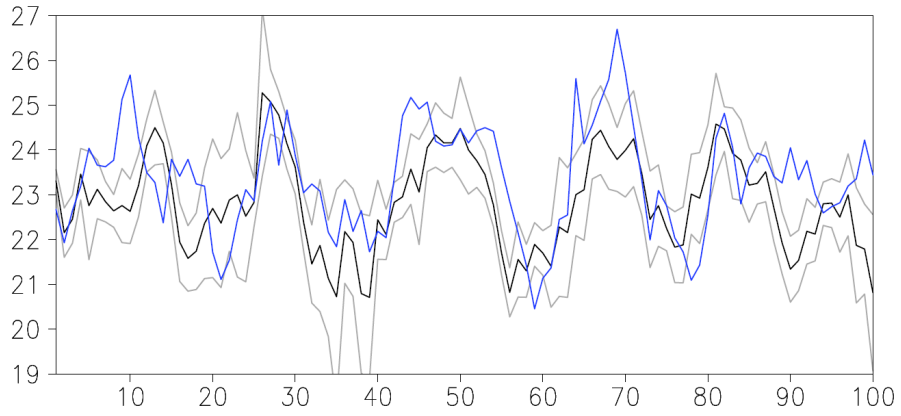

Figure 4.4: Time series of the annual mean of the MOC maximum in the North Atlantic (*Sv*). The blue line represents the pseudo-observations, and the black line corresponds to the result of the model simulation constrained by pseudo-observations of 800 *hPa* geopotential height using the particle filter. The grey lines are the mean of the ensemble plus and minus one standard deviation of the ensemble.

4.4.3 Assimilating real surface temperature observations

Considering that observations of surface temperature provide a good constraint to the MOC, and keeping in mind the weaknesses of the method (discussed also in Section 4.5), we used this property to study the behaviour of the MOC during the past 155 years by assimilating instrumental data of surface temperature (Brohan et al., 2006). The comparison between two different experiments, one performed using all the data available in the Northern Hemisphere northwards of 30°N (ALL experiment) and another one using only the data of the North Atlantic region (0°- 80°W, 0°- 75°N) (ATL experiment), pro-

vides an estimate about the robustness of the results. Indeed, as an important constraint of the MOC is coming from the North Atlantic in LOVECLIM, significant differences between the two experiments would indicate that the model is not constrained enough by the surface temperature.

The first verification consists of checking whether the observations of surface temperature have been assimilated correctly in the model. The evolution over the last 155 years of the mean surface temperature in the region northwards of 30°N is depicted in Fig. 4.5. The ALL and ATL experiments (in blue and green respectively) follow correctly the observations (in black). The peak of temperature observed around the year 1940 is satisfactorily reproduced in the data assimilation experiments. This constitutes an improvement compared to simulations without data assimilation (in red), since LOVECLIM does not simulate it when using only the natural and anthropogenic forcings. The correlation between the observations and the ALL and ATL experiments reaches 0.80 and 0.79, respectively, without applying any temporal filter, but this is not different from the correlation between the observations and the no assimilated experiment.

The MOC corresponding to that state of the climate can now be analysed and compared with other studies. The evolutions of the MOC strength in the ALL

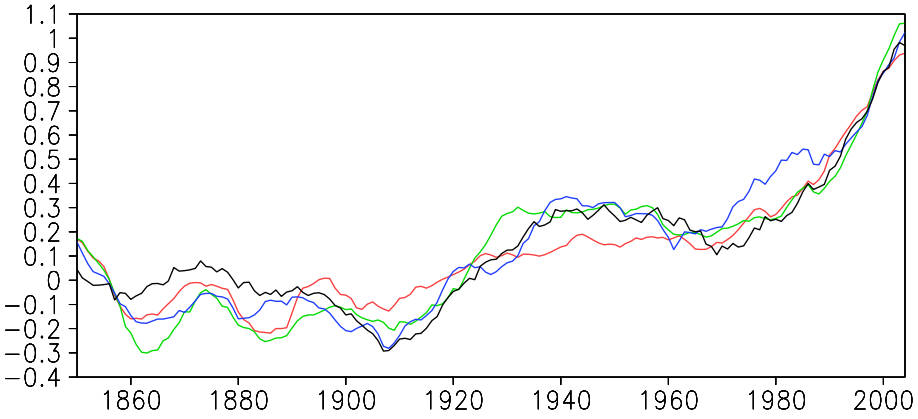

Figure 4.5: Anomaly in annual mean surface temperature (°C) for the Northern Hemisphere (region north of 30°N) over the past 155 years. The ALL experiment is in blue, the ATL experiment in green, the mean of an ensemble of 10 simulations made without data assimilation in red, and the observations in black. An 11-year running mean has been applied to the time series. The reference period is 1880-1950.

and ATL experiments show similar tendency and decadal variability (Fig. 4.6) (Corr = 0.42). Both experiments agree on a general decrease of the intensity of MOC since 1860 ($-0.10 \pm 0.04\ Sv/decade$ in ALL and $-0.15 \pm 0.03\ Sv/decade$ in ATL). This trend is close to the one obtained in the simulation without data assimilation ($-0.07 \pm 0.02\ Sv/decade$) and is thus likely related to the model response to forcing changes. ALL and ATL also display some clear episodes where the MOC strengthened. The most important peaks of the MOC are found approximately in 1860, 1920 and 1980 in both experiments. The simulation without data assimilation behaves in a similar way but with a lower decreasing trend and lower decadal variability. The assimilation of surface temperature in LOVECLIM results in a stronger decrease of the MOC than the one obtained using only external forcings.

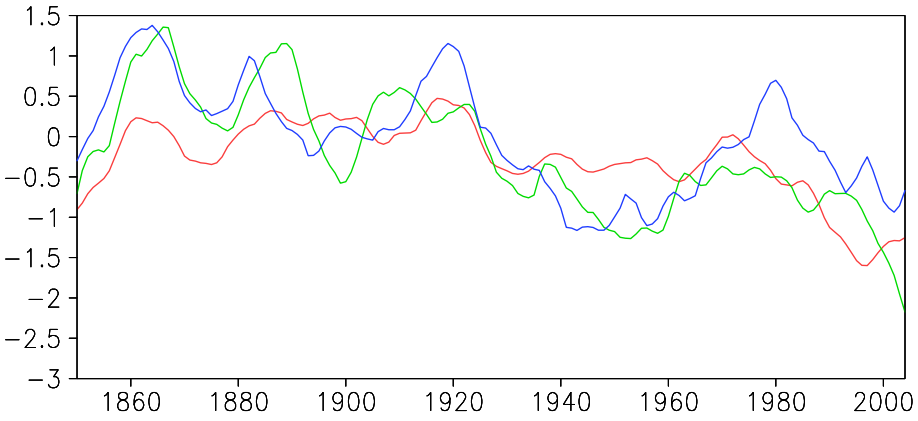

Figure 4.6: Time series of the annual mean of the MOC maximum anomaly in the North Atlantic (Sv). The ALL experiment is in blue, the ATL experiment in green, and the mean of an ensemble of 10 simulations made without data assimilation in red. An 11-year running mean has been applied to the time series. The reference period is 1880-1950.

Among the observational and modelling studies focusing on MOC changes over the last decades (Sections 4.2.2 and 4.2.3), some of them agree with our decreasing MOC, such as the studies presented in Menary et al. (2013) suggesting a decline in the MOC since 1860. The comparison is less convincing when it concerns very short time scales. For instance, in the review of Cunningham and Marsh (2010), the MOC between the 1990s and early 2000s showed a decrease in many studies, with a magnitude from 1 to 3 Sv. This is difficult to compare with LOVECLIM results, since no consistent trend between ATL and ALL is discernible for that short time period. Balmaseda et al. (2007) found a

decline of around 6 Sv during the period 1995-2005 at 25°N. Our simulations also suggest a decline but not such large amplitude. Our results also agree in part with the results of Köhl and Stammer (2008), who proposed an increase of the MOC of 4 Sv from the 1960s to the mid-1990s, followed by a decline. Our increase is not as high as theirs and ends approximately a decade earlier. In their study, Swingedouw et al. (2013) simulate two MOC maxima around 1980 and 1995. In our model, we find the first one, but the MOC then decreased almost continuously until the end of the simulation. Finally, a recent set of 10 ocean reanalyses reveals a general increase in the MOC magnitude at 45°N from 1960 to the mid 1990s followed by a decrease thereafter (Pohlmann et al., 2013). These results are in agreement with ours, with the difference that the strengthening of the MOC ends a decade earlier in LOVECLIM. The conclusions proposed by the existent studies are so diverse that we can state that the agreement between different reconstructions of the MOC changes over the last decades is not better between the different studies together than between LOVECLIM results and the other studies.

The processes responsible for those changes in the MOC can now be briefly discussed, a deeper analysis being out of the scope of this study. The main cause of a decline of the MOC in the North Atlantic in LOVECLIM is an increase of the surface temperature. If a warming of the air occurs, the ocean heat transfer from the ocean to the atmosphere is reduced, especially during winter, the season with the highest depth of convection. This results in an increase of the surface water temperature and hence a decrease of its density. A decrease in the surface heat flux from the ocean to the atmosphere and in the depth of convection can indeed be seen in the Nordic Seas in our simulations during a decrease of the MOC such as for instance between 1920 and 1950 (not shown). In our experiments, the peaks of high or low MOC intensity corresponds then approximately to periods of low or high air surface temperature in the North Atlantic, respectively, with a lag of several years due to the thermal inertia of the system.

4.5 Conclusions

First, we have proved that the new data assimilation method works successfully and constitutes a big improvement compared to the previous simplified version of the method (in which only one particle is kept at each assimilation step). The tests carried out within this study have highlighted the fact that a better use of the information within the ensemble is needed during the assimilation process compared to the previous method, otherwise the method might become degenerative. This is especially true when one deals with

oceanic variables. When one uses the particle filter with the same number of particles, the range of model states obtained at each time step is found to be wider and the chance to find a good analog of the observations within this range is bigger. This new data assimilation method has been used successfully in different studies about past climate (Dubinkina et al., 2011; Goosse et al., 2012c,b,a; Mathiot et al., 2013; Mairesse et al., 2013). The tests performed here contributed to its implementation.

In the twin experiments, we are able to satisfactory reproduce the evolution of the intensity of the MOC in our model using the information obtained from annual mean surface temperature. Less satisfactory results are obtained when one assimilates the geopotential height, suggesting that wind patterns may not constraint sufficiently the evolution of the MOC. We also tried to assimilate temperature and geopotential height at the same time, and no improvement is shown either. In this case, the degrees of freedom of the system are probably too high and the sample is then probably too small to have the chance to find particles displaying reasonable agreement with both the temperature and geopotential height.

The results obtained from the experiments using pseudo-observations of temperature suggest that our method can propose a reasonable reconstruction of the MOC evolution for the last 155 years making use only of surface air temperature data. The results display a general decline of the MOC over this period but with some episodes of stronger intensity. A LOVECLIM simulation without data assimilation for the same period also shows a decreasing trend, but with a much lower decadal variability. The higher variability of the MOC obtained with the assimilation of surface temperature data in the model is consistent with the simulated temperature. For instance, the data assimilation helps the model to follow the 1940 peak of temperature, and consequently simulates a MOC minimum at this time, which was not present in the experiment without data assimilation. We have to keep in mind that those results depend on the physics of LOVECLIM, and the use of a different model could of course lead to different results. However, the method ensures that the results obtained are in agreement not only with the physics of the model, but also with the observational data.

Although our results are in good agreement with some other studies, several other ones do not present the same conclusions. According to Balmaseda et al. (2007), no consistent evidence of a trend in the MOC over the last 50 years exists because of the conflict between observational and modelling studies. Cunningham and Marsh (2010) also warn that the available observations of

the MOC are still not long enough to detect a trend or to attribute some climate variability to MOC changes, and that another several decades of measurement would be necessary. However, for the most recent period, i.e., the last decade, observations of the strength of the MOC show a decline, which is suggested by Robson et al. (2014), using observations and model simulations, to be part of a long-term reduction of the MOC instead of a temporary fluctuation. Here we propose a new reconstruction of the evolution of the MOC but, for the reasons just mentioned, it is impossible to further test its validity compared to other studies. The twin experiments gives reasonably good results, but certainly not sufficiently good to be confident about our method being able to provide a totally reliable reconstruction. The differences and lack of robustness between the tests conducted here (ALL and ATL experiments, and several other similar tests not shown) lead us to conclude that, even if the information of surface temperature helps to constrain the MOC, it is not enough to have an accurate estimate of interannual variations of the MOC. A solution, for instance, would be to use a more complete set of data in the assimilation process to even better constrain the ocean dynamics, essentially 3D oceanic data. However, this is unfortunately not conceivable for long-term studies, as this kind of data is available only for the recent decades. The study presented in this chapter has thus pointed out the interest but also the limitations of our methodology, leaving the question about past reconstructions of the MOC still open.

CHAPTER 5

ASSIMILATION OF INDIVIDUAL ARCTIC PROXY RECORDS IN LOVECLIM: IMPACT OF THE CALIBRATION METHOD ON THE RESULTS

5.1 Introduction

Different statistical methods can be used to calibrate proxy records against local temperatures and to combine them in order to provide reconstructions of hemispheric or global mean temperature, or to reconstruct entire climate fields, e.g. spatial patterns of past surface temperature (Section 1.2). In the previous studies performed using our data assimilation methods, both local and field reconstructions of surface temperature based on proxy records were used. First, 56 individual local proxy-based reconstructions of temperature (Mann et al., 2008) have been directly assimilated in LOVECLIM using the simplified data assimilation method (Crespin et al., 2009; Goosse et al., 2009, 2010b). The selected time series span at least the last 6 centuries and were scaled locally to instrumental data as described in Chapter 2. Second, in more recent studies (Goosse et al., 2012c,b), the improved version of the data assimilation method (detailed in Chapter 4) has been applied in LOVECLIM.

In those studies, the data constraint is not anymore based on the individual proxies but on the large-scale surface temperature spatial reconstruction from Mann et al. (2009), which spans the past 1500 years and uses a larger network of 1209 proxies. The 56 individual series used in the first studies were processed to obtain a homogeneous data set. The records with sub-annual resolution were converted to annual mean values, and the records available only at decadal resolution were interpolated to annual resolution. As both annually and decadally-resolved records were selected, they were all decadally-smoothed in order to have a common effective temporal resolution. If a grid-box of the model included more than one proxy, the average was taken before being scaled to the nearest instrumental grid box. The second reconstruction also has a decadal resolution and focuses on large-scale features (Mann et al., 2009). Those procedures result in smoothed time series, or spatially smoothed fields, that can be efficiently assimilated in LOVECLIM (e.g. Goosse et al., 2010b, 2012c,b).

Because of this temporal and/or spatial filtering, part of the information included in the recorded signal is lost. Consequently, in the present study, we conduct simulations with the new data assimilation method (Section 4.3.1) but using directly the raw local proxy-based reconstructions, taking advantage of additional proxies available over the Arctic to complete the coverage in this region. The aim of this chapter is similar to the one of Chapter 2, that is, to obtain a model simulation of past Arctic climate that would be in good agreement with all proxies located in that region. Like in Chapter 2, the a priori goal was to provide a deeper understanding of mechanisms explaining warm episodes during the past millennium, but, as explained below, our focus progressively changed to methodological issues. The novelty of the present study is the use of the improved version of the data assimilation method and an enlarged proxy coverage, as well as different ways to process proxy data before the assimilation. The additional proxy series are selected according to the significance of their correlation with local temperature, in order to obtain an estimate of temperature variations at the model grid scale (see Section 5.2.2). The time series are centered and scaled to produce an estimate of the target climate variable. The scaling coefficient can be determined in various ways (Jones et al., 2009). Here we focus on the influence of the choice of this coefficient on the results of our data assimilation simulations. Three different ways to determine this coefficient of calibration are tested: (1) matching the variance of the record to the one of the temperature record, (2) regression of the proxy record onto the temperature (direct regression), and (3) regression of the temperature onto the proxy record (inverse regression). By using the raw individual proxies, we do not have to rely on reconstructions that assume

a stability of the teleconnections (Section 1.2) as done in the previous simulations with data assimilation using this new method. However, we still have to rely on the stationarity of the link between the proxy time series and local temperature.

In the first part of this chapter, we present the experimental design, and we describe the proxy network as well as the different calibration methods. The results obtained using reconstructions calibrated in different ways are compared in Section 5.3.1, and the results of the most satisfying simulations are analysed and described in more detail in Section 5.3.2.

5.2 Method and data

5.2.1 Proxy data set

The additional proxy data used in this study have been compiled by the PAGES Working Group on Arctic climate during the last two millennia (Arctic2k, http://www.pages-igbp.org/workinggroups/arctic2k). This group is part of the PAGES 2k Network, composed by 9 regional working groups, focusing on 8 continental-scale regions and the oceans (PAGES 2k Consortium, 2013). In this framework, 52 time series have been selected for the Arctic region, defined as the region located north of 60°N. The climate parameter recorded by those proxies is considered to be the temperature, but the relationship between the signal and temperature is not always thought to be linear. The part of the year represented in the signal varies between the different proxy records. Some of them reflect annual conditions, but many are representative of just one month or season. The proxy sources are diverse but are essentially coming from lake sediments, ice cores and tree rings, and to a lesser extent from speleothems, marine sediments and historic documents. The set of proxy data is publicly available (PAGES 2k Consortium, 2013).

After a selection among those records, explained in the following subsection, 10 series have been retained here (Table 5.1). Eight of those proxies come from tree rings and two from ice cores. The period covered by the records starts in -100 AD for the longest and 1259 AD for the shortest time series, and finishes between 1973 AD and 2007 AD. Those new records were combined with the proxy series from Mann et al. (2008), already used in Chapter 2, to obtain a good coverage for the whole Northern Hemisphere. The locations of all the proxies in the Arctic are depicted in Fig. 5.1.

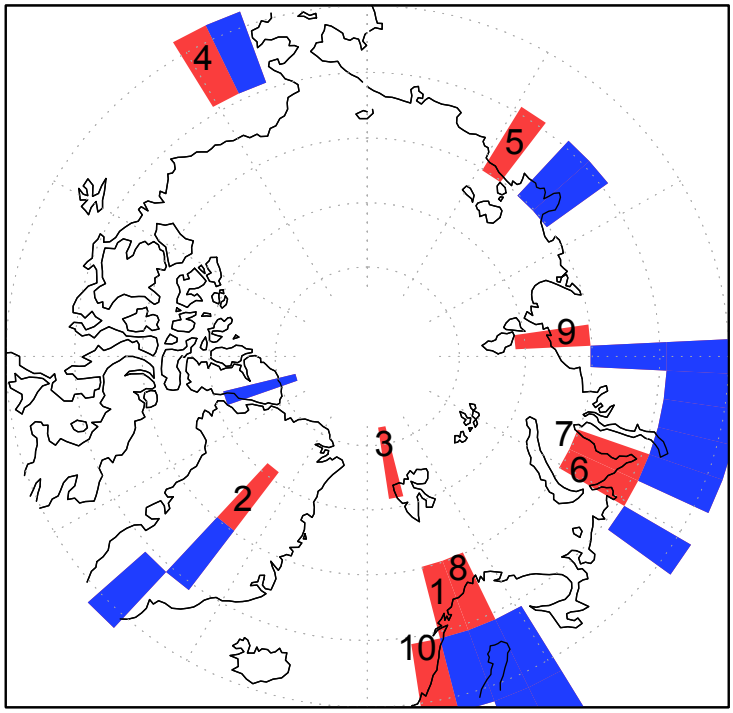

Figure 5.1: Location of the model gridboxes that contains the 26 proxies in the Arctic region. The red boxes are the 10 new proxies from PAGES 2k and the blue ones are from Mann et al. (2008).

5.2.2 Screening procedure

The new proxy records were required to meet a series of objective criteria to be included in the study. First, they must extend back to at least 1400 AD, as in Chapter 2. Secondly, only the proxy records having an annual resolution have been kept, corresponding to 34 over the 52 proxies of the database. Lower resolution proxies, such as those derived from marine sediment cores for instance, were excluded since they do not allow a meaningful calibration against instrumental data. They have indeed too few degrees of freedom over the instrumental period, with data available only for the last one or two centuries at the best. Finally, the proxies had to be significantly correlated with co-located instrumental temperature data. In order to be coherent when merging the two data sets, a similar screening procedure as in Mann et al. (2008) is applied here. Each series was required to have a statistically significant correlation ($p < 0.10$) with the closest instrumental surface temperature gridbox. This correlation is computed over the entire common time period between proxy

Proxy	Reference	Site	Coordinates	Proxy type	Period	Season represented	Corr.
1	Grudd (2008)	Scandinavia	68.26°N 19.6°E	Tree ring	500-2004	Summer	0.65
2	Vinther et al. (2010)	Greenland	71.12°N 37.32°W	Ice core	553-1973	Annual	0.17
3	Divine et al. (2011)	North Atlantic	78.25°N 15.5°E	Ice core	769-1997	Dec-Feb	0.25
4	D'Arrigo et al. (2006)	Alaska	61.03°N 146.59°W	Tree ring	724-2002	Annual	0.23
5	Hughes et al. (1999)	Eastern Russia	69.5°N 147°E	Tree ring	1259-1994	Jun-Jul	0.41
6	Esper et al. (2002)	Central Russia	66.83°N 65.75°E	Tree ring	778-1990	Jun-Jul	0.50
7	Briffa et al. (2008)	Central Russia	67.5°N 70°E	Tree ring	1-1996	Jun-Jul	0.53
8	Helama et al. (2010)	Scandinavia	69°N 25°E	Tree ring	0-2005	Jun-Jul	0.44
9	Briffa et al. (2008)	Central Russia	72°N 101°E	Tree ring	-100-2003	Jun-Jul	0.46
10	Gunnarson et al. (2011)	Scandinavia	63.5°N 15.5°E	Tree ring	1107-2007	Summer	0.64

Table 5.1: Description of the 10 additional proxy records included in this study. The last column corresponds to the correlation between the proxy data and HadCRUT3 instrumental data over the calibration period. The calibrations of proxies 2 and 5 are performed with an instrumental data located next to the nearest gridbox, owing to the scarcity of data in the region.

and instrumental data to have the largest number of degrees of freedom (Table 5.1). It is estimated for annual, seasonal or monthly averages according to the seasonal sensitivity of the proxy.

The instrumental data used to assess the climate signal in the proxy is the HadCRUT3 surface temperature observations (Brohan et al., 2006), with $5^\circ \times 5^\circ$ resolution. This calibration against local temperature instrumental data is challenging in a region such as the Arctic, where data are very sparse. In the case instrumental data are not available in the gridbox where the proxy record is located, a neighboring grid point is taken.

5.2.3 Calibration of proxies against instrumental temperature data

After the screening of the proxy data, the local temperature is reconstructed through a linear regression using the HadCRUT3 data. Simple standard methods determine the relationship between the two series over a calibration period during which they are both available. The climate variable of interest is then deduced from this relationship over the whole reconstruction period (e.g. Juckes et al., 2007). According to the method employed, different ways to carry out this operation can be considered (Jones et al., 2009). In this study, three different approaches of calibration have been used and tested. First, the variance of the proxy record is matched to the one of the instrumental record. We have also considered two different linear regression models, the direct and indirect regression, differing on the choice of the variable considered independent and the variable considered dependent. These different approaches are explained in the following subsections.

Matching variance

The calibration is performed here as it was done, for instance, by Mann et al. (2008) in the CPS (composite-plus-scale) approach (see also Mann and Jones, 2003; Moberg et al., 2005; D'Arrigo et al., 2006). This scaling approach consists in adjusting the mean and variance of the proxy to the instrumental temperature data over the calibration period (here the entire common time period between proxy and instrumental data). Each proxy record is first standardized by removing the long-term mean and by dividing it by the standard deviation. The proxy series is then centered so that the mean of the time series is equal to the mean of the target instrumental series, over the defined period of overlap, and finally multiplied to have the same standard deviation as the nearest available proxy data. This technique, referred to as "inflating" in statistical downscaling, is not meaningful according to von Storch (1999),

because it does not guarantee that the climatic signal have the right variance, since all local variability is not related to large-scale variability.

Direct regression

The direct regression is another CPS method (e.g. Briffa and Osborn, 2002). In this approach, we are interested in predicting the temperature T from the proxy time series P, and choose the temperature T as the dependent variable and the proxy data P as the independent variable. The corresponding equation is

$$T = \alpha P + \beta$$

where the equation coefficients α and β are determined by least square fit. This approach is known to significantly underestimate the amplitude of the variability and of the trends (e.g. Christiansen, 2011). Indeed, the reconstructed amplitudes are scaled by the correlation between T and P: $\alpha = \sigma_{P,T}/\sigma_P^2$, where $\sigma_{P,T}$ denotes the covariance and σ_P^2 the variance. Then $\alpha = \rho\sigma_T/\sigma_P$, where ρ is the correlation between T and P ($\rho < 1$, mostly on the order of 0.2 to 0.6 (Table 5.1)). Then, the variance of the estimated temperature T^* is $\sigma_{T^*}^2 = \rho^2\sigma_T^2 < \sigma_T^2$ (von Storch et al., 2004).

Indirect regression

Here, the calibration of each proxy against local temperature is done by regressing the proxy on the instrumental data and then by inverting the regression slope to predict the local temperature at each proxy location (Moberg, 2012). This is done, for instance, in the so-called LOC (local) method (Christiansen, 2011; Christiansen and Ljungqvist, 2011). The proxy data P is then the dependent variable and the temperature T is the independent variable. The indirect regression equation is

$$P = \gamma T + \delta$$

where the equation coefficients γ and δ are determined by least square fit. The equation relating a proxy P to the corresponding local temperature T is then

$$T = (P - \delta)/\gamma$$

The disadvantage of this method is that, preserving the low-frequency variability, it results in an exaggerated high-frequency variability (Moberg, 2012).

5.2.4 Experimental design

The model LOVECLIM, described in Sections 2.2 and 3.2, is constrained by the proxy-based reconstructions calibrated as explained in Section 5.2.3 using a particle filter. The data assimilation method is applied as in Chapter 4. Please refer to Section 4.3.1 for the details about this technique. The version of the model used here, LOVECLIM1.3, slightly differs from the version used in the 3 previous chapters, the main improvement is in the way the perturbations within the ensemble are applied in order to avoid a bias present in the previous approach. The perturbed variable is now the air surface temperature instead of the atmospheric streamfunction, as tests using this methodology have shown that it assumes a more symmetric distribution of the ensemble around its mean compared to the previous one. The experiments starts in 850 AD, the initial conditions being derived as for the simulations presented in Chapter 3. Three different simulations are conducted, differing in the way the assimilated reconstructions are calibrated: matching variance, direct regression and indirect regression. They are named VAR, DIR and IND, respectively. As the indirect regression calibration method provides a more noisy signal than the direct regression method, a larger proxy error is chosen in this case. This choice is made arbitrarily here. The value of the error is $2.0^{\circ}C$ for IND, compared to $0.5^{\circ}C$ for VAR and DIR. The scaling factor for the error of representativeness is fixed to 1.5. The choice of a different proxy error or scaling factor would lead to a different number of particles kept at each analysis step.

Acronym	Data assimilation method	Proxy series assimilated
NOD	None, Ensemble mean	None
ONE	None, Single simulation	None
SPA	Particle filter	Spatial reconstruction (Mann et al., 2009)
OLD	Simplified particle filter	(Mann et al., 2008) + new set of proxies, variance matching calibration
VAR	Particle filter	(Mann et al., 2008) + new set of proxies, variance matching calibration
DIR	Particle filter	(Mann et al., 2008) + new set of proxies, direct regression calibration
IND	Particle filter	(Mann et al., 2008) + new set of proxies, indirect regression calibration

Table 5.2: List of the experiments performed or analysed in this study.

A simulation, named OLD, is also run with the previous version of the data assimilation method (Chapter 2), using the proxies calibrated by matching variance. As the proxy records from Mann et al. (2008) end in 1996, the simulations are stopped at this time. Those simulations are compared with a simulation (SPA) in which the spatial reconstruction of temperature of Mann et al. (2009) was assimilated. The results of this experiment are discussed in Goosse et al. (2012c,b). An ensemble of 10 simulations without data assimilation (NOD) is also provided as a reference. This ensemble is similar to the one described in Chapter 3, but runs with the version 1.3 of LOVECLIM. Both the ensemble mean and a single member of this ensemble (ONE) are analysed, the latter being used to estimate the magnitude of the internal climate variability of LOVECLIM without data assimilation. A summary of the different experiments is given in Table 5.2.

5.3 Results

5.3.1 Comparison of the different simulations

By comparing the different types of simulations described above, this section aims to answer some questions about the methodology, both about the data assimilation method employed and about the proxy data used and the way to treat them. We can summarize those questions as follows.

- What are the skills and improvements of the new data assimilation method compared to the previous one?
- Are local constraints obtained by individual proxies enough to obtain good results at a much larger scale?
- What is the best way to calibrate local proxies in data assimilation experiments?

The main results of this section are grouped in Tables 5.3 to 5.7, where the model results are compared to proxy data through the computation of correlations. They are separated in two periods: the last 1150 years and the last 150 years. The surface temperature results of all the simulations performed in the framework of this study, for each location where the new proxies are available, are depicted in Fig. 5.2. The proxy-based reconstructions that have been calibrated by variance matching are also depicted. The reconstructions calibrated in a different way have the same evolution but different variances. The results are compared with the PAGES2k proxy-based reconstruction of Arctic temperature and the available instrumental data (Fig. 5.4 and 5.5).

Simulations without and with data assimilation

As already pointed out in the previous chapters of this thesis, the simulations performed with LOVECLIM without data assimilation, driven by anthropogenic and natural forcings over the last millennium, are able to capture the general tendencies of regional or global mean climate, but have nearly no skill at the local scale compared to observational and proxy data. As expected, the simulations with data assimilation using the new set of proxies (OLD, VAR, DIR and IND) provide surface temperatures that are locally much more consistent with those assimilated proxies than the results obtained from the simulations without data assimilation (NOD). This is true for the period covering the last millennium (Table 5.3, Fig. 5.2) as well as the industrial period (Table 5.4). The mean of the correlation between model and proxies at the 10 locations is almost zero for the NOD experiment for both periods.

The model results over the industrial period have also been compared with the instrumental data that have been used to calibrate the assimilated new set of proxies (Brohan et al., 2006). The correlation between those instrumental data and the proxies that passed the screening procedure is never very high, due to the fact that proxy data include not only a climatic signal, but also a residual variance, uncorrelated with the true state of the climate, considered as noise. On average for the 10 new proxies, this correlation is 0.43 (Table 5.1). The relatively weak common climatic signal between model results and HadCRUT3 data suggests that the signal to noise ratio is small in the proxies. The correlations between model simulations with data assimilation and the proxies over the industrial period are similar, and even better at some locations (Table 5.4). Unfortunately, the correlations between the simulated local temperature and the instrumental data at the locations of proxies (Table 5.5) are far from reaching the correlations obtained over the calibration period between the proxy and instrumental data. The improvement brought by data assimilation is much larger when the proxy themselves are considered instead of the HadCRUT3 data. This means that the simulations with data assimilation are not able to extract the climatic signal from the proxies but follow as well the non-climatic noise.

On a regional average over the Arctic (defined as the region located northward of 60°N), the quality of the results is not considerably different in the model without data assimilation than in the experiments with data assimilation. The correlation over the last millennium between the mean of the proxies in that region (10 new proxies + 16 proxies from Mann et al. (2008)) and the NOD experiment is nearly the same as the mean of the correlations for the four

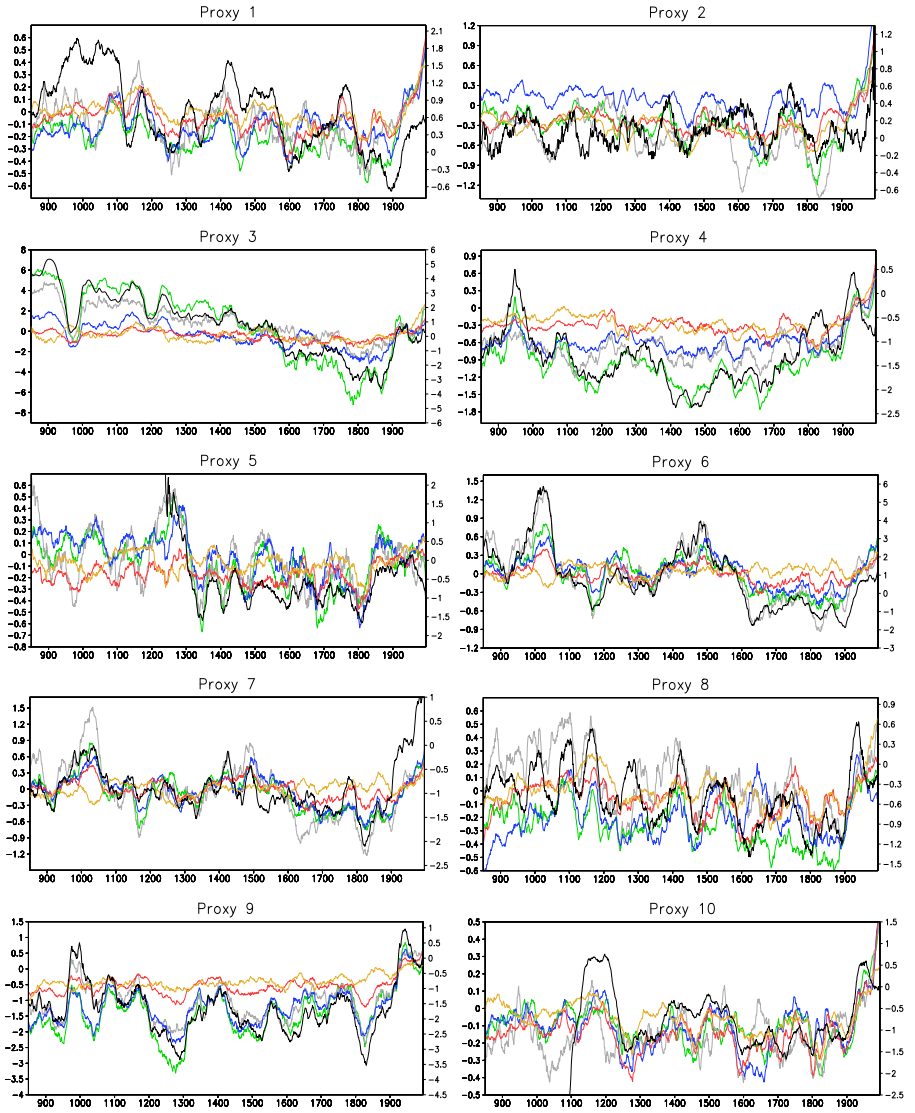

Figure 5.2: Time series of the proxy-based reconstructions calibrated by variance matching (black, right axis) and the surface temperature anomaly (°C) for the different model simulations (left axis): NOD (yellow), OLD (gray), VAR (blue), DIR (red), IND (green), for seasonal or annual mean, depending on the part of the year influencing the proxy signal (Table 5.1). The reference period is 1901-1970. A 41-year running mean has been applied to the time series. The correlation between each time series and the proxy-based reconstruction is given in Table 5.3.

mentioned simulations with data assimilation (Table 5.6). The correlation for the last 150 years is a little bit smaller in NOD compared to the others but remains similar. The reason of this relatively good correlation between the Arctic mean proxy series and NOD is interpreted here by the fact that the forcing anomalies are sufficiently strong to drive the dominant long-term tendencies. A single simulation (ONE) has a lower correlation, since the noise due to the internal variability masks the forced signal, which is not the case in an ensemble mean, where this noise is reduced because of the averaging. The results of the correlation with NOD have, however, to be taken with caution, because even though some long-term trends are correct, the multidecadal variability is less consistent. Some special events are not captured in this simulation, as for instance the warming peak in the 1930s (Figs. 5.3 and 5.4).

Proxy	NOD	ONE	SPA	OLD	VAR	DIR	IND
1	0.11	0.04	0.24	0.22	0.34	0.32	0.27
2	0.02	0.02	-0.04	0.21	0.30	0.09	0.60
3	0.04	0.07	0.08	0.42	0.51	0.22	0.82
4	0.10	0.02	0.20	0.34	0.43	0.15	0.71
5	0.03	0.00	-0.02	0.41	0.66	0.48	0.70
6	0.00	0.03	0.10	0.68	0.60	0.50	0.66
7	0.10	0.04	0.10	0.52	0.53	0.45	0.58
8	0.08	0.00	0.12	0.21	0.39	0.30	0.35
9	0.04	-0.01	0.03	0.66	0.78	0.66	0.81
10	0.23	0.09	0.31	0.16	0.41	0.35	0.27
Mean	0.08	0.03	0.11	0.38	0.50	0.35	0.58

Table 5.3: Local correlation for the 1147 years of simulations (850-1996) between the surface temperatures from each simulation and the individual proxy data.

Simple and improved data assimilation methods

The improvement obtained using the particle filter instead of the previous data assimilation method has already been illustrated for the ocean in the experiments performed in Chapter 4. In this study, the difference is not as marked, but some improvement can be pointed out, particularly at local scale. The comparison between experiments OLD and VAR over the entire past millennium (Table 5.3, Fig. 5.2) indicates a better correlation between individual proxies and model results at the proxy locations, at every point except one. The mean of the correlations at the 10 locations rises from 0.38 to 0.50. This indicates a better capacity of the particle filter to capture the local information of proxy records.

Proxy	NOD	ONE	SPA	OLD	VAR	DIR	IND
1	0.34	0.11	0.37	0.2	0.44	0.45	0.42
2	0.02	-0.06	-0.03	0.03	0.3	0.04	0.57
3	0.11	0.07	0.15	0.35	0.59	0.28	0.69
4	0.10	0.07	0.12	0.37	0.41	0.18	0.72
5	-0.10	-0.13	-0.1	0.26	0.66	0.45	0.68
6	0.07	-0.09	0.24	0.48	0.54	0.46	0.59
7	0.05	-0.04	0.16	0.46	0.59	0.47	0.66
8	0.10	-0.02	0.17	0.15	0.53	0.28	0.36
9	0.12	-0.01	0.06	0.58	0.86	0.71	0.85
10	0.30	0.26	0.51	0.07	0.42	0.46	0.37
Mean	0.11	0.02	0.16	0.30	0.53	0.38	0.59

Table 5.4: Local correlation over the period 1850-1996 between the surface temperatures from each simulation and the individual proxy data.

Location	NOD	ONE	SPA	OLD	VAR	DIR	IND
1	0.11	0.1	0.22	0.14	0.32	0.24	0.28
2	0.26	0.14	0.34	0.29	-0.01	0.28	0.33
3	-0.15	-0.03	-0.01	0.17	0.04	-0.07	0.11
4	0.07	-0.02	0.09	0.11	0.14	0.07	0.31
5	-0.13	-0.37	-0.05	-0.16	0.11	-0.13	0.08
6	0.12	-0.03	0.16	0.12	0.2	0.17	0.14
7	-0.10	-0.22	0.15	-0.14	0.08	-0.06	0.07
8	0.20	0.01	0.17	0.16	0.39	0.19	0.35
9	0.03	-0.09	0.18	0.07	-0.13	-0.1	-0.09
10	0.23	0.15	0.25	0.22	0.29	0.4	0.29
Mean	0.06	-0.04	0.15	0.10	0.14	0.10	0.19

Table 5.5: Local correlation over the period 1850-1996 between the surface temperatures from each simulation and the HadCRUT3 data, at the locations of the new proxy data.

Nevertheless, this seems not to be enough to improve the constraint at a larger scale. The correlation between the model results averaged over the Arctic region and the mean of the proxies is lower when using the particle filter (Table 5.6, Fig. 5.3). That means that the model, trying to follow as closely as possible each individual proxy (the correlation is sometimes locally higher between model simulations and proxies than between proxies and instrumental data), fails to catch the more global picture. This will be discussed in more detail in Section 5.4. Focusing the analysis over the last 150 years, the conclusions remain the same.

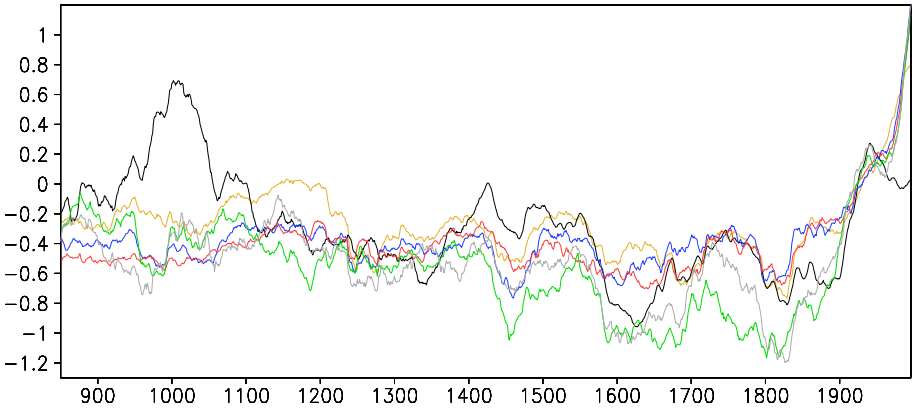

Figure 5.3: Anomaly in annual mean surface temperature (°C) averaged over the Arctic for the different model simulations: NOD (yellow), OLD (gray), VAR (blue), DIR (red), IND (green). The black line corresponds to the average of the proxy series used to constrain the model over the Arctic (calibration of the new proxies using variance matching). The reference period is 1901-1970. A 41-year running mean has been applied to the time series. The correlation between each time series and the proxies is given in Table 5.6.

An additional experiment has been run using the particle filter and only the proxies from Mann et al. (2008), as in Chapter 2, to analyse the effect of adding the new proxies (not shown). As expected, the correlation with the individual new proxies is similar to NOD. Those proxies are not used in the assimilation process and the constraint from the selected data is not able to bring consistent information at the location of those new proxies. However, interestingly enough, the correlation for the Arctic region between this experiment and the PAGES2k reconstruction over the last 1150 years (0.42), or the correlation with the mean of all the proxies over the last 150 years (0.73), is higher than for the experiments using also the 10 new proxies. This suggests that an incoherence between these new proxies prevents the model to find spatial patterns in good agreement with the Arctic mean (see Section 5.4).

Spatial and individual proxy-based reconstructions

The experiment conducted with a spatial reconstruction (SPA) demonstrates the higher consistency between model results and the assimilated data when the latter are processed and filtered via a statistical model (reconstruction from Mann et al. (2009)). Implicitely, using such an approach is a convenient way to take into account the limitations of the model. The filtering process reduces considerably the noise in the proxies, and the spatial coherency within the

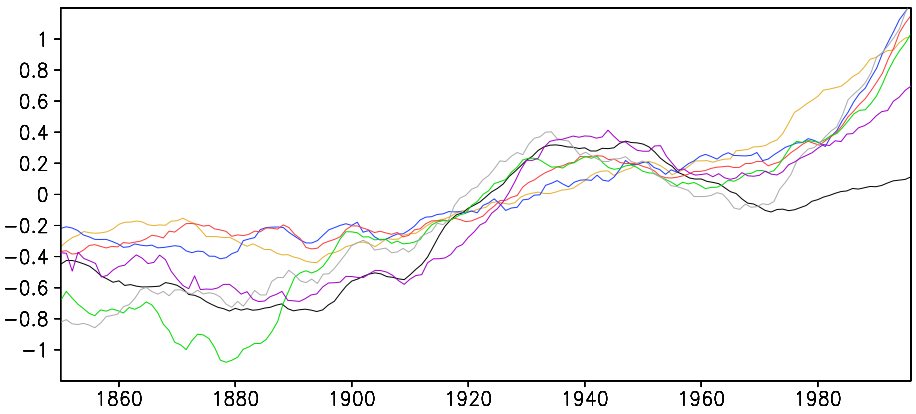

Figure 5.4: Anomaly in annual mean surface temperature (°C) averaged over the Arctic for the different model simulations: NOD (yellow), OLD (gray), VAR (blue), DIR (red), IND (green). The black line corresponds to the average of the proxy series used to constrain the model over the Arctic (calibration of the new proxies using variance matching) and the purple line to the HadCRUT3 data (Brohan et al., 2006). The reference period is 1901-1970. A 21-year running mean has been applied to the time series. The correlation between each time series and the proxies is given in Table 5.6.

data is much better compared to individual proxy records. Consequently, the model can more easily follow this clear large-scale spatial structure and then the Arctic mean. Indeed, the correlation between the Arctic mean temperature from the spatial reconstruction (not shown) and the model results is high in the SPA experiment (almost 0.80), and the correlation between the mean of the individual proxies and SPA is also higher than the correlations between the mean of the individual proxies and the experiments with assimilation of these proxies (Table 5.6). The correlation between the SPA experiment and the PAGES2k reconstruction is less satisfactory, which is explained by the fact that the selected proxy data and the reconstruction method are not the same than those of the spatial reconstruction. It is, however, the highest from all the experiments. On the other hand, this high consistency at the scale of the Arctic comes along with a much lower local correlation with the new individual proxy data, reaching a mean similar to NOD (0.11) (Table 5.3). Nevertheless, at the locations of the new proxies, the local correlation between model results and the spatial reconstruction assimilated in SPA is good, averaging 0.66 for the 5 series available in this area. This proves that there is not much local common signal between the individual new proxies and the spatial reconstruction from Mann et al. (2009).

	Corr with	NOD	ONE	SPA	OLD	VAR	DIR	IND
850-1996	Proxies mean	0.33	0.17	0.50	0.40	0.20	0.30	0.38
	Pages2k	0.41	0.21	0.48	0.35	0.29	0.32	0.36
1850-1996	Proxies mean	0.50	0.24	0.63	0.62	0.48	0.55	0.67
	HadCRUT3	0.48	0.28	0.60	0.47	0.38	0.44	0.47

Table 5.6: Correlation for the periods 850-1996 and 1850-1996 between Arctic mean temperature for each simulation and different time series: the mean over the Arctic of the set of proxy-based reconstructions used in this study (calibrated by variance matching, except for DIR and IND, where the corresponding calibration method is used), the Arctic reconstruction of PAGES2k, and the HadCRUT3 data averaged over the Arctic.

Effect of the proxies calibration method

Among the three different simulations using the particle filter (VAR, DIR and IND), the one that assimilates the proxies having been calibrated with the indirect regression method, IND, provides the best results, both at local and Arctic scales (Tables 5.3 to 5.6, Figs. 5.2 and 5.3). The local temperature correlations with the local proxy time series are better than any other simulation, reaching up to 0.82 at one location point, and the comparison with the Arctic mean series has a similar value than in OLD. On the other hand, the DIR experiment is clearly the less satisfactory one, with local correlations with the proxies similar to OLD.

The results obtained assimilating the new set of proxies are unfortunately not entirely satisfactory for Arctic mean conditions, since they do not bring any improvement to the agreement with Arctic mean proxy-based temperature reconstructions or HadCRUT3 data (Table 5.6). Here again, an incompatibility between the various proxies according to the physics of the model might be a possible explanation (see Section 5.4). The model is probably not able to follow all the time series simultaneously. As the average of the available proxies over the Arctic are not necessarily representative of the mean conditions in that region, the comparison is also made for the reconstruction of Arctic temperatures from the PAGES2k group (Table 5.6). The comparison with this reconstruction gives the same conclusions (Fig. 5.5, the only depicted experiment is IND to improve readability). The correlation between the mean of the individual proxy-based and PAGES2k reconstructions is 0.60 over the period 850-1996 and 0.74 over 1850-1996.

In addition to the information brought by the correlations, the magnitude of the signal for the last 150 years has been estimated by computing the standard deviation of temperature time series from simulations and proxy-based

reconstructions (Table 5.7). This enables us to assess if the signal simulated by LOVECLIM preserves the amplitude of the observed one. The variances of NOD and ONE experiments inform us about the magnitude of the forced and natural variabilities respectively, simulated by LOVECLIM during this period and at these particular locations. An individual simulation is characterized by a standard deviation of 1.75 on average, while the ensemble mean of ten simulations has a value smaller by a factor of 2.8 (the reduction of the internal variability in an ensemble mean decreases as the inverse square root of the number of members, a factor three in this case). Compared to the corresponding standard deviation in the HadCRUT3 temperature data, which is approximately 1.50 (same as proxies VAR in Table 5.7), it shows the expected lack of variability in NOD, confirmed when looking at the time series depicted in Fig. 5.2. The standard deviation in SPA is of the same order of magnitude as in NOD and has then the same problem. Concerning the other data assimilation experiments, their variances strongly depend on the method selected to calibrate the proxies and the data assimilation method. As only one member is kept during the data assimilation procedure in OLD, the variance is not reduced by an average of several ensemble members. It is thus of the same order as ONE and very similar to the instrumental data or the assimilated proxy VAR variances. The signal simulated in DIR appears clearly underestimated, just as the signal recorded in the proxy-based reconstructions calibrated by direct regression, and has a similar amplitude as in NOD. The calibration via the

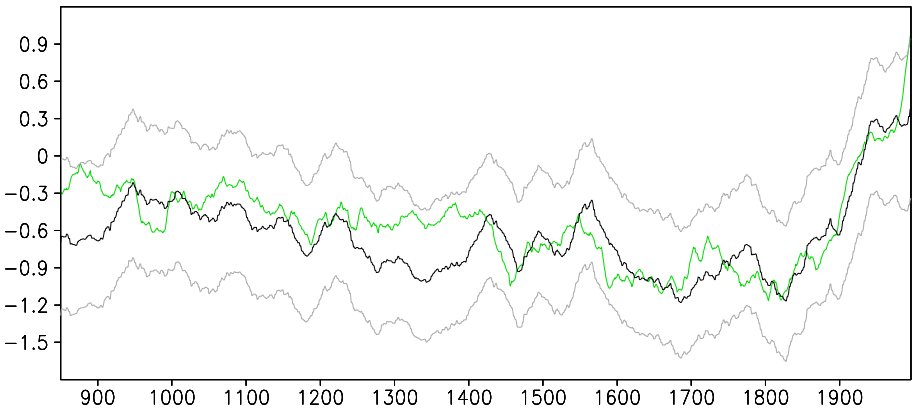

Figure 5.5: Anomaly in annual mean surface temperature (°C) averaged over the Arctic for the IND simulation (green) and the PAGES2k reconstruction (black) with error bars (grey). The reference period is 1901-1970. A 41-year running mean has been applied to the time series. The correlation between the time series is given in Table 5.6.

indirect regression and the variance matching leads to higher variances of the proxy-based reconstructions that consequently drive a higher variance of the simulation which uses them. This still leads to a clear underestimation of the variance in VAR. The indirect regression overestimates the variability of the proxy-based reconstructions inducing a higher variability in IND, but which is much lower than the one of the reconstructions themselves. So, the IND simulation has the advantage of following the low frequency forced signal, but without neglecting the high frequency variability, resulting in a variance not so far from the instrumental data. It is important to note at this point that the amount of kept particles in VAR, DIR and IND are approximately the same, 20, 25 and 24%, respectively, and the ensemble mean is then not responsible for the difference in the computed variances. Furthermore, the local variance in IND is similar to the one of OLD, but the local correlation is much lower for the latter, meaning that a large part of the variability is unconstrained noise.

5.3.2 Warm periods

The previous section has allowed selecting IND as the simulation that is the most consistent with the proxy-based temperature reconstructions at both local and Arctic scales. We focus here on five 40-year long warm periods observed during the last 1000 years in the mean of the 26 proxy series located north of 60°N (Fig. 5.6). Specifically, the goal is to understand, by analysing the spatial patterns of anomalies, the reasons for potential mismatches between the results of IND, the assimilated proxy series, and other statistical reconstructions. The results are also compared to NOD to identify the forced signal in LOVECLIM. Considering the low skills of the method, we will not enter into much details, as these results are not presented as a realistic representation of past climate changes, but just as a qualitative indication of the behaviour of our model with data assimilation. The five warm periods were chosen as the five maxima in the time series of the proxy data average over the Arctic, after applying a 41-year running mean (black curve in Fig. 5.3).

The first warm period (990-1030) is characterized by much warmer conditions in the mean of the proxies than in the model simulations (Fig. 5.3). Positive anomalies of surface temperature (compared to the period 1600-1950) are recorded in all the proxies, except for 2 proxies located in Alaska and the Canadian Archipelago (Fig. 5.6). The variability of the signal of some proxies is particularly large (Fig. 5.2), and the temperature anomaly recorded is probably exaggerated by the calibration using the indirect regression method. This seems particularly clear for the northernmost proxy (proxy 3), the one situated near Svalbard, which probably highly influences the warming observed in the

Proxy	NOD	ONE	SPA	Proxy VAR	OLD	VAR	Proxy DIR	DIR	Proxy IND	IND
1	0.29	0.9	0.26	0.99	0.68	0.46	0.65	0.34	1.52	0.5
2	0.42	0.96	0.43	1.11	0.89	0.64	0.19	0.47	6.34	0.79
3	2.30	6.67	2.28	2.73	4.96	3.2	0.69	2.48	10.70	5.67
4	0.44	1.06	0.48	1.16	0.92	0.62	0.27	0.5	5.08	0.81
5	0.39	1.11	0.32	1.33	0.94	0.63	0.54	0.38	3.25	0.67
6	0.48	1.25	0.35	1.64	0.97	0.75	0.82	0.57	3.27	0.73
7	0.54	1.38	0.4	1.56	1.15	0.9	0.83	0.65	2.91	0.8
8	0.40	1.17	0.34	1.37	0.85	0.53	0.60	0.42	3.13	0.55
9	0.74	2.41	0.66	2.01	1.98	1.47	0.93	0.85	4.36	1.78
10	0.23	0.59	0.24	1.20	0.53	0.38	0.78	0.32	1.86	0.34
Mean	0.62	1.75	0.58	1.51	1.39	0.96	0.63	0.70	4.24	1.26

Table 5.7: Standard deviation of the surface temperature time series for the period 1850-1996 from the different simulations and proxy-based reconstructions, at the location where the new proxy data is available.

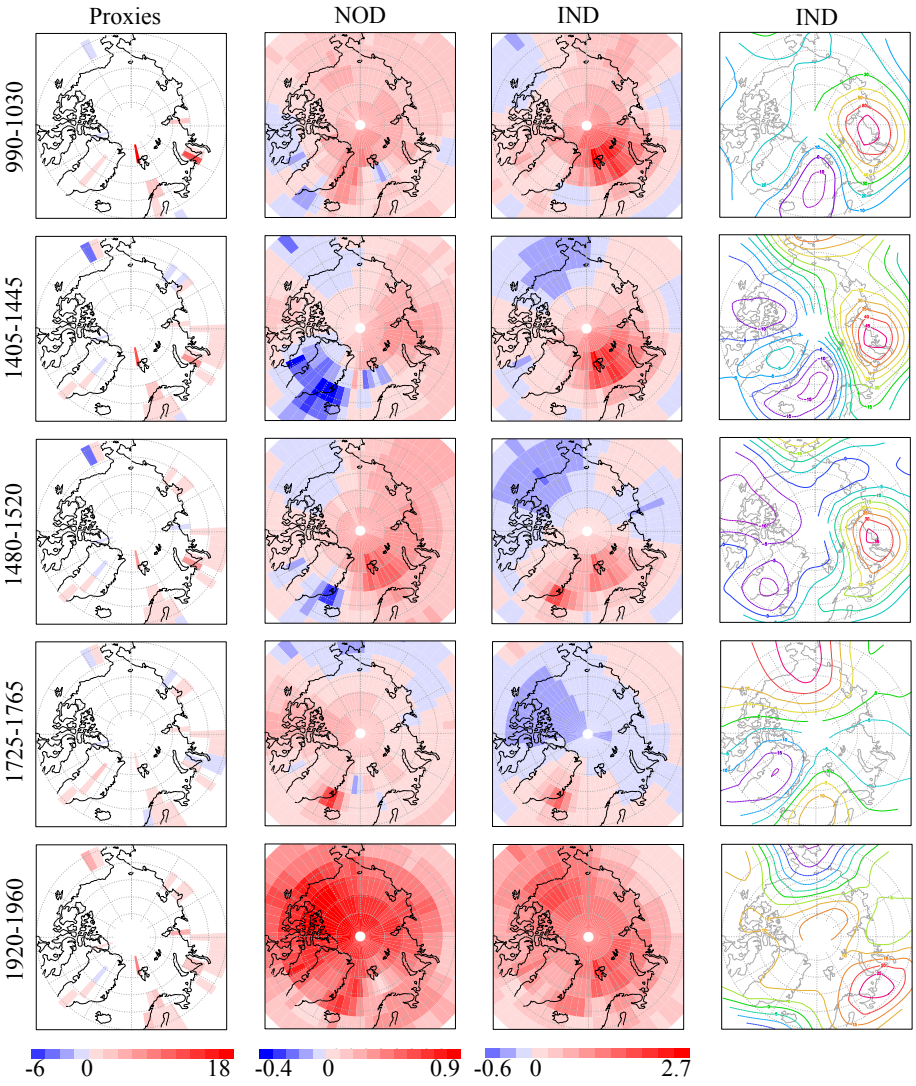

Figure 5.6: Anomaly in annual mean surface temperature (°C) over 5 different warm periods for the proxy-based reconstructions calibrated by indirect regression and the NOD and IND simulations (3 first columns) (note that the scale is different in the different columns). Anomaly in annual mean geopotential height at 800 hPa ($m^2 s^{-2}$) over the 5 warm periods for the IND simulation (last column). The reference period is 1600-1950.

Barents Sea in IND. The NOD experiment displays also a warming but the signal is more homogeneous, with a maximum west of Svalbard. A cooling present in NOD over Baffin Bay is also shifted westwards in IND, likely following the signal of the cooler proxy located in Alaska. In this region, a record became available after year 1200, close to the longer one. These two proxies seem to be in contradiction with each other over a large period (correlation of 0.04). The dynamics of the model is not able to follow the two opposite anomalies in neighboring grids and will favor the negative anomaly in the 3 following warm periods. Periods spanning 1405-1445 and 1480-1520 present similar patterns of anomaly. The main differences before and after the assimilation of proxy-based reconstructions is an important cooling over Greenland in NOD almost nonexistent in IND (here again, two opposite estimates of surface temperature are deduced from the proxies in this area), a stronger warming over the Barents Sea in IND (always imposed by the very warm proxy near Svalbard), and a stronger and more extended cooling in Alaska and northern Canada. As there is no difference between the external forcing applied in the simulations with and without data assimilation, the differences between the spatial patterns of surface temperature between NOD and IND can be explained by dynamical changes. The magnitude of the changes in atmospheric circulation are generally higher in IND than in NOD in the different warm periods (not shown). The spatial patterns of anomaly related to the first three warm periods in IND (Fig. 5.6) are explained by similar modes in the model: lower geopotential height over the Nordic Seas and Greenland, and higher geopotential height over the Eurasian Arctic. This leads to a strengthening of the southerly winds in the Barents Seas. A lower geopotential height over the Canadian Archipelago and a higher one over the Pacific Ocean explain the cooling over Alaska by enhanced northerly winds. The 1480-1520 period was analysed also in Chapter 2. The spatial pattern of anomaly obtained with the previous data assimilation method is not consistent everywhere with the new one. The warming over the Barents Sea is common to both simulations and is explained by the negative anomaly in geopotential height over Greenland. However, while the previous method presents a warming over the Canadian Archipelago, IND suggests a cooling there, which is most probably due to the constraint of the cold proxy in Alaska that was not present before. The lower geopotential height present over Alaska in the previous simulation, is now located over the Canadian Archipelago.

During the relatively warm episode which occurs between 1725 and 1765, the period known as the Little Ice Age, the warming of the Arctic deduced from the proxy records is less obvious in IND. A cooling over a large area, not simulated in NOD, seems to predominate. Three proxies located in the western

Siberian region (around 70°E) record a cooling that is probably responsible for the changes in wind patterns (enhanced winds from Siberia to the north) and then for the cooling in central Arctic, northern Canada and Alaska. The increase of mean surface temperature starting at the end of the 17th century in IND ends earlier than in the proxies, and the temperature is already decreasing when the maximum is reached in the proxies (Fig. 5.3).

The warming over the period 1920-1960 is more spatially homogeneous. All the proxies indicate a warming, expect one over Greenland that is not followed by the model. The higher warming over Svalbard leads to a higher warming over that region in IND, as in the other periods. The mean temperatures during this period are not correctly represented in LOVECLIM without data assimilation (Fig. 5.4), the warming of the 20th century is constant and does not peak around 1930 as it should according to the proxy or instrumental data. In this case, the data assimilation helps the model in the good direction, provided that the variability of the assimilated proxies is not underestimated as it is in DIR.

5.4 Discussion and conclusions

Our simulations without data assimilation have informed us that LOVECLIM fails to reproduce the observed local changes in the Arctic over the last millennium, but that the forcings anomalies are sufficiently strong to drive the principal tendencies for the large-scale or globally averaged changes. In an attempt of improving the local agreement, the use of data assimilation proves to be an efficient and robust constraint on the simulated climate variability, as already showed in previous studies using data assimilation over the last millennium (Crespin et al., 2009; Goosse et al., 2010b, 2012c,b). The improvement at the scale of the Arctic is, however, relatively low.

The possible reasons that could explain the mediocre correlation of the averaged conditions between model results and proxy data in the Arctic are numerous. Firstly, the comparison between the Arctic mean simulated temperature and the mean of the 26 assimilated proxies has to be tempered, as the number of those proxies is probably too small to estimate correctly the mean over the region. Indeed, the proxy records do not cover the entire region, but just some specific locations that might not be representative of the averaged conditions. Furthermore, the model results and proxy data do not necessarily represent the climate at the same scale, the model gridbox representing much larger-scale conditions than the proxy data which can be influenced by local

climate variations.

Secondly, the proxy information can be in disagreement with the physics of the model. The proxy series themselves are characterized by a high uncertainty concerning their ability to reproduce both high and low frequency climate variations, and contains then a big part of non-climatic information. There is also uncertainties in the forcing and in certain physical processes simulated by LOVECLIM. The fact that our model simulations with data assimilation are not strongly correlated with the instrumental data, but present much better correlations with the proxy series over that period, suggests that the model might be reproducing a large part of the non-climatic noise recorded in the proxies. Also, the individual proxies are not correlated one to the other, and certain patterns imposed by the proxies may present spatial inconsistencies that the model will be unable to follow. Opposite information between the signals recorded by nearby located proxies can lead to bias in the teleconnections simulated in the model. Ideally, the model should follow the proxy time series that are the most consistent with the large-scale dynamics of the model. For instance, Mairesse et al. (2013) arrive to the same conclusion concerning proxies of the Holocene. The comparison of our results with the experiment SPA suggests that the statistical models used to spatially reconstruct temperature from proxy data are more efficient than the climate simulation with data assimilation used here to get rid of the noise in the proxies. The filtering processes applied in those reconstructions reduce the spatial inconsistencies that exist with individual and non-treated proxies. This advantage comes along with the disadvantage of a reconstruction based on the stability of teleconnections, as discussed in Section 1.2.

Keeping in mind the limitations of the proxies, one goal of the present study was to determine the best way to calibrate the proxy series using instrumental data. In our study, the best calibration option is the indirect regression. This is consistent with the assumption of the data assimilation technique that the assimilated data contain both the climatic signal and an additional noise. Because of the assumed presence of non-climatic noise, the magnitude of the variance of assimilated data has then to be higher than the one of the less noisy observations. This is obtained using the indirect regression, contrarily to the direct regression which underestimates the variance of the signal. This result is in agreement with the study of Sundberg et al. (2012) who also propose to use indirect regression in their statistical framework for evaluation of climate model simulations.

Finally, we have shown that the skill of our method is low at local scale. The model is able to follow the signal recorded in the assimilated proxies, but is not able to reconstruct the signal where no proxy series exists. Furthermore, the method is extremely sensitive to one additional proxy, and thus to the potential biases in this proxy. This leads us to conclude on the necessity of applying a spatial filter to the proxy-based reconstructions before assimilation, since the model is not able to filter the signal during the process. This seems particularly essential when the information recorded in different proxies seems too disparate. A larger number of climatic proxies and a spatial filtering of those proxies appear then to be required to get the best of the assimilation method in the present framework.

CHAPTER 6

CONCLUSION

In this final section, a synthesis of the answers to the main questions raised in the introduction of this thesis is proposed. The principal limitations of our methodology are then summarized, and, finally, some perspectives for future studies are presented.

The main goal of this PhD thesis was to propose an interpretation of some important past changes in the Arctic climate and possible explanations of their origins. In this context, the data assimilation technique proved to be a very useful tool. It can provide information that cannot be obtained using uniquely the "ground truth" (that is the proxy data), such as physically consistent large-scale patterns, climate variables not recorded in the proxies, etc. This allows formulating hypotheses of dynamical processes and mechanisms that could explain the observed changes in past Arctic climate.

The first application of the data assimilation method led us to propose a mechanism explaining the cause of a particularly warm period simulated in the Arctic at the end of the 15th century, a period that appears in our simulations to be one of the warmest episodes of the last millennium before the industrial period. As expected, the simulations obtained follow the signal recorded in the majority of the proxies. The results obtained with data assimilation, used

in conjunction with those from simulations without data assimilation (which estimate the response of the system to external forcings), helped us to establish qualitatively the role of internal versus external causes in Arctic climate variations. In particular, the changes occurring during the 15th century warming appear to be related to the internal variability of the system. In parallel to the simulation with data assimilation, we took advantage of a set of simulations run with different external forcings taken individually, in order to clarify the role played by each of them in the observed variations of past Arctic climate as summarized below.

The analysis of the role of internal variability and external forcings in the observed changes was a central theme of this thesis, and was successfully accomplished. Our approach permitted to estimate whether a particular event appeared related to any forcing or not. The main outcomes resulting from this analysis are as follows. The relative contribution of forced and internal variability is principally dependent on the time scale. External forcings seem to play a larger role for low frequency variations, while at shorter time scales, such as multidecadal variations, the response generally appears largely dominated by internal variability. Such events can be identified if they are reproduced by the model only if it is constrained by data assimilation. The different external forcings all contribute to the simulated temperature changes, but in different proportions, and with some marked differences according to the period of the year considered. The influence of the astronomical forcing, for instance, is very low on an annual average, but it plays a dominant role on long-term trends with a magnitude (and sign) that differs from one season to another. It is at the origin of the positive long-term temperature trend in spring and of the negative one during the other seasons, before the beginning of the industrial period. The magnitude of the response to greenhouse gas and, more surprisingly, land use forcings is also different between seasons. On the other hand, the impact of solar and volcanic forcings is similar throughout the year. Finally, the responses to all the external forcings are amplified in the Arctic region by positive feedbacks involving sea ice and snow.

Despite those satisfactory results, many aspects of the data assimilation method appeared to leave considerable room for improvement. A main part of this thesis was devoted to this improvement of the methodology, keeping in mind the original aim to obtain a satisfactory reconstruction of Arctic past climate as a necessary step for a better understanding of the dynamics of the system. A better use of the information contained in the different ensemble members, a more efficient way to generate the different initial conditions for each member, and the inclusion of proxy data uncertainties, were some as-

pects of the method that were refined in collaboration with colleagues of the Georges Lemaître Centre for Earth and Climate Research. In the context of this thesis, we first tackled the problem of the oceanic variability which appeared unconstrained by the data assimilation process in our first experiments. However, it is essential to estimate correctly the changes of oceanic heat transport from the North Atlantic to the Arctic. To respond to this concern, we tested a new methodology to reconstruct past changes of the MOC. With a series of simulations that contributed to the development of a new version of the data assimilation method, we proved that this new version brought large improvements to the results. We were able to satisfactorily estimate past changes of the MOC in twin experiments using only annual mean surface temperature data. The lack of robustness among the existent reconstructions of the MOC unfortunately prevented us to validate our methodology in realistic conditions.

With the revisited and improved version of the data assimilation method, we undertook another attempt of reconstructing and interpret climate changes of the past millennium in the Arctic. A major novelty, additionally to the new data assimilation method, was to extend the set of assimilated proxies. Those new proxies were not treated the same way as the ones used in our first study. The results obtained after their assimilation opened a new important question on the best way to calibrate the proxy data against observed temperature data to take the recorded signal into account in an optimal way during the assimilation process. Our conclusion is that a calibration by indirect regression must be preferred, leading to a variance of the assimilated data larger than the one of the instrumental observations.

Limitations

The results obtained in this thesis have to be interpreted taking into account the limitations of our methodology. An important obstacle is the lack of available proxy data, particularly in the Arctic region. Although important efforts are being made to increase the coverage in that region, there are still important gaps. Because of this, the results of the simulations with data assimilation are less robust in areas with poor data coverage as, for instance, in regions such as eastern Siberia or northern Canada and over the oceans. Another problem concerning proxy data is the incompatibility that they sometimes present between each other. When the local temperature reconstructions derived from nearby proxies are inconsistent according to the model physics, i.e., the model is not able to follow the constraint imposed by the proxy time series, the data assimilation is not performed properly in that region, the system being gener-

ally not able to distinguish which one is the most reliable.

We also have to keep in mind that LOVECLIM is an Earth system model of intermediate complexity, with a coarse resolution and a highly simplified representation of the atmospheric dynamics. The dynamical response of the atmosphere to forcings can thus be biased, and we may attribute to an internal cause a change that should in reality be attributed to a response to an external forcing. More generally, it is challenging to determine the origin of a particular pattern observed during a past period and the true role of internal variability compared to the forced one in circulation changes. For instance, when attributing a change to the internal variability of the system rather than to an external cause, we cannot exclude a bias in the model response to the forcings, but also in the reconstructions of forcings used in our simulations. Indeed, our results depend on our choice of forcing estimates and their uncertainties. Selecting another solar forcing, for example, could lead to different conclusions on the interpretation of past climate changes.

Finally, because of the low robustness of some of our results, one of the aims of this thesis could not be totally achieved: the uncertainties in the simulations with data assimilation did not allow us to perform an extensive analysis of the mechanisms driving the climate variability. More particularly, we could not conclude our study of warm episodes of the last millennium in the Arctic and their common characteristics, with the purpose to be placed in the context of the recent warming. For instance, the pattern of temperature anomaly of the late 15th century that was studied in Chapter 2 had some similarities with the one obtained with new additional proxies in Chapter 5, but also clear differences. In particular, the cold conditions imposed by a new proxy in Alaska induced a pattern of atmospheric circulation that was different in this region from the one obtained in Chapter 2. Therefore, it was not possible to study with high confidence the processes responsible for the changes at that period. This leads to the conclusion that significant problems may result from the assimilation of a limited number of proxies and that the sensitivity of the method to the addition of one or few supplementary proxies must be tested whenever this is possible.

Perspectives

The interesting results obtained within this PhD thesis can certainly be used as a base for further work. Here are some hints that should be addressed in priority:

First, it would be very interesting to compare our interpretation of the origin of past climate variations in the Arctic with those obtained by more sophisticated models, in order to assess the robustness of our conclusions. Simulations covering the last millennium performed with GCMs have become available in recent years, and their more complex representation of atmospheric processes could provide complementary or alternatives explanations concerning these processes.

Determining the number of proxies needed to have a good representation of Arctic mean conditions is an important issue. In this context, perfect model studies could probably provide useful informations, but a high quantity of tests would be needed if using the methodology applied here. Although a larger amount of proxies series would benefit to our methodology, the first aspect that needs to be refined in order to obtain more robust results concerns the way to treat the proxy data before or during their assimilation. Indeed, it is not useful to add more proxies, i.e. to increase the number of degrees of freedom of the system, if there is an incompatibility between them according to the physics of the model. Increasing the number of particles to deal with a larger number of degrees of freedom would be of limited help in this case. Instead, the focus should be put on the way to extract the common climatic signal in the proxy data before the assimilation, in order to get rid of the spatial inconsistencies. Indeed, the data assimilation method proved to be efficient when used with smoothed data. Our approach consisting in assimilating raw proxies was probably too optimistic and demanding in the present framework. Our model, struggling to follow each individual time series, is unable to reconstruct properly the large-scale patterns from noisy local proxy data. The reason for this behaviour is still an open question. But including an additional constraint from the mean of the proxies in the computation of the likelihood seems promising.

The results obtained by data assimilation could also be used to identify the key locations where additional proxy data should be collected, because of a poor coverage, or inconsistencies between the signals recorded by the proxies. Identifying those inconsistencies could help to understand the differences between our results and the reconstructions based on statistical methods, but this would require additional experiments using different sets of proxies to constrain the model.

Another aspect that must be improved is the way we include the uncertainties of the proxies in the assimilation process. We could, for instance, give less weight in the computation of the likelihood to those proxies that display a

smaller correlation with instrumental estimates. However, this step is not effortless, since the proxy non-climatic signals are difficult to estimate. The classical statistical methods are used to identify a relationship between proxy data and a single climate variable that is assumed to be dominant. This is done usually by linear regression. However, this assumption of linear and stationary relationships is not always satisfying. To avoid this aspect, a promising method is the forward proxy modelling, which estimates directly from a model output the variable recorded in the archive. This approach could certainly contribute to reduce the uncertainties in the quantification of the model-data agreement (Hughes et al., 2010). This is a challenging process, but the satisfactory results obtained with our method up to now seems to justify, however, additional investigations of more sophisticated approaches.

REFERENCES

ACIA, 2005. Arctic Climate Impact Assessment. Cambridge University Press. Cited in pages 1, 2, and 5.

Alexander, M. A., Bhatt, U. S., Walsh, J. E., Timlin, M. S., Miller, J. S., Scott, J. D., 2004. The atmospheric response to realistic Arctic sea ice anomalies in an AGCM during winter. Journal of climate 17 (5). Cited in page 38.

Allan, R. J., Ansell, T. J., 2006. A new globally complete monthly historical gridded mean sea level pressure dataset (HadSLP2): 1850–2004. Journal of Climate 19, 5816–5838. Cited in page 63.

Ammann, C. M., Wahl, E. R., 2007. The importance of the geophysical context in statistical evaluations of climate reconstruction procedures. Climatic Change 85, 71–88. Cited in page 8.

Annan, J. D., Hargreaves, J. C., 2012. Identification of climatic state with limited proxy data. Climate of the Past 8, 1141–1151. Cited in page 76.

Baehr, J., 2010. Influence of the 26°N RAPID–MOCHA array and Florida Current cable observations on the ECCO–GODAE state estimate. Journal of Physical Oceanography 40, 865–879. Cited in page 67.

Baehr, J., Haak, H., Alderson, S., Cunningham, S. A., Jungclaus, J. H., Marotzke, J., 2007. Timely detection of changes in the meridional overturning circulation at 26°n in the Atlantic. Journal of Climate 20, 5827–5841. Cited in pages 65 and 68.

Balmaseda, M. A., Smith, G. C., Haines, K., Anderson, D., Palmer, T. N., Vidard, A., 2007. Historical reconstruction of the Atlantic meridional overturning circulation from the ECMWF operational ocean reanalysis. Geophysical Research Letters 34 (23). Cited in pages 18, 67, 79, and 81.

Bauer, E., Claussen, M., 2006. Analyzing seasonal temperature trends in forced climate simulations of the past millennium. Geophysical research letters 33 (2). Cited in pages 46, 56, 57, and 61.

Bauer, E., Claussen, M., Brovkin, V., Huenerbein, A., 2003. Assessing climate forcings of the earth system for the past millennium. Geophysical Research Letters 30 (6). Cited in page 11.

Bengtsson, L., Semenov, V. A., Johannessen, O. M., 2004. The early twentieth-century warming in the Arctic—a possible mechanism. Journal of Climate 17 (20). Cited in pages 23, 39, and 42.

Berger, A., 1978. Long-term variations of daily insolation and Quaternary climatic changes. Journal of the Atmospheric Sciences 35 (12), 2362–2367. Cited in pages 25 and 49.

Berger, A., Loutre, M.-F., Tricot, C., 1993. Insolation and Earth's orbital periods. Journal of Geophysical Research: Atmospheres 98, 10341–10362. Cited in pages 5, 55, and 57.

Bindoff, N. L., Willebrand, J., Artale, V., Cazenave, A., Gregory, J. M., Gulev, S., Hanawa, K., Le Quere, C., Levitus, S., Nojiri, Y., et al., 2007. Observations: Oceanic climate change and sea level. In: Climate Change 2007: The Physical Science Basis. Contribution of Working Group I to the Fourth Assessment Report of the Intergovernmental Panel on Climate Change [Solomon, S., D. Qin, M. Manning, Z. Chen, M. Marquis, K.B. Averyt, M. Tignor and H.L. Miller (eds.)]. Cambridge University Press, Cambridge, United Kingdom and New York, NY, USA. Cited in page 64.

Bingham, F. M., Howden, S. D., Koblinsky, C. J., 2002. Sea surface salinity measurements in the historical database. Journal of Geophysical Research: Oceans 107 (C12), 8019. Cited in page 63.

Bird, B. W., Abbott, M. B., Finney, B. P., Kutchko, B., 2009. A 2000 year varve-based climate record from the central Brooks Range, Alaska. Journal of Paleolimnology 41, 25–41. Cited in page 40.

Black, D. E., Peterson, L. C., Overpeck, J. T., Kaplan, A., Evans, M. N., Kashgarian, M., 1999. Eight centuries of North Atlantic Ocean atmosphere variability. Science 286, 1709–1713. Cited in page 39.

Böning, C. W., Scheinert, M., Dengg, J., Biastoch, A., Funk, A., 2006. Decadal variability of subpolar gyre transport and its reverberation in the North Atlantic overturning. Geophysical Research Letters 33 (21). Cited in page 67.

Briffa, K. R., Jones, P. D., Schweingruber, F. H., 1994. Summer temperatures across northern North America: Regional reconstructions from 1760 using tree-ring densities. Journal of Geophysical Research: Atmospheres 99 (D12), 25835–25844. Cited in page 7.

Briffa, K. R., Osborn, T. J., 2002. Blowing hot and cold. Science 295, 2227–2228. Cited in pages 61 and 89.

Briffa, K. R., Osborn, T. J., Schweingruber, F. H., Harris, I. C., Jones, P. D., Shiyatov, S. G., Vaganov, E. A., 2001. Low-frequency temperature variations from a northern tree ring density network. Journal of Geophysical Research 106, 2929–2941. Cited in pages 23 and 46.

Briffa, K. R., Shishov, V. V., Melvin, T. M., Vaganov, E. A., Grudd, H., Hantemirov, R. M., Eronen, M., Naurzbaev, M. M., 2008. Trends in recent temperature and radial tree growth spanning 2000 years across northwest Eurasia. Philosophical Transactions of the Royal Society B: Biological Sciences 363, 2269–2282. Cited in page 87.

Broecker, W. S., Denton, G. H., 1989. The role of ocean-atmosphere reorganizations in glacial cycles. Geochimica et Cosmochimica Acta 53, 2465–2501. Cited in page 65.

Brohan, P., Kennedy, J. J., Harris, I., Tett, S. F., Jones, P. D., 2006. Uncertainty estimates in regional and global observed temperature changes: A new data set from 1850. Journal of Geophysical Research 111 (D12). Cited in pages 27, 29, 30, 63, 71, 77, 88, 92, and 97.

Brovkin, V., Bendtsen, J., Claussen, M., Ganopolski, A., Kubatzki, C., Petoukhov, V., Andreev, A., 2002. Carbon cycle, vegetation, and climate dynamics in the Holocene: Experiments with the CLIMBER-2 model. Global Biogeochemical Cycles 16 (4), 1139. Cited in pages 25 and 48.

Bryden, H. L., Longworth, H. R., Cunningham, S. A., 2005. Slowing of the Atlantic meridional overturning circulation at 25°N. Nature 438, 655–657. Cited in pages 65 and 66.

Calvo, E., Grimalt, J., Jansen, E., 2002. High resolution U^k_{37} sea surface temperature reconstruction in the Norwegian Sea during the Holocene. Quaternary Science Reviews 21, 1385–1394. Cited in page 64.

Chapman, W. L., Walsh, J. E., 1993. Recent variations of sea ice and air temperature in high latitudes. Bulletin of the American Meteorological Society 74, 33–47. Cited in page 49.

Charlson, R. J., Langner, J., Rodhe, H., Leovy, C. B., Warren, S. G., 1991. Perturbation of the Northern Hemisphere radiative balance by backscattering from anthropogenic sulfate aerosols. Tellus A 43, 152–163. Cited in pages 25 and 49.

Christiansen, B., 2011. Reconstructing the NH mean temperature: Can underestimation of trends and variability be avoided? Journal of Climate 24, 674–692. Cited in page 89.

Christiansen, B., Ljungqvist, F. C., 2011. Reconstruction of the extratropical NH mean temperature over the last millennium with a method that preserves low-frequency variability. Journal of Climate 24, 6013–6034. Cited in page 89.

Comiso, J. C., Nishio, F., 2008. Trends in the sea ice cover using enhanced and compatible AMSR-E, SSM/I, and SMMR data. Journal of Geophysical Research: Oceans 113 (C2). Cited in page 49.

Crespin, E., Goosse, H., Fichefet, T., Mairesse, A., Sallaz-Damaz, Y., 2012. Arctic climate over the past millennium: Annual and seasonal responses to external forcings. The Holocene 23, 321–329. Cited in pages 11 and 18.

Crespin, E., Goosse, H., Fichefet, T., Mann, M. E., 2009. The 15th century Arctic warming in coupled model simulations with data assimilation. Climate of the Past 5, 389–401. Cited in pages 16, 17, 48, 68, 83, and 104.

Crowley, T. J., 2000. Causes of climate change over the past 1000 years. Science 289, 270–277. Cited in pages 7, 11, 23, 25, 26, 46, and 57.

Crowley, T. J., Zielinski, G., Vinther, B., Udisti, R., Kreutz, K., Cole-Dai, J., Castellano, E., 2008. Volcanism and the little ice age. PAGES news 16, 22–23. Cited in page 5.

Cunningham, S. A., Kanzow, T., Rayner, D., Baringer, M. O., Johns, W. E., Marotzke, J., Longworth, H. R., Grant, E. M., Hirschi, J. J.-M., Beal, L. M., et al., 2007. Temporal variability of the Atlantic meridional overturning circulation at 26.5°N. science 317, 935–938. Cited in page 65.

Cunningham, S. A., Marsh, R., 2010. Observing and modeling changes in the Atlantic MOC. Wiley Interdisciplinary Reviews: Climate Change 1, 180–191. Cited in pages 66, 67, 79, and 81.

D'Arrigo, R., Wilson, R., Jacoby, G., 2006. On the long-term context for late twentieth century warming. Journal of Geophysical Research: Atmospheres 111 (D3). Cited in pages 87 and 88.

D'Arrigo, R. D., Jacoby, G. C., 1993. Secular trends in high northern latitude temperature reconstructions based on tree rings. Climatic Change 25, 163–177. Cited in page 23.

Delaygue, G., Bard, E., 2011. An Antarctic view of Beryllium-10 and solar activity for the past millennium. Climate Dynamics 36, 2201–2218. Cited in page 49.

Delworth, T. L., Knutson, T. R., 2000. Simulation of early 20th century global warming. Science 287, 2246–2250. Cited in page 23.

Delworth, T. L., Mann, M. E., 2000. Observed and simulated multidecadal variability in the Northern Hemisphere. Climate Dynamics 16, 661–676. Cited in pages 23 and 43.

Denton, G. H., Broecker, W. S., 2008. Wobbly ocean conveyor circulation during the Holocene? Quaternary Science Reviews 27, 1939–1950. Cited in page 65.

Divine, D., Isaksson, E., Martma, T., Meijer, H. A., Moore, J., Pohjola, V., van de Wal, R. S., Godtliebsen, F., 2011. Thousand years of winter surface air temperature variations in Svalbard and northern Norway reconstructed from ice-core data. Polar Research 30 (1). Cited in page 87.

Driesschaert, E., Fichefet, T., Goosse, H., Huybrechts, P., Janssens, I., Mouchet, A., Munhoven, G., Brovkin, V., Weber, S. L., 2007. Modeling the influence of Greenland ice sheet melting on the Atlantic meridional overturning circulation during the next millennia. Geophysical Research Letters 34 (10). Cited in pages 24 and 48.

Drijfhout, S. S., Hazeleger, W., 2007. Detecting Atlantic MOC changes in an ensemble of climate change simulations. Journal of climate 20, 1571–1582. Cited in page 67.

Dubinkina, S., Goosse, H., Sallaz-Damaz, Y., Crespin, E., Crucifix, M., 2011. Testing a particle filter to reconstruct climate changes over the past centuries. International Journal of Bifurcation and Chaos 21 (12), 3611–3618. Cited in pages 14, 15, 16, 70, 72, and 81.

Eby, M., Weaver, A. J., Alexander, K., Zickfeld, K., Abe-Ouchi, A., Cimatoribus, A. A., Crespin, E., Drijfhout, S. S., Edwards, N. R., Eliseev, A. V., et al., 2013. Historical and idealized climate model experiments: an intercomparison of earth system models of intermediate complexity. Climate of the Past 9, 1111–1140. Cited in page 16.

Eiríksson, J., Bartels-Jonsdottir, H. B., Cage, A. G., Gudmundsdottir, E. R., Klitgaard-Kristensen, D., Marret, F., Rodrigues, T., Abrantes, F., Austin, W. E., Jiang, H., et al., 2006. Variability of the North Atlantic Current during

the last 2000 years based on shelf bottom water and sea surface temperatures along an open ocean/shallow marine transect in western Europe. The Holocene 16, 1017–1029. Cited in page 39.

Esper, J., Cook, E. R., Schweingruber, F. H., 2002. Low-frequency signals in long tree-ring chronologies for reconstructing past temperature variability. Science 295, 2250–2253. Cited in pages 23 and 87.

Fichefet, T., Morales Maqueda, M., 1997. Sensitivity of a global sea ice model to the treatment of ice thermodynamics and dynamics. Journal of Geophysical Research: Oceans 102, 12609–12646. Cited in page 48.

Forster, P., Ramaswamy, V., Artaxo, P., Berntsen, T., Betts, R., Fahey, D. W., Haywood, J., Lean, J., Lowe, D. C., Myhre, G., et al., 2007. Changes in atmospheric constituents and in radiative forcing. In: Climate Change 2007: The Physical Science Basis. Contribution of Working Group I to the Fourth Assessment Report of the Intergovernmental Panel on Climate Change [Solomon, S., D. Qin, M. Manning, Z. Chen, M. Marquis, K.B. Averyt, M.Tignor and H.L. Miller (eds.)]. Cambridge University Press, Cambridge, United Kingdom and New York, NY, USA. Cited in page 4.

Foukal, P., Fröhlich, C., Spruit, H., Wigley, T. M., 2006. Variations in solar luminosity and their effect on the Earth's climate. Nature 443, 161–166. Cited in page 53.

Gerdes, R., Karcher, M. J., Kauker, F., Schauer, U., 2003. Causes and development of repeated Arctic Ocean warming events. Geophysical research letters 30 (19). Cited in page 43.

González-Rouco, J. F., Beltrami, H., Zorita, E., Von Storch, H., 2006. Simulation and inversion of borehole temperature profiles in surrogate climates: Spatial distribution and surface coupling. Geophysical Research Letters 33 (1). Cited in pages 46 and 57.

Goosse, H., Arzel, O., Luterbacher, J., Mann, M. E., Renssen, H., Riedwyl, N., Timmermann, A., Xoplaki, E., Wanner, H., 2006a. The origin of the European "Medieval Warm Period". Climate of the Past 2, 99–113. Cited in pages 46 and 48.

Goosse, H., Braida, M., Crosta, X., Mairesse, A., Masson-Delmotte, V., Mathiot, P., Neukom, R., Oerter, H., Philippon, G., Renssen, H., et al., 2012a. Antarctic temperature changes during the last millennium: evaluation of simulations and reconstructions. Quaternary Science Reviews 55, 75–90. Cited in pages 16 and 81.

Goosse, H., Brovkin, V., Fichefet, T., Haarsma, R., Huybrechts, P., Jongma, J., Mouchet, A., Selten, F., Barriat, P.-Y., Campin, J.-M., et al., 2010a. Description of the Earth system model of intermediate complexity LOVECLIM version 1.2. Geoscientific Model Development Discussions 3, 309–390. Cited in pages 16, 47, 48, 58, 59, 71, and 72.

Goosse, H., Crespin, E., de Montety, A., Mann, M. E., Renssen, H., Timmermann, A., 2010b. Reconstructing surface temperature changes over the past 600 years using climate model simulations with data assimilation. Journal of Geophysical Research: Atmospheres (1984–2012) 115 (D9). Cited in pages 16, 46, 49, 57, 68, 73, 83, 84, and 104.

Goosse, H., Crespin, E., Dubinkina, S., Loutre, M.-F., Mann, M. E., Renssen, H., Sallaz-Damaz, Y., Shindell, D., 2012b. The role of forcing and internal dynamics in explaining the "Medieval Warm Period". Climate dynamics 39, 2847–2866. Cited in pages 16, 81, 83, 84, 91, and 104.

Goosse, H., Driesschaert, E., Fichefet, T., Loutre, M.-F., 2007. Information on the early Holocene climate constrains the summer sea ice projections for the 21st century. Climate of the Past 3, 683–692. Cited in pages 24 and 25.

Goosse, H., Fichefet, T., 1999. Importance of ice-ocean interactions for the global ocean circulation: A model study. Journal of Geophysical Research: Oceans 104, 23337–23355. Cited in pages 25 and 48.

Goosse, H., Guiot, J., Mann, M. E., Dubinkina, S., Sallaz-Damaz, Y., 2012c. The medieval climate anomaly in Europe: Comparison of the summer and annual mean signals in two reconstructions and in simulations with data assimilation. Global and Planetary Change 84, 35–47. Cited in pages 16, 81, 83, 84, 91, and 104.

Goosse, H., Lefebvre, W., de Montety, A., Crespin, E., Orsi, A. H., 2009. Consistent past half-century trends in the atmosphere, the sea ice and the ocean at high southern latitudes. Climate Dynamics 33, 999–1016. Cited in pages 16, 25, 29, 68, and 83.

Goosse, H., Mann, M. E., Renssen, H., 2008. What we can learn from combining paleoclimate proxy data and climate model simulations of past centuries. Natural Climate Variability and Global Warming: A Holocene Perspective, Blackwell Pusblishing, 163–188. Cited in pages 10 and 23.

Goosse, H., Renssen, H., 2004. Exciting natural modes of variability by solar and volcanic forcing: idealized and realistic experiments. Climate Dynamics 23, 153–163. Cited in pages 35 and 61.

Goosse, H., Renssen, H., Timmermann, A., Bradley, R. S., 2005. Internal and forced climate variability during the last millennium: a model-data comparison using ensemble simulations. Quaternary Science Reviews 24, 1345–1360. Cited in pages 4, 11, 16, 23, 42, and 48.

Goosse, H., Renssen, H., Timmermann, A., Bradley, R. S., Mann, M. E., 2006b. Using paleoclimate proxy-data to select optimal realisations in an ensemble of simulations of the climate of the past millennium. Climate Dynamics 27, 165–184. Cited in pages 12, 13, 15, 25, and 72.

Goosse, H., Selten, F., Haarsma, R., Opsteegh, J., 2003. Large sea-ice volume anomalies simulated in a coupled climate model. Climate dynamics 20, 523–536. Cited in page 39.

Gregory, J. M., Dixon, K. W., Stouffer, R. J., Weaver, A. J., Driesschaert, E., Eby, M., Fichefet, T., Hasumi, H., Hu, A., Jungclaus, J. H., et al., 2005. A model intercomparison of changes in the Atlantic thermohaline circulation in response to increasing atmospheric CO_2 concentration. Geophysical Research Letters 32 (12). Cited in page 64.

Grist, J. P., Marsh, R., Josey, S. A., 2009. On the relationship between the North Atlantic meridional overturning circulation and the surface-forced overturning streamfunction. Journal of Climate 22, 4989–5002. Cited in pages 66, 67, and 68.

Groll, N., Widmann, M., 2006. Sensitivity of temperature teleconnections to orbital changes in AO-GCM simulations. Geophysical research letters 33. Cited in page 8.

Grudd, H., 2008. Torneträsk tree-ring width and density AD 500–2004: a test of climatic sensitivity and a new 1500-year reconstruction of north Fennoscandian summers. Climate Dynamics 31, 843–857. Cited in page 87.

Guemas, V., Salas-Mélia, D., 2008. Simulation of the Atlantic meridional overturning circulation in an atmosphere-ocean global coupled model. Part II: weakening in a climate change experiment: a feedback mechanism. Climate dynamics 30, 831–844. Cited in page 39.

Guiot, J., Corona, C., et al., 2010. Growing season temperatures in Europe and climate forcings over the past 1400 years. PloS one 5, 1–15. Cited in page 46.

Gunnarson, B. E., Linderholm, H. W., Moberg, A., 2011. Improving a tree-ring reconstruction from west-central Scandinavia: 900 years of warm-season temperatures. Climate Dynamics 36, 97–108. Cited in page 87.

Hawkins, E., Sutton, R., 2009. The potential to narrow uncertainty in regional climate predictions. Bulletin of the American Meteorological Society 90, 1095–1107. Cited in page 4.

Hegerl, G., Luterbacher, J., González-Rouco, F., Tett, S. F., Crowley, T., Xoplaki, E., 2011. Influence of human and natural forcing on European seasonal temperatures. Nature Geoscience 4, 99–103. Cited in page 46.

Hegerl, G. C., Zwiers, F. W., Braconnot, P., Gillett, N., Luo, Y., Marengo Orsini, J., Nicholls, N., Penner, J., Stott, P., 2007. Understanding and attributing climate change. In: Climate Change 2007: The Physical Science Basis. Contribution of Working Group I to the Fourth Assessment Report of the Intergovernmental Panel on Climate Change [Solomon, S., D. Qin, M. Manning, Z. Chen, M. Marquis, K.B. Averyt, M. Tignor and H.L. Miller (eds.)]. Cambridge University Press, Cambridge, United Kingdom and New York, NY, USA. Cited in page 11.

Helama, S., Fauria, M. M., Mielikäinen, K., Timonen, M., Eronen, M., 2010. Sub-milankovitch solar forcing of past climates: mid and late Holocene perspectives. Geological Society of America Bulletin 122, 1981–1988. Cited in page 87.

Hirschi, J., Baehr, J., Marotzke, J., Stark, J., Cunningham, S., Beismann, J.-O., 2003. A monitoring design for the Atlantic meridional overturning circulation. Geophysical Research Letters 30 (7). Cited in page 65.

Holland, M. M., Bitz, C. M., 2003. Polar amplification of climate change in coupled models. Climate Dynamics 21, 221–232. Cited in page 47.

Hughes, M. K., Guiot, J., Ammann, C. M., 2010. Emerging techniques and concepts offer ways to improve the use of process knowledge in reconstructions of past climate, and to make more comprehensive estimates of the uncertainties associated with them. PAGES news 18, 87–89. Cited in page 112.

Hughes, M. K., Vaganov, E. A., Shiyatov, S., Touchan, R., Funkhouser, G., 1999. Twentieth-century summer warmth in northern Yakutia in a 600-year context. The Holocene 9, 629–634. Cited in page 87.

IPCC, 2013. Annex I: Atlas of global and regional climate projections [van Oldenborgh, G.J., M. Collins, J. Arblaster, J.H. Christensen, J. Marotzke, S.B. Power, M. Rummukainen and T. Zhou (eds.)]. In: Climate Change 2013: The Physical Science Basis. Contribution of Working Group I to the Fifth Assessment Report of the Intergovernmental Panel on Climate Change [Stocker, T.F., D. Qin, G.-K. Plattner, M. Tignor, S.K. Allen, J. Boschung, A. Nauels,

Y. Xia, V. Bex and P.M. Midgley (eds.)]. Cambridge University Press, Cambridge, United Kingdom and New York, NY, USA. Cited in page 2.

Jacoby, G. C., D'Arrigo, R., 1989. Reconstructed Northern Hemisphere annual temperature since 1671 based on high-latitude tree-ring data from North America. Climatic Change 14, 39–59. Cited in page 23.

Jansen, E., Overpeck, J., Briffa, K., Duplessy, J.-C., Joos, F., Masson-Delmotte, V., Olago, D., Otto-Bliesner, B., Peltier, W., Rahmstorf, S., Ramesh, R., Raynaud, D., Rind, D., Solomina, O., Villalba, R., D. Zhang, 2007. Palaeoclimate. In: Climate Change 2007: The Physical Science Basis. Contribution of Working Group I to the Fourth Assessment Report of the Intergovernmental Panel on Climate Change [Solomon, S., D. Qin, M. Manning, Z. Chen, M. Marquis, K.B. Averyt, M. Tignor and H.L. Miller (eds.)]. Cambridge University Press, Cambridge, United Kingdom and New York, NY, USA. Cited in pages 23 and 33.

Jennings, A. E., Weiner, N. J., 1996. Environmental change in eastern Greenland during the last 1300 years: evidence from foraminifera and lithofacies in Nansen Fjord, 68°N. The Holocene 6, 179–191. Cited in page 23.

Jiang, H., Eiríksson, J., Schulz, M., Knudsen, K.-L., Seidenkrantz, M.-S., 2005. Evidence for solar forcing of sea-surface temperature on the North Icelandic Shelf during the late Holocene. Geology 33, 73–76. Cited in pages 23 and 64.

Jiang, H., Seidenkrantz, M.-S., Knudsen, K. L., Eríksson, J., 2002. Late-Holocene summer sea-surface temperatures based on a diatom record from the north Icelandic shelf. The Holocene 12, 137–147. Cited in page 39.

Johannessen, O. M., Bengtsson, L., Miles, M. W., Kuzmina, S. I., Semenov, V. A., Alekseev, G. V., Nagurnyi, A. P., Zakharov, V. F., Bobylev, L. P., Pettersson, L. H., et al., 2004. Arctic climate change: Observed and modelled temperature and sea-ice variability. Tellus A 56, 328–341. Cited in pages 22 and 23.

Jones, P. D., Briffa, K. R., Osborn, T. J., 2003. Changes in the Northern Hemisphere annual cycle: Implications for paleoclimatology? Journal of Geophysical Research: Atmospheres 108 (D18). Cited in pages 46 and 61.

Jones, P. D., Briffa, K. R., Osborn, T. J., Lough, J. M., Van Ommen, T. D., Vinther, B. M., Luterbacher, J., Wahl, E. R., Zwiers, F. W., Mann, M. E., et al., 2009. High-resolution palaeoclimatology of the last millennium: a review of current status and future prospects. The Holocene 19, 3–49. Cited in pages 7, 46, 61, 84, and 88.

Jones, P. D., Mann, M. E., 2004. Climate over past millennia. Reviews of Geophysics 42 (2). Cited in pages 3, 7, 23, 35, 39, 46, and 61.

Jones, P. D., Osborn, T. J., Briffa, K. R., 2001. The evolution of climate over the last millennium. Science 292, 662–667. Cited in page 23.

Joos, F., Spahni, R., 2008. Rates of change in natural and anthropogenic radiative forcing over the past 20.000 years. Proceedings of the National Academy of Sciences 105, 1425–1430. Cited in page 49.

Josey, S. A., Grist, J. P., Marsh, R., 2009. Estimates of meridional overturning circulation variability in the North Atlantic from surface density flux fields. Journal of Geophysical Research: Oceans 114 (C9). Cited in page 66.

Juckes, M. N., Allen, M. R., Briffa, K. R., Esper, J., Hegerl, G. C., Moberg, A., Osborn, T. J., Weber, S., 2007. Millennial temperature reconstruction intercomparison and evaluation. Climate of the Past 3, 591–609. Cited in page 88.

Jungclaus, J. H., Lorenz, S. J., Timmreck, C., Reick, C. H., Brovkin, V., Six, K., Segschneider, J., Giorgetta, M. A., Crowley, T. J., Pongratz, J., et al., 2010. Climate and carbon-cycle variability over the last millennium. Climate of the Past 6, 723–737. Cited in page 11.

Kalnay, E., 2003. Atmospheric modeling, data assimilation, and predictability. Cambridge university press. Cited in pages 12 and 13.

Kaplan, J. O., Krumhardt, K. M., Ellis, E. C., Ruddiman, W. F., Lemmen, C., Goldewijk, K. K., 2011. Holocene carbon emissions as a result of anthropogenic land cover change. The Holocene 21, 775–791. Cited in page 61.

Kaufman, D. S., Schneider, D. P., McKay, N. P., Ammann, C. M., Bradley, R. S., Briffa, K. R., Miller, G. H., Otto-Bliesner, B. L., Overpeck, J. T., Vinther, B. M., et al., 2009. Recent warming reverses long-term Arctic cooling. Science 325, 1236–1239. Cited in pages 7, 8, 9, 45, 47, 58, 59, and 60.

Keigwin, L. D., 1996. The little ice age and medieval warm period in the Sargasso Sea. Science 274, 1503–1508. Cited in page 64.

Keigwin, L. D., Boyle, E. A., 2000. Detecting Holocene changes in thermohaline circulation. Proceedings of the National Academy of Sciences 97, 1343–1346. Cited in page 65.

Kekonen, T., Moore, J., Perämäki, P., Mulvaney, R., Isaksson, E., Pohjola, V., van de Wal, R. S., 2005. The 800 year long ion record from the Lomonosovfonna (Svalbard) ice core. Journal of Geophysical Research: Atmospheres 110 (D7). Cited in page 40.

Kerr, R. A., 2005. The Atlantic Conveyor may have slowed, but don't panic yet. Science 310, 1403–1404. Cited in page 65.

Kinnard, C., Zdanowicz, C. M., Fisher, D. A., Isaksson, E., de Vernal, A., Thompson, L. G., 2011. Reconstructed changes in Arctic sea ice over the past 1.450 years. Nature 479, 509–512. Cited in pages 58, 59, and 60.

Klitgaard Kristensen, D., Sejrup, H. P., Haflidason, H., Berstad, I. M., Mikalsen, G., 2004. Eight-hundred-year temperature variability from the Norwegian continental margin and the North Atlantic thermohaline circulation. Paleoceanography 19 (2). Cited in page 39.

Knight, J. R., Allan, R. J., Folland, C. K., Vellinga, M., Mann, M. E., 2005. A signature of persistent natural thermohaline circulation cycles in observed climate. Geophysical Research Letters 32 (20). Cited in pages 43, 66, and 67.

Köhl, A., Stammer, D., 2008. Variability of the meridional overturning in the North Atlantic from the 50-year GECCO state estimation. Journal of Physical Oceanography 38, 1913–1930. Cited in pages 67 and 80.

Kuzmina, S. I., Johannessen, O. M., Bengtsson, L., Aniskina, O. G., Bobylev, L. P., 2008. High northern latitude surface air temperature: comparison of existing data and creation of a new gridded data set 1900–2000. Tellus A 60, 289–304. Cited in page 22.

Latif, M., Böning, C., Willebrand, J., Biastoch, A., Dengg, J., Keenlyside, N., Schweckendiek, U., Madec, G., 2006. Is the thermohaline circulation changing? Journal of Climate 19, 4631–4637. Cited in pages 66 and 67.

Latif, M., Roeckner, E., Botzet, M., Esch, M., Haak, H., Hagemann, S., Jungclaus, J., Legutke, S., Marsland, S., Mikolajewicz, U., et al., 2004. Reconstructing, monitoring, and predicting multidecadal-scale changes in the North Atlantic thermohaline circulation with sea surface temperature. Journal of Climate 17, 1605–1614. Cited in pages 66 and 67.

Lee, S.-K., Park, W., van Sebille, E., Baringer, M. O., Wang, C., Enfield, D. B., Yeager, S. G., Kirtman, B. P., 2011. What caused the significant increase in Atlantic Ocean heat content since the mid-20th century? Geophysical Research Letters 38 (17). Cited in page 67.

Lherminier, P., Mercier, H., Gourcuff, C., Alvarez, M., Bacon, S., Kermabon, C., 2007. Transports across the 2002 Greenland-Portugal Ovide section and comparison with 1997. Journal of Geophysical Research: Oceans 112 (C7). Cited in page 66.

Liu, J. S., Chen, R., 1998. Sequential Monte Carlo methods for dynamic systems. Journal of the American statistical association 93, 1032–1044. Cited in page 70.

Ljungqvist, F. C., 2009. Temperature proxy records covering the last two millennia: a tabular and visual overview. Geografiska Annaler: Series A, Physical Geography 91, 11–29. Cited in page 7.

Ljungqvist, F. C., 2010. A new reconstruction of temperature variability in the extra-tropical Northern Hemisphere during the last two millennia. Geografiska Annaler: Series A, Physical Geography 92, 339–351. Cited in page 7.

Lohmann, G., Rimbu, N., Dima, M., 2005. Where can the Arctic oscillation be reconstructed? towards a reconstruction of climate modes based on stable teleconnections. Climate of the Past Discussions 1. Cited in page 8.

Lozier, M. S., 2012. Overturning in the North Atlantic. Annual review of marine science 4, 291–315. Cited in page 64.

Lozier, M. S., Roussenov, V., Reed, M. S., Williams, R. G., 2010. Opposing decadal changes for the North Atlantic meridional overturning circulation. Nature Geoscience 3, 728–734. Cited in page 67.

Lumpkin, R., Speer, K. G., Koltermann, K. P., 2008. Transport across 48°N in the Atlantic Ocean. Journal of Physical Oceanography 38, 733–752. Cited in pages 65 and 66.

Lund, D. C., Lynch-Stieglitz, J., Curry, W. B., 2006. Gulf Stream density structure and transport during the past millennium. Nature 444, 601–604. Cited in pages 39 and 66.

Luterbacher, J., Dietrich, D., Xoplaki, E., Grosjean, M., Wanner, H., 2004. European seasonal and annual temperature variability, trends, and extremes since 1500. Science 303, 1499–1503. Cited in pages 7 and 46.

Mairesse, A., Goosse, H., Mathiot, P., Wanner, H., Dubinkina, S., 2013. Investigating the consistency between proxy-based reconstructions and climate models using data assimilation: a mid-Holocene case study. Climate of the Past 9, 3953–3991. Cited in pages 16, 81, and 105.

Manabe, S., Spelman, M. J., Stouffer, R. J., 1992. Transient responses of a coupled ocean-atmosphere model to gradual changes of atmospheric CO_2. Part II: Seasonal response. Journal of Climate 5, 105–126. Cited in page 50.

Mann, M. E., Bradley, R. S., Hughes, M. K., 1998. Global-scale temperature patterns and climate forcing over the past six centuries. Nature 392, 779–787. Cited in page 8.

Mann, M. E., Bradley, R. S., Hughes, M. K., 1999. Northern Hemisphere temperatures during the past millennium: Inferences, uncertainties, and limitations. Geophysical research letters 26, 759–762. Cited in pages 8 and 23.

Mann, M. E., Cane, M. A., Zebiak, S. E., Clement, A., 2005a. Volcanic and solar forcing of the tropical pacific over the past 1000 years. Journal of Climate 18, 447–456. Cited in page 35.

Mann, M. E., Jones, P. D., 2003. Global surface temperatures over the past two millennia. Geophysical Research Letters 30 (15). Cited in pages 23 and 88.

Mann, M. E., Park, J., 1994. Global-scale modes of surface temperature variability on interannual to century timescales. Journal of Geophysical Research: Atmospheres 99, 25819–25833. Cited in page 23.

Mann, M. E., Rutherford, S., Wahl, E., Ammann, C., 2005b. Testing the fidelity of methods used in proxy-based reconstructions of past climate. Journal of Climate 18, 4097–4107. Cited in page 23.

Mann, M. E., Zhang, Z., Hughes, M. K., Bradley, R. S., Miller, S. K., Rutherford, S., Ni, F., 2008. Proxy-based reconstructions of hemispheric and global surface temperature variations over the past two millennia. Proceedings of the National Academy of Sciences 105, 13252–13257. Cited in pages 7, 8, 17, 23, 24, 25, 27, 33, 35, 46, 83, 85, 86, 88, 90, 91, 92, and 96.

Mann, M. E., Zhang, Z., Rutherford, S., Bradley, R. S., Hughes, M. K., Shindell, D., Ammann, C., Faluvegi, G., Ni, F., 2009. Global signatures and dynamical origins of the Little Ice Age and Medieval Climate Anomaly. Science 326, 1256–1260. Cited in pages 7, 8, 46, 64, 84, 90, 91, 96, and 97.

Marsh, R., De Cuevas, B. A., Coward, A. C., Bryden, H. L., Álvarez, M., 2005. Thermohaline circulation at three key sections in the North Atlantic over 1985–2002. Geophysical Research Letters 32 (10). Cited in page 67.

Massé, G., Rowland, S. J., Sicre, M.-A., Jacob, J., Jansen, E., Belt, S. T., 2008. Abrupt climate changes for Iceland during the last millennium: evidence

from high resolution sea ice reconstructions. Earth and Planetary Science Letters 269, 565–569. Cited in page 23.

Mathiot, P., Goosse, H., Crosta, X., Stenni, B., Braida, M., Renssen, H., Van Meerbeeck, C. J., Masson-Delmotte, V., Mairesse, A., Dubinkina, S., 2013. Using data assimilation to investigate the causes of Southern Hemisphere high latitude cooling from 10 to 8 ka BP. Climate of the Past 9, 887–901. Cited in pages 16 and 81.

McBean, G., Alekseev, G., Chen, D., Foerland, E., Fyfe, J., Groisman, P. Y., King, R., Melling, H., Vose, R., Whitfield, P. H., 2005. Arctic Climate: past and present. In: Arctic Climate Impact Assessment. Cambridge University Press. Cited in page 47.

Meier, W., Stroeve, J., Fetterer, F., Knowles, K., 2005. Reductions in Arctic sea ice cover no longer limited to summer. Eos, Transactions American Geophysical Union 86, 326–326. Cited in page 22.

Menary, M. B., Roberts, C. D., Palmer, M. D., Halloran, P. R., Jackson, L., Wood, R. A., Müller, W. A., Matei, D., Lee, S.-K., 2013. Mechanisms of aerosol-forced AMOC variability in a state of the art climate model. Journal of Geophysical Research: Oceans 118, 2087–2096. Cited in pages 67 and 79.

Mercier, H., Lherminier, P., Sarafanov, A., Gaillard, F., Daniault, N., Desbruyères, D., Falina, A., Ferron, B., Gourcuff, C., Huck, T., et al., 2013. Variability of the meridional overturning circulation at the Greenland–Portugal OVIDE section from 1993 to 2010. Progress in Oceanography. Cited in page 66.

Mikalsen, G., Sejrup, H. P., Aarseth, I., 2001. Late-Holocene changes in ocean circulation and climate: foraminiferal and isotopic evidence from Sulafjord, western Norway. The Holocene 11, 437–446. Cited in page 39.

Miller, G. H., Geirsdóttir, Á., Zhong, Y., Larsen, D. J., Otto-Bliesner, B. L., Holland, M. M., Bailey, D. A., Refsnider, K. A., Lehman, S. J., Southon, J. R., et al., 2012. Abrupt onset of the Little Ice Age triggered by volcanism and sustained by sea-ice/ocean feedbacks. Geophysical Research Letters 39 (2). Cited in page 65.

Moberg, A., 2012. Comments on 'Reconstruction of the extratropical NH mean temperature over the last millennium with a method that preserves low-frequency variability'. Journal of Climate 25. Cited in page 89.

Moberg, A., 2013. Comparisons of simulated and observed Northern Hemisphere temperature variations during the past millennium-selected lessons learned and problems encountered. Tellus B 65. Cited in pages 4 and 5.

Moberg, A., Alexandersson, H., Bergström, H., Jones, P. D., 2003. Were southern Swedish summer temperatures before 1860 as warm as measured? International Journal of Climatology 23, 1495–1521. Cited in page 23.

Moberg, A., Sonechkin, D. M., Holmgren, K., Datsenko, N. M., Karlén, W., 2005. Highly variable Northern Hemisphere temperatures reconstructed from low-and high-resolution proxy data. Nature 433, 613–617. Cited in pages 7 and 88.

Muscheler, R., Joos, F., Beer, J., Müller, S. A., Vonmoos, M., Snowball, I., 2007. Solar activity during the last 1000yr inferred from radionuclide records. Quaternary Science Reviews 26, 82–97. Cited in pages 25 and 26.

Ogilvie, A. E., Jónsson, T., 2001. "Little Ice Age" Research: A perspective from Iceland. Climatic Change 48, 9–52. Cited in page 23.

Opsteegh, J. D., Haarsma, R. J., Selten, F. M., Kattenberg, A., 1998. ECBILT: A dynamic alternative to mixed boundary conditions in ocean models. Tellus A 50, 348–367. Cited in pages 24 and 48.

Osborn, T. J., Briffa, K. R., 2006. The spatial extent of 20th-century warmth in the context of the past 1200 years. Science 311, 841–844. Cited in pages 46 and 57.

Osborn, T. J., Raper, S. C., Briffa, K. R., 2006. Simulated climate change during the last 1.000 years: comparing the ECHO-G general circulation model with the MAGICC simple climate model. Climate Dynamics 27, 185–197. Cited in pages 46 and 57.

Overland, J. E., Spillane, M. C., Percival, D. B., Wang, M., Mofjeld, H. O., 2004. Seasonal and regional variation of pan-Arctic surface air temperature over the instrumental record. Journal of Climate 17, 3263–3282. Cited in pages 22, 23, and 42.

Overland, J. E., Wang, M., 2005. The third Arctic climate pattern: 1930s and early 2000s. Geophysical Research Letters 32 (23). Cited in page 43.

Overpeck, J., Hughen, K., Hardy, D., Bradley, R., Case, R., Douglas, M., Finney, B., Gajewski, K., Jacoby, G., Jennings, A., et al., 1997. Arctic environmental change of the last four centuries. Science 278, 1251–1256. Cited in pages 7, 8, 9, 23, 32, 33, and 47.

PAGES 2k Consortium, 2013. Continental-scale temperature variability during the past two millennia. Nature Geoscience 6, 339–346. Cited in pages 8, 9, and 85.

Pithan, F., Mauritsen, T., 2014. Arctic amplification dominated by temperature feedbacks in contemporary climate models. Nature Geoscience 7, 181–184. Cited in page 3.

Pohlmann, H., Smith, D. M., Balmaseda, M. A., Keenlyside, N. S., Masina, S., Matei, D., Müller, W. A., Rogel, P., 2013. Predictability of the mid-latitude Atlantic meridional overturning circulation in a multi-model system. Climate dynamics 41, 775–785. Cited in page 80.

Polyakov, I. V., Johnson, M. A., 2000. Arctic decadal and interdecadal variability. Geophysical Research Letters 27, 4097–4100. Cited in page 22.

Pongratz, J., Reick, C., Raddatz, T., Claussen, M., 2008. A reconstruction of global agricultural areas and land cover for the last millennium. Global Biogeochemical Cycles 22 (3). Cited in pages 5 and 49.

Przybylak, R., 2000. Temporal and spatial variation of surface air temperature over the period of instrumental observations in the Arctic. International Journal of Climatology 20, 587–614. Cited in page 23.

Ramankutty, N., Foley, J. A., 1999. Estimating historical changes in global land cover: Croplands from 1700 to 1992. Global biogeochemical cycles 13, 997–1027. Cited in pages 5, 25, and 49.

Renssen, H., Goosse, H., Fichefet, T., Brovkin, V., Driesschaert, E., Wolk, F., 2005. Simulating the Holocene climate evolution at northern high latitudes using a coupled atmosphere-sea ice-ocean-vegetation model. Climate Dynamics 24, 23–43. Cited in page 48.

Robock, A., 2000. Volcanic eruptions and climate. Reviews of Geophysics 38, 191–219. Cited in page 61.

Robson, J., Hodson, D., Hawkins, E., Sutton, R., 2014. Atlantic overturning in decline? Nature Geoscience 7, 2–3. Cited in page 82.

Rogers, J. C., 1985. Atmospheric circulation changes associated with the warming over the northern North Atlantic in the 1920s. Journal of Climate and Applied Meteorology 24, 1303–1310. Cited in page 23.

Rutherford, S., Mann, M. E., Osborn, T. J., Bradley, R. S., Briffa, K. R., Hughes, M. K., Jones, P. D., 2005. Proxy-based Northern Hemisphere surface temperature reconstructions: Sensitivity to method, predictor network, target season, and target domain. Journal of climate 18, 2308–2329. Cited in pages 7 and 46.

Schmidt, G. A., Jungclaus, J. H., Ammann, C. M., Bard, E., Braconnot, P., Crowley, T. J., Delaygue, G., Joos, F., Krivova, N. A., Muscheler, R., et al., 2011. Climate forcing reconstructions for use in PMIP simulations of the last millennium (v1.0). Geoscientific Model Development 4, 33–45. Cited in pages 10, 49, 52, and 55.

Schmidt, G. A., Jungclaus, J. H., Ammann, C. M., Bard, E., Braconnot, P., Crowley, T. J., Delaygue, G., Joos, F., Krivova, N. A., Muscheler, R., et al., 2012. Climate forcing reconstructions for use in PMIP simulations of the last millennium (v1.1). Geoscientific Model Development 5, 185–191. Cited in pages 5, 53, and 61.

Schmittner, A., Latif, M., Schneider, B., 2005. Model projections of the North Atlantic thermohaline circulation for the 21st century assessed by observations. Geophysical Research Letters 32 (23). Cited in page 64.

Schott, F. A., Fischer, J., Dengler, M., Zantopp, R., 2006. Variability of the deep western boundary current east of the Grand Banks. Geophysical Research Letters 33 (21). Cited in page 66.

Sejrup, H. P., Lehman, S. J., Haflidason, H., Noone, D., Muscheler, R., Berstad, I. M., Andrews, J. T., 2010. Response of Norwegian Sea temperature to solar forcing since 1000 ad. Journal of Geophysical Research: Oceans 115 (C12). Cited in page 64.

Serreze, M. C., Barry, R. G., 2011. Processes and impacts of Arctic amplification: A research synthesis. Global and Planetary Change 77, 85–96. Cited in page 3.

Serreze, M. C., Francis, J. A., 2006. The Arctic amplification debate. Climatic Change 76, 241–264. Cited in page 47.

Serreze, M. C., Walsh, J. E., Chapin, F. S., Osterkamp, T., Dyurgerov, M., Romanovsky, V., Oechel, W. C., Morison, J., Zhang, T., Barry, R. G., 2000. Observational evidence of recent change in the northern high-latitude environment. Climatic Change 46, 159–207. Cited in page 22.

Shapiro, A. I., Schmutz, W., Rozanov, E., Schoell, M., Haberreiter, M., Shapiro, A. V., Nyeki, S., 2011. A new approach to long-term reconstruction of the

solar irradiance leads to large historical solar forcing. Astronomy & Astrophysics 529, A67. Cited in pages 53 and 61.

Shi, F., Yang, B., Ljungqvist, F. C., Yang, F., 2012. Multi-proxy reconstruction of arctic summer temperatures over the past 1400 years. Climate Research 54, 113–128. Cited in pages 8 and 9.

Shindell, D. T., Schmidt, G. A., Mann, M. E., Rind, D., Waple, A., 2001. Solar forcing of regional climate change during the Maunder Minimum. Science 294, 2149–2152. Cited in pages 35 and 61.

Shindell, D. T., Schmidt, G. A., Miller, R. L., Mann, M. E., 2003. Volcanic and solar forcing of climate change during the preindustrial era. Journal of Climate 16, 4094–4107. Cited in page 46.

Sicre, M.-A., Hall, I. R., Mignot, J., Khodri, M., Ezat, U., Truong, M.-X., Eiríksson, J., Knudsen, K.-L., 2011. Sea surface temperature variability in the subpolar Atlantic over the last two millennia. Paleoceanography 26 (4). Cited in page 64.

Sicre, M.-A., Jacob, J., Ezat, U., Rousse, S., Kissel, C., Yiou, P., Eiríksson, J., Knudsen, K. L., Jansen, E., Turon, J.-L., 2008. Decadal variability of sea surface temperatures off North Iceland over the last 2000 years. Earth and Planetary Science Letters 268, 137–142. Cited in page 39.

Slonosky, V. C., Mysak, L. A., Derome, J., 1997. Linking Arctic sea-ice and atmospheric circulation anomalies on interannual and decadal timescales. Atmosphere-Ocean 35, 333–366. Cited in page 38.

Spangehl, T., Cubasch, U., Raible, C., Schimanke, S., Körper, J., Hofer, D., 2010. Transient climate simulations from the maunder minimum to present day: Role of the stratosphere. Journal of Geophysical Research: Atmospheres 115 (D1). Cited in page 11.

Spielhagen, R. F., Werner, K., Sørensen, S. A., Zamelczyk, K., Kandiano, E., Budeus, G., Husum, K., Marchitto, T. M., Hald, M., 2011. Enhanced modern heat transfer to the Arctic by warm Atlantic water. Science 331, 450–453. Cited in page 64.

Stammer, D., Wunsch, C., Giering, R., Eckert, C., Heimbach, P., Marotzke, J., Adcroft, A., Hill, C. N., Marshall, J., 2002. Global ocean circulation during 1992–1997, estimated from ocean observations and a general circulation model. Journal of Geophysical Research: Oceans 107 (C9). Cited in pages 18 and 67.

Stendel, M., Mogensen, I. A., Christensen, J. H., 2006. Influence of various forcings on global climate in historical times using a coupled atmosphere–ocean general circulation model. Climate dynamics 26, 1–15. Cited in page 11.

Stroeve, J., Holland, M. M., Meier, W., Scambos, T., Serreze, M., 2007. Arctic sea ice decline: Faster than forecast. Geophysical research letters 34 (9). Cited in page 49.

Sundberg, R. M., Anders, Hind, A., 2012. Statistical framework for evaluation of climate model simulations byuse of climate proxy data from the last millennium: Part 1: Theory. Climate of the Past 8, 1339–1353. Cited in page 105.

Swingedouw, D., Mignot, J., Labetoulle, S., Guilyardi, E., Madec, G., 2013. Initialisation and predictability of the AMOC over the last 50 years in a climate model. Climate dynamics 40, 2381–2399. Cited in pages 67 and 80.

Thomas, E. K., Briner, J. P., 2009. Climate of the past millennium inferred from varved proglacial lake sediments on northeast Baffin Island, Arctic Canada. Journal of Paleolimnology 41, 209–224. Cited in page 40.

Timmermann, A., Goosse, H., 2004. Is the wind stress forcing essential for the meridional overturning circulation? Geophysical research letters 31 (4). Cited in pages 64 and 77.

Trenberth, K. E., Jones, P. D., Ambenje, P., Bojariu, R., Easterling, D., Tank, A. K., Parker, D., Rahimzadeh, F., Renwick, J. A., Rusticucci, M., et al., 2007. Observations: Surface and atmospheric climate change. In: Climate Change 2007: The Physical Science Basis. Contribution of Working Group I to the Fourth Assessment Report of the Intergovernmental Panel on Climate Change [Solomon, S., D. Qin, M. Manning, Z. Chen, M. Marquis, K.B. Averyt, M. Tignor and H.L. Miller (eds.)]. Cambridge University Press, Cambridge, United Kingdom and New York, NY, USA. Cited in pages 8 and 22.

Trouet, V., Scourse, J. D., Raible, C. C., 2012. North Atlantic storminess and Atlantic meridional overturning circulation during the last millennium: reconciling contradictory proxy records of NAO variability. Global and Planetary Change 84, 48–55. Cited in page 65.

Våge, K., Pickart, R. S., Thierry, V., Reverdin, G., Lee, C. M., Petrie, B., Agnew, T. A., Wong, A., Ribergaard, M. H., 2009. Surprising return of deep convection to the subpolar North Atlantic Ocean in winter 2007–2008. Nature Geoscience 2, 67–72. Cited in page 66.

van der Schrier, G., Barkmeijer, J., 2005. Bjerknes' hypothesis on the coldness during AD 1790–1820 revisited. Climate Dynamics 25, 537–553. Cited in page 13.

van Leeuwen, P. J., 2009. Particle filtering in geophysical systems. Monthly Weather Review 137, 4089–4114. Cited in pages 13, 14, and 69.

Vaughan, D. G., Comiso, J. C., Allison, I., Carrasco, J., Kaser, G., Kwok, R., Mote, P., Murray, T., Paul, F., Ren, J., Rignot, E., Solomina, O., Steffen, K., Zhang, T., 2007. Observations: Cryosphere. In: Climate Change 2013: The Physical Science Basis. Contribution of Working Group I to the Fifth Assessment Report of the Intergovernmental Panel on Climate Change [Stocker, T.F., D. Qin, G.-K. Plattner, M. Tignor, S.K. Allen, J. Boschung, A. Nauels, Y. Xia, V. Bex and P.M. Midgley (eds.)]. Cambridge University Press, Cambridge, United Kingdom and New York, NY, USA. Cited in page 2.

Vavrus, S. J., Holland, M. M., Jahn, A., Bailey, D. A., Blazey, B. A., 2012. Twenty-first-century Arctic climate change in CCSM4. Journal of Climate 25, 2696–2710. Cited in page 50.

Vellinga, M., Wood, R. A., 2002. Global climatic impacts of a collapse of the Atlantic thermohaline circulation. Climatic change 54, 251–267. Cited in page 64.

Vinther, B. M., Andersen, K. K., Jones, P. D., Briffa, K. R., Cappelen, J., 2006. Extending Greenland temperature records into the late eighteenth century. Journal of Geophysical Research: Atmospheres 111 (D11). Cited in page 23.

Vinther, B. M., Jones, P. D., Briffa, K. R., Clausen, H. B., Andersen, K. K., Dahl-Jensen, D., Johnsen, S. J., 2010. Climatic signals in multiple highly resolved stable isotope records from Greenland. Quaternary Science Reviews 29, 522–538. Cited in page 87.

von Storch, H., 1999. On the use of "inflation" in statistical downscaling. Journal of Climate 12, 3505–3506. Cited in page 88.

von Storch, H., Cubasch, U., Gonzalez-Rouco, J. F., Jones, J. M., Voss, R., Widmann, M., Zorita, E., 2000. Combining paleoclimatic evidence and GCMs by means of data assimilation through upscaling and nudging (DATUN). Proceedings of the 11th symposium on Gobal Change Studies, AMS Long Beach, CA. Cited in page 13.

von Storch, H., Zorita, E., Jones, J. M., Dimitriev, Y., González-Rouco, F., Tett, S. F., 2004. Reconstructing past climate from noisy data. Science 306, 679–682. Cited in page 89.

Wanamaker, A. D., Butler, P. G., Scourse, J. D., Heinemeier, J., Eiríksson, J., Knudsen, K. L., Richardson, C. A., 2012. Surface changes in the North Atlantic meridional overturning circulation during the last millennium. Nature communications 3, 899. Cited in pages 65 and 66.

Wang, Y.-M., Lean, J. L., Sheeley, N. R., 2005. Modeling the Sun's magnetic field and irradiance since 1713. The Astrophysical Journal 625, 522–538. Cited in page 49.

Weaver, A. J., Sedláček, J., Eby, M., Alexander, K., Crespin, E., Fichefet, T., Philippon-Berthier, G., Joos, F., Kawamiya, M., Matsumoto, K., et al., 2012. Stability of the Atlantic meridional overturning circulation: A model intercomparison. Geophysical Research Letters 39 (20). Cited in page 16.

Weckström, J., Korhola, A., Erästö, P., Holmström, L., 2006. Temperature patterns over the past eight centuries in Northern Fennoscandia inferred from sedimentary diatoms. Quaternary Research 66, 78–86. Cited in page 40.

Widmann, M., Goosse, H., van der Schrier, G., Schnur, R., Barkmeijer, J., 2010. Using data assimilation to study extratropical Northern Hemisphere climate over the last millennium. Climate of the Past 6, 627–644. Cited in page 13.

Willis, J. K., 2010. Can in situ floats and satellite altimeters detect long-term changes in Atlantic Ocean overturning? Geophysical Research Letters 37 (6). Cited in page 65.

Wunsch, C., Heimbach, P., 2006. Estimated decadal changes in the North Atlantic meridional overturning circulation and heat flux 1993–2004. Journal of Physical Oceanography 36, 2012–2024. Cited in pages 18 and 67.

Xoplaki, E., Luterbacher, J., Paeth, H., Dietrich, D., Steiner, N., Grosjean, M., Wanner, H., 2005. European spring and autumn temperature variability and change of extremes over the last half millennium. Geophysical Research Letters 32 (15). Cited in pages 7 and 46.

Zhang, J., Rothrock, D. A., Steele, M., 1998. Warming of the Arctic Ocean by a strengthened Atlantic inflow: Model results. Geophysical Research Letters 25, 1745–1748. Cited in page 43.

Zhang, R., Delworth, T. L., Held, I. M., 2007. Can the Atlantic Ocean drive the observed multidecadal variability in Northern Hemisphere mean temperature? Geophysical Research Letters 34 (2). Cited in page 43.

Zickfeld, K., Eby, M., Weaver, A. J., Alexander, K., Crespin, E., Edwards, N. R., Eliseev, A. V., Feulner, G., Fichefet, T., Forest, C. E., et al., 2013. Long-term climate change commitment and reversibility: An EMIC intercomparison. Journal of Climate 26, 5782–5809. Cited in page 16.

Zunz, V., Goosse, H., Massonnet, F., 2013. How does internal variability influence the ability of CMIP5 models to reproduce the recent trend in Southern Ocean sea ice extent? Cryosphere 7, 451–468. Cited in page 16.

Zveryaev, I. I., Gulev, S. K., 2009. Seasonality in secular changes and interannual variability of European air temperature during the twentieth century. Journal of Geophysical Research: Atmospheres 114 (D2). Cited in page 46.